The golden age of wasted TVs

Regaining precious metals and critical raw materials from low and medium grade PCBs within the EU, including a technical case study for FDP TVs and monitors

by

Max van Beek BSc.

Student number: s1851535 (Leiden), 4630181 (Delft)
Project duration: February, 2022 – November, 2022
Thesis committee: Dr. F. Di Maio, TU Delft, main supervisor
Prof. dr. E. van der Voet, Universiteit Leiden, secondary supervisor
Dr. L. Wang, TU Delft, daily supervisor

TU Delft

Universiteit Leiden
The Netherlands

Abstract

In recent decades Europe has been increasing its demand and consumption of electronics. This has in turn resulted in major outflows of waste electronics (WEEE) that are usually not properly dealt with. This is especially the case for low to medium grade printed circuit boards (PCBs) which unlike higher grade electronics such as computers are currently not profitable to recycle. Therefore this thesis, as a part of the Peacoc project, investigated the low energy separation methods roll sorting, magnetic separation and magnetic density separation to concentrate the precious and critical metals found in the components of these discarded PCBs. The resulting secondary material flows were then evaluated on their impact in the EU from a material and energetical perspective.

The roll sorter was able to significantly increase the concentrations of the precious metal rich target components (*Central processing units*, *IC chips and transistors*, *MLCC + Ta capacitors*, *Small transistors and IC chips* and *Connectors of plastic with golden pins*). The machine sorted the feed into multiple width sizes (< 3.0, 3.0 - 5.0, 5.0 - 7.0 and > 7.0 mm) of which all except > 7.0 were used for further processing, increasing the overall grade from 18.66 to 42.61 wt%. This was further increased by the magnetic separator (lightly and non magnetic fractions for < 3.0 mm and only the non magnetic fraction for 3.0 - 7.0 mm) to 53.69 wt% and magnetic density separation (only for non magnetic 5.0 - 7.0 mm) to 66.23 wt%. Recovery for all target categories was near 100% with the exception of *Connectors of plastic with golden pins* as these were too large for the roll sorter to sort.

The thesis also took a broader approach by employing a dynamic material flow analysis to determine the low to medium grade PCBs and their accompanying precious metal flows in the EU. The expected metal flows were low (~4%) compared to the EU's overall demand in 2020 and expected to decrease over the years due to miniaturisation (decreasing size and weight) of the components. Furthermore, only around 36.68 wt% of the maximum precious metal flows were expected to be captured due to low collection rates of WEEE and small loses in separation and metallurgical recovery. Nonetheless, a sizeable fraction of the EU's electronics sector's demand (over 10%) could be supplied. These results were confirmed by modelling different future scenarios, a Monte-Carlo uncertainty and sensitivity analysis of the model.

Lastly, the thesis explored the topic of critical raw materials (CRMs) and the direct energy requirements of Peacoc's recovery system. It was found that beryllium, antimony, platinum and palladium were the only CRMs that had any significant potential to supply the EU (9.13% for beryllium, 1.58% for antimony, 1.32% for platinum and 4.02% for palladium). If only looking at the electronics sector this was also the case for cobalt and vanadium. The newly captured secondary precious metals were shown to require significantly less energy to produce, around an order of magnitude, compared to primary production but were similar to other recycling pathways. Furthermore, the majority of energy was required during metallurgical recovery showing a potential for further mechanical concentration during separation.

In conclusion it can be stated that the separation technologies (roll sorting, magnetic separation and magnetic density separation) are effective methods for separating the components of low to medium grade PCBs. However, their impact on the circularity and energetical footprint of the whole EU are expected to be small.

Acknowledgements

During my thesis I had help of numerous people and would therefore like to thank them.

First of all I would like to thank my two main supervisors Francesco Di Maio and Ester van der Voet for all their support, input and guiding me through the project. I would also like to thank my daily supervisor Lin Wang for having a partner to discuss the topic with and Peter Rem for acting as a de facto third supervisor, especially during the summer. Ron Penners, Richard Idzes and the others at Resources & Recycling should also not be forgotten for their great help during the experiments in the lab and their expertise. Last but not least I would like to thank my friends for proofreading my thesis.

Contents

List of Figures

List of Tables

List of abbreviations

Ag	Silver
Au	Gold
BAU	Business as usual
CE	Circular economy
CPU	Central processing unit
CRM	Critical raw material
CRT	Cathode-ray tube
EEE	Electrical and Electronic Equipment
EI	Economic importance
EoL	End-of-life
EoL-RIR	End-of-life recycling input rate
FDP	Flat display panel
GDEx	Gas diffusion electrocrystallization
IR	Import ratio
MDS	Magnetic density separation
MFA	Material flow analysis
MS	Magnetic separation
PCB	Printed circuit board
Pd	Palladium
PGM	Platinum Group Metal
RQ	Research question
RS	Roll sorter
SR	Supply risk
Unu	United nations university
WEEE	Waste Electrical and Electronic Equipment

1 Introduction

The philosopher's stone is one of the most famous and elusive mythical devices known to humanity, both through ancient and modern stories [1, 2]. According to myth, the stone can convert or transmutate base metals (e.g. lead) to precious metals such as gold [3]. Many people have dedicated their lives to the continued search, yet to no avail. Even though we nowadays know the stone cannot exist, the persistence of this legend shows the continued interest that we as humanity hold in our most beloved precious metals: gold, silver and platinum.

Throughout history, precious metals have been used in a multifold of applications such as coins, jewellery or simply to store wealth [4]. This continued demand is due to their beauty, rarity, resistance to corrosion and ease of working [5]. Therefore, it should come as no surprise that they have also historically been some of the most recycled and reused metals [6].

Over time our usage of these metals has shifted. New commercial and industrial applications to improve our lives have been found such as paints for silver and auto-catalysts for platinum [7, 8]. Except, these products use the precious metals as an additive and not as their main material. This results in low concentrations and/or complex forms, such as alloys and nanoparticles, making it hard to recycle [9]. For example, the catalyst in a car contains only 0.179 wt% platinum [10]. However, the precious metals still encompass the majority of the product's value, showing their importance again [11].

Low concentrations and negligible recycling rates are not unique to precious metals and can also be found in a group of materials called the critical raw materials (CRMs). CRMs are materials (metals, organics and minerals) which have a high vulnerability to supply chain disruptions while being of high economic importance [12, 13]. CRMs are often mined/refined in small quantities or as a companion to a major metal [14]. For example, all indium is currently won as a by-product of zinc mining thus disabling normal supply demand behaviour [15]. Furthermore, primary production tends to be highly centralised in a limited number of countries/regions. For instance, China produces 89% of all magnesium worldwide [8]. Yet at the same time CRMs are essential to the economy and have therefore been called the vitamins of the economy and industry [16, 17].

Modern electronics might be one of the best examples of the problem at hand. Gold and silver are a preferred metal in electronics as they are great electrical conductors, while being strong and resistant against damage [18, 19]. However, due to their cost they are only used in small amounts and in a select number of components, such as the central processing units (CPUs) and connectors [20, 21]. Furthermore, we as humanity have developed an insatiable hunger with ever increasing needs for these electronics, thus also increasing our demand for the metals. At the same time we are also quick to replace our electronics with new products resulting in very short lifespans [22]. After they become waste, known as waste electrical and electronic equipment (WEEE), we exert minimal effort trying to regain them and dump, export or burn them instead [23]. And even if we put in the effort, the methods we use tends to be unselective and energy intensive, such as Umicore's Precious Metal Refining [24].

Therefore, a new way has to be found. The EU has recognised this problem and started the Peacoc Project in 2021 [25]. As a part of this project, the Resources & Recycling research group at the TU Delft has the goal of separating the components found on discarded printed circuit boards (PCBs) in a cheap, effective and energetically efficient way. This will allow metallurgical recyclers to tailor their hydrometallurgical processes to the specific composition of the components resulting in improved energetical and material efficiency. Furthermore, electronics' producers can learn from and aid in the separation by designing their products for recycling [26, 27].

This thesis will take a wide and in-depth view at the WEEE issue and Peacoc project. A technical case study will be presented regarding the separation of components found on PCBs taken from flat display panel TVs and monitors. Here, different methods will be employed such as sieving, magnetic separation and magnetic density separation. From a birds eye view, an overview of the stocks and flows for PCBs of low and medium grade electronics in the EU and their accompanying critical/precious metals will be presented using a material flow analysis (MFA). This will be compared with the current demand of these metals within the EU and its impact on their criticality for the CRMs. Lastly, the energy requirements for the recovery of precious metals will be determined and compared to primary production and current recycling methods.

This thesis report will start out with a theoretical background, followed by the research questions. The technical case study will be presented in chapter 2, followed by the stocks and flows in chapter 3. In chapter 4 the topic of CRMs will be addressed and chapter 5 covers the energy requirements of the Peacoc project. Finally, a conclusion and recommendation will finish the thesis report in chapter 6.

1.1. Sorting technologies

1.1.1. Roll sorter (RS)

The roll sorter (RS), also known as roller or fruit grader, is a shape separation method. It is a well established separation method in the food industry for separating fruit, fish and seeds [28–33]. The oldest patents stem from the early 20th century [34–36]. However, outside of this field little to no research or adoption has taken place, except one patent from 2004 on regenerating spent catalysts and another from 2009 on separating plastic flakes from rubber [37, 38].

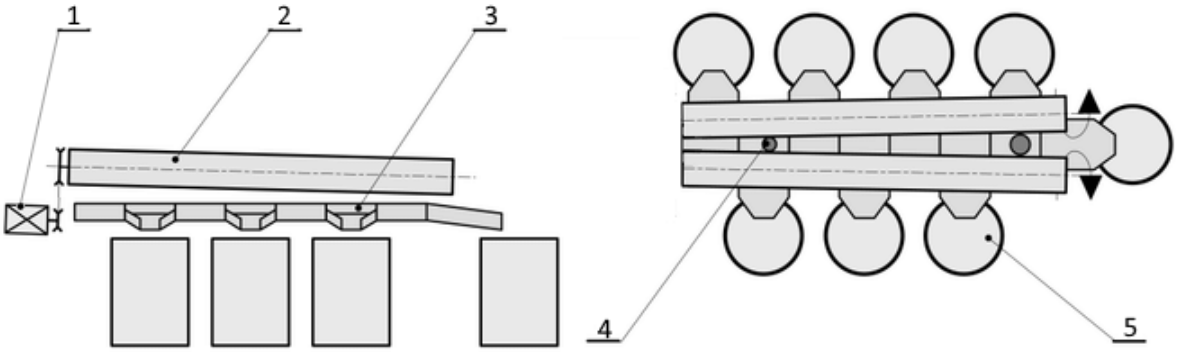

Figure 1.1: A side (left) and top (right) view diagram of a roll sorter: 1 engine, 2 sorting rollers, 3 classification chute, 4 feed particle, 5 container. Adapted from [39].

A roll sorter is operated by two counter rotating cylinders/rollers, which are placed at an angle with a small gap in between (see figure 1.1). By decreasing the width of the cylinders or increasing the distance between them, a widening of the gap can be achieved [39, 40]. The feedstock can only pass through the two rollers when the gap is wide enough for its smallest dimension. For example, a postcard can pass easily, but a cube will not. This allows the machine to sieve/sort the feedstock along its thinnest axis [41]. To avoid crushing the feedstock between the rollers, an inside to outside rotation of the cylinders is implemented. Furthermore, the cylinders should be placed at an angle which will allow the feedstock to be gravity fed over the whole length of the machine [42, 43].

1.1.2. Magnetic separation (MS)

The magnetic separator (MS), also known as magnetic concentrator, was invented in the late 19th century and exploits the magnetic properties that are found in metals [44]. It has been adopted by a multitude of sectors including microbiology, mining and waste separation [45–47].

A (stationary) magnetic field is created through the use of a permanent magnet or electromagnet. Ferromagnetic (and paramagnetic if the field is strong enough) particles are attracted by the magnet and can overcome gravity leaving the feed stream, thus allowing their separation from the feed [44]. Out of the ferromagnetic materials iron, nickel and cobalt are the most important targets [48].

One of the methods to achieve magnetic separation is the overbelt magnet, see figure 1.2. A magnet is hung above to the feeding stream. The magnetic particles (blue in the figure) will leave the feed stream due to the magnetic field, removing them from the non magnetic particles [50].

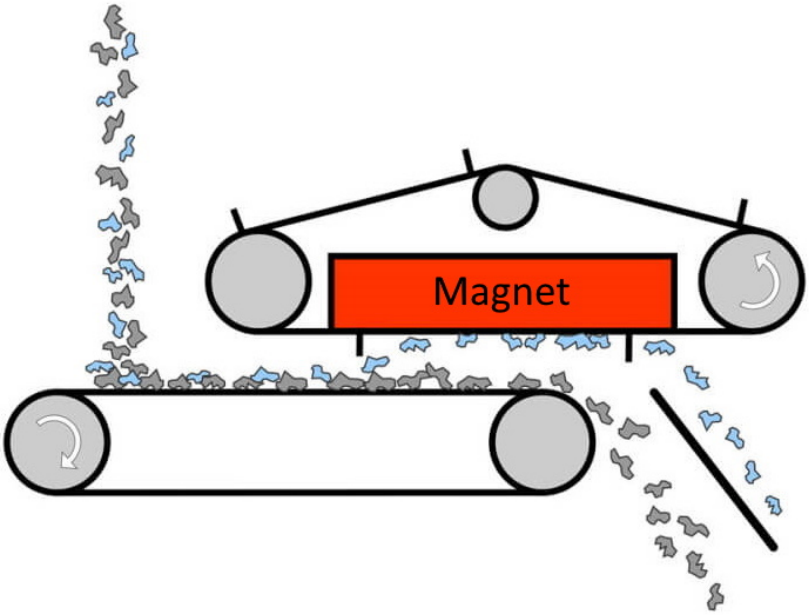

Figure 1.2: A schematic diagram for an overbelt magnetic separator with the blue particles being magnetically susceptible, adapted from [49]

1.2. Magnetic density separation (MDS)

Magnetic density separation (MDS) is a novel separation technology in development at the Resources & Recycling department of the TU Delft [51]. It can best be seen as an advanced form of the sink-float separator, allowing the feedstock to be sorted based on its density [52]. In a normal sink-float separator, the feedstock is released in a liquid medium with a preselected density (usually water). If the feedstock particle has a higher density than the medium it will sink (heavy fraction), while a lower density will result in a floating particle (light fraction) [53]. However, this method is limited by the fact that only two fractions are produced. The novelty of MDS stems from its ability to create a density gradient in the medium, thus creating more than two density fractions.

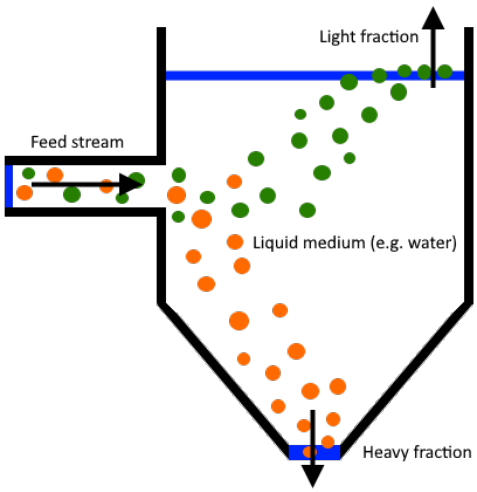

Figure 1.3: A schematic overview of a sink-float separator with the particles possessing either a higher (orange) or lower (green) density than water.

The gradient in density (see figure 1.4) is achieved by using a magnetic fluid as medium and a magnet [54]. The magnet is placed below or above the separator, which in turn attracts the magnetic particles in the fluid. If the magnet is placed below the fluid, the attraction increases the (effective) density of the

fluid near the bottom. By carefully selecting the size and shape of the magnet it is possible to have a uniform magnetic field and density gradient in the horizontal axis while decreasing in the vertical axis, see figure 1.4. This allows the particles to settle at their preferred density while flowing from left to right [55]. As creating this magnet setup has been extensively explored by Jaap Kosse of Twente University, it is considered outside the scope of this thesis [56–58].

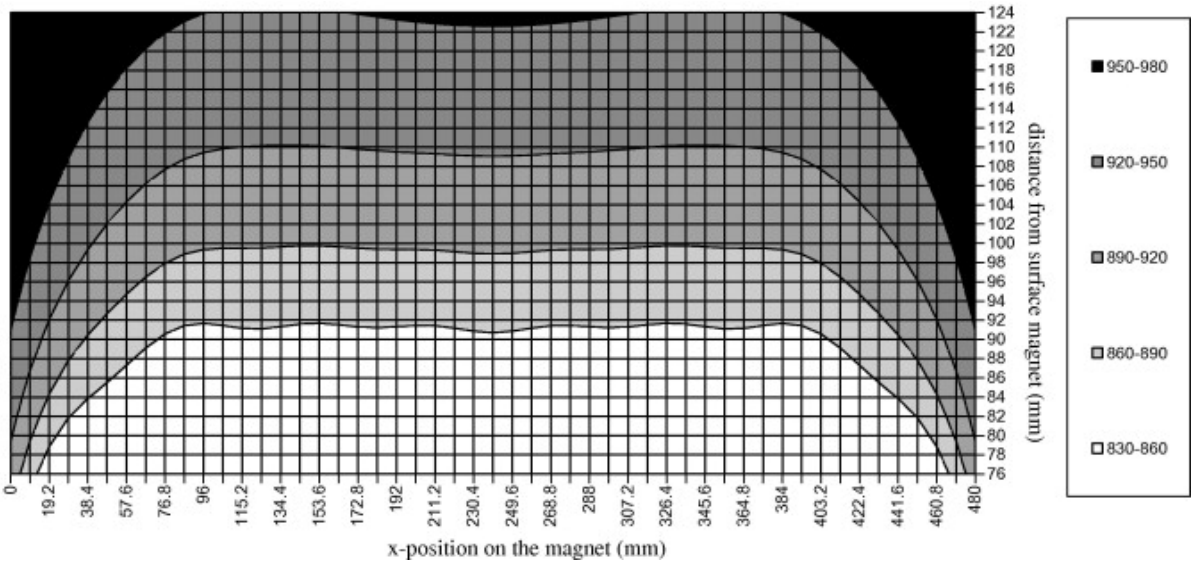

Figure 1.4: An example of the density gradient in a MDS for plastics with the magnet at the bottom, taken from [55].

The (effective) density ($\rho_{apparent}$) a particle feels depends on several parameters. Most important during operation is the distance from the magnet (z). Other variables include the original density of the liquid (ρ), the magnetisation of the liquid (M), the strength of magnetic induction at the surface of the magnet (B_0), the wavelength of the field (w) and gravity (g) [59].

$$\rho_{apparent} = \rho + \frac{2\pi M B_0}{gw} e^{-2\pi z/w} \tag{1.1}$$

Two limitations for accurate sorting regarding the feedstock can be found. First of all, it is not possible to sort magnetic particles on their density as they will be attracted to the magnet. The magnetic particles either have to be removed beforehand (as a pre-processing step) or are collected during the MDS process as a magnetic, instead of density, fraction. Secondly, care must be taken to avoid the formation of air bubbles on the particles as these will influence the density of the particle [59–61]. This can be achieved through steaming or boiling the feed particles with tap water which deposits a thin layer of water and calcium carbonate [62].

MDS is already a technology with proven success. It has been applied to a multitude of feedstocks including vegetable seeds, bottom ash from incineration and plastics [55, 63, 64]. Furthermore in the case of plastics, a commercial scale has been achieved by the Umincorp company [65].

1.3. Material flow analysis (MFA)

Material/substance flow analysis (MFA/SFA) is a non-standardised analytical method based on the mass-balance [66]. It is used to quantify the stocks and flows of materials in a pre-defined system (both by geography and time) [67]. The mass-balance exploits the conservation of mass (what flows in must leave again or accumulate) to analyse, visualise and predict the behaviour of the materials.

In an MFA, there are processes, stocks and flows (see figure 1.5). A process is an operation where the material is created, changed or used (e.g. manufacturing, consumption or stockpiling) and is represented by a square box [68]. A stock is a special process where (a part of) the material stays within the process for longer than the time step of the model (e.g. a house on a yearly timescale) and is represented as a rectangle within the process box [66]. A flow is a movement of the material between two processes and is represented by an arrow [68]. It should also be noted that a process/stock always uses a non time-dependent unit (e.g. kg of iron or number of TVs), while a flow is time-dependent (e.g. tons of concrete per year) [66].

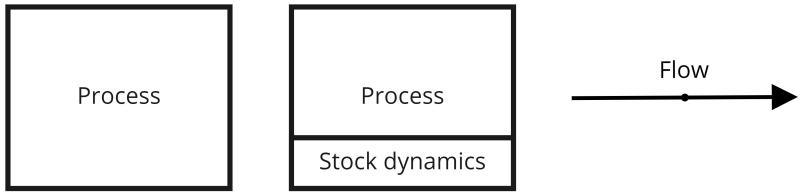

Figure 1.5: The representations of a process (left), stock (middle) and flow (right) in a material flow analysis (MFA).

An MFA model can either be accounting, static or dynamic in nature. An accounting model is purely based on historical data and the principle of mass-balance within processes. A static model introduces causality within processes using Transfer Coefficients (TC), which tell the process what fraction of inflow x goes to outflow y [68]. Therefore, not all flows have to be known in advance if enough TCs are known.

Even though accounting and static models might keep track of the size and in/outflows of a stock they do not properly interact with the stock. As these models take the form of a “snapshot” (e.g. one year), the model does not know how its stocks are composed or when an inflow will flow out again in the future (the model does not have a memory). This is not the case in a dynamic model, where time does play a role [69]. The model keeps track of each individual inflow into a stock and when (parts of this) inflow flows out again based on a predefined lifespan [67]. Therefore, a better understanding of the flows can be achieved. Furthermore, it is even possible to go beyond the historical data to future periods for prediction/exploration [67]. However, dynamic modelling does have some disadvantages such as requiring historical data for multiple years, lifespan distributions and a better understanding of the driving forces of the flows [66].

1.3.1. Scenarios

Even with the usage of stock dynamics it will not be possible to accurately predict the future. For instance, it is near impossible to predict unexpected events (e.g. Covid-19 pandemic) or completely understand the complexity of human society. However, it is possible to create several potential futures called scenarios which present paths humanity can take [70]. By carefully choosing the input parameters of these scenarios it is possible to create a “realistic” scenario (usually called Business as Usual or BAU). However, the technique is probably best for creating best and worst case scenarios where significant deviations from the current status quo are taken. All three of these types will be explored in this research.

1.3.2. Uncertainty and sensitivity

One of the major drawbacks of MFA is that it is deterministic in nature as it uses the mass-balance. This means that it does not take variability or uncertainty into account [71]. This can give a skewed image of reality as a lot of assumptions and simplifications are usually made for an MFA. One of the ways to investigate and evaluate this problem is a Monte Carlo uncertainty analysis [72]. During a Monte Carlo analysis multiple runs (> 1,000) are performed where all the input variables of the model are randomised. The input variables can use multiple statistical methods for randomisation including

normal distributions, estimates by the researcher and triangle functions [73–75]. This will provide a range of outputs which in turn can be statistically analysed for its variability showing how robust the system and its data inputs are. Furthermore, it can also show the impact of each individual input variable.

1.4. Critical raw material analysis

As mentioned before, critical raw materials (CRMs) suffer from supply restrictions while being of great economic importance. They are often used in high-tech applications (e.g. electronics or green technologies) and their demand is expected to increase 20 fold by 2030 [76, 77]. At the same time, their production is often coupled to other materials as they are mined as a by-product [15]. Furthermore, recycling rates tend to be poor as well due to low concentrations [78]. Therefore, CRMs have been a rising topic in the last couple of decades.

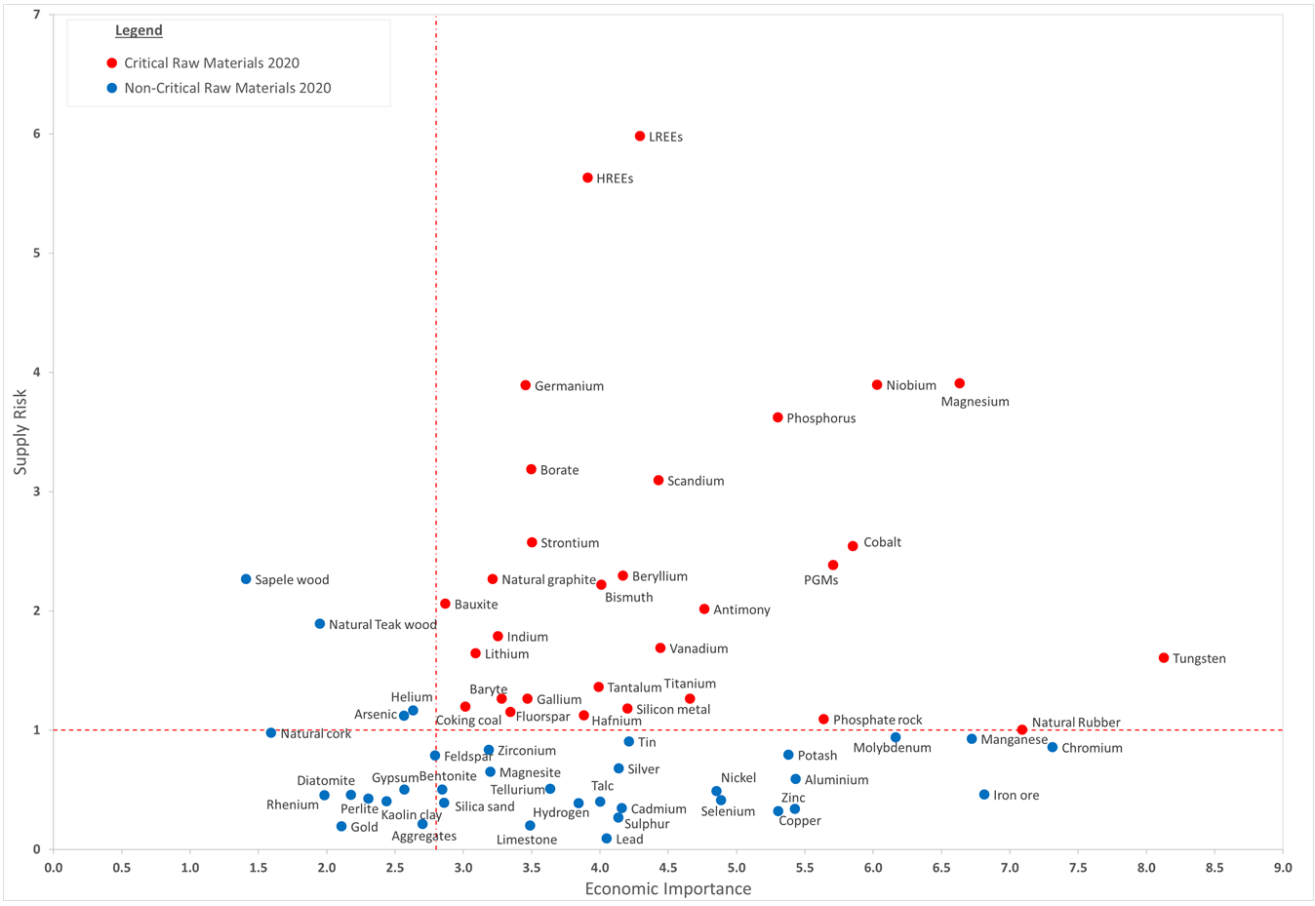

Figure 1.6: The EU's critical raw materials according to the 2020 EU report [79].

This interest in CRMs has also resulted in methods to identify, analyse and track CRMs called critical raw material analysis. A CRM analysis is usually performed as a form of risk assessment and multiple methods have joined the scene with different scopes, goals and approaches [80]. One of the most popular methods is the supply risk (SR) and economic importance (EI) two axis system [81]. A potential CRM is scored on each axis and is deemed critical if it scores higher than a preset threshold on both axes or if an overall score is high enough [80, 82]. However, other forms do exist such as the three axis system developed by *Graedel et al.* which also includes environmental impacts in addition to the original two [83].

1.4.1. The EU's CRM methodology

The EU is currently one of the major leading parties in CRM analysis. Back in 2011 the EU published their first report on critical raw materials within the EU and has updated these every three years (2014, 2017 and 2020) [79, 84–86]. This has resulted in a standardised and adopted methodology using the two axis system [87].

Economic importance (EI)
The economic importance (EI) axis shows the EU's economic dependency on a material. Materials that play an important role in the EU's economy tend to score highly on this axis. For instance, sapele wood is not deemed critical due to its low economic importance (1.4) even though its supply risk (SR) score is high enough for criticality (2.3). Yet, a material does not necessarily have to be used in great quantities to score highly as even a small quantity can be essential for a product.

$$EI = \sum_{s} (A_s * Q_s) * SI_{EI} \tag{1.2}$$

As can be seen in equation 1.2, the EI score is composed of three main variables. The first two are calculated for each NACE sector of the EU's economy and summed into one value. These two are the share of end use of a raw material (A_s) and the sector's added value (Q_s). This score is combined with the economic substitution score (SI_{EI}), which is dependent on the cost-performance of potential substitutes.

Supply risk (SR)
The vertical axis in the EU's criticality method is SR. Supply risk shows how likely a material is to suffer a potential supply disruption. For instance, if all material production originates from a single mine the SR is high as any disruptions in this location will stall all supply. SR is broken into multiple variables that combine to the SR score according to formula 1.3. The SR is applied to the most vulnerable/bottlenecked step in production (usually extraction, but refining is also possible).

$$SR = \left[(HHI_{WGI,t})_{GS} * \frac{IR}{2} + (HHI_{WGI,t})_{EUsourcing} * (1 - \frac{IR}{2}) \right] * (1 - EoL_{RIR}) * SI_{SR} \tag{1.3}$$

Import Reliance (*IR*) is a variable that shows how dependent the EU is on external production. Thus, a material which is not sourced from within the EU will have an *IR* of 1, while an *IR* of 0 means that all consumption is sourced from within the EU. If the EU is a net exporter, *IR* will be limited to 0.

$$IR = \frac{import - export}{domestic\ production + import - export} \tag{1.4}$$

The second variable is the HHI_{WGI} which is the Herfindahl-Hirschman Index scaled with the World Governance Index of the countries in question. This variable shows how concentrated the production (S_c) of the material is, corrected for the countries' governance (WGI_c) and trade restrictions (t_c). This variable is calculated for global sourcing (*GS*) and EU sourcing ($EU_{sourcing}$).

$$HHI_{WGI} = \sum_{c} (S_c)^2 WGI_c * t_c \tag{1.5}$$

The most relevant variable for this thesis is the End-of-Life Recycling Input Rate (*EoL-RIR*). This variable shows the ratio between reused old scrap (End-of-Life products) and total consumption. As the EU assumes these secondary materials do not yield any supply risks, this factor acts as a reducing factor on the total SR. Furthermore, it also indirectly shows the EU's dependency on primary production. It is

important to note that only old scrap (end-of-life) is taken into account and any new scrap (production scrap) is not counted.

$$EoL_{RIR} = \frac{Old\ scrap\ input}{Primary\ material\ input + Old\ scrap\ input} \tag{1.6}$$

The last variable is the supply risk Substitution Index (SI_{SR}), which shows how effectively the material can be substituted in the case of a supply restriction. This score is based on the worldwide production (scale and if it is a by-product) and criticality of the substitute.

1.5. Energy consumption

Back in 2015 the production of precious metals comprised 0.59% of all carbon emissions worldwide [88]. Even though this is only a small amount compared to other materials such as steel (8.68%) and concrete (7.06%), the energy intensity and carbon emissions per kg is significantly higher. For instance, the embodied energy in 1.0 kg of primary produced gold is between 240,000 and 265,000 MJ, compared to only 25 - 28 and 1.0 - 1.3 kg MJ/kg for low carbon steel and concrete, respectively [89]. Therefore, reducing the emissions generated by the production of these materials through recycling should be explored.

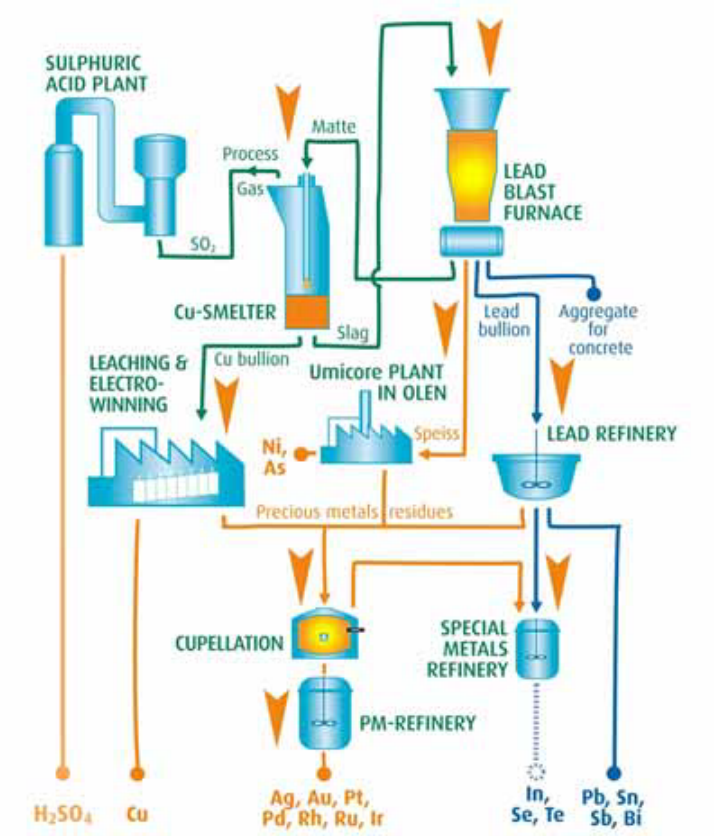

Figure 1.7: Umicore's precious metal recycling plant for E-waste [90].

Currently the main recycling method employed for WEEE is pyrometallurgical recycling, such as Umicore's precious metal refining (see figure 1.7). Here the discarded PCBs are processed under high temperatures (> 1,000°C). The plastics in the PCBs are burned for the required heat (e.g. 7431 kJ/kg for mobile phones) and the metals are extracted from the slag [91]. However, this method is energy intensive and causes the loss of the plastics as a potential material. Therefore Peacoc aims to instead

employ less energy intensive hydrometallurgical methods instead [92].

1.6. PCB grading

As this thesis only focuses on low to medium grade PCBs, it should be properly defined what falls under this category. Prior literature does not seem to adhere to a consistent definition, except that higher grades possess a higher value per kg or have specific origins (e.g. WEEE category) [93, 94]. For instance, *Goosey and Kellner* define medium grade PCBs as £2.74 per kg and *Bigum et al.* define high grade PCBs as originating from category 3 or 4 (old WEEE classification system) [95, 96].

In this report, grade will be defined using the origin method with the smallest unit being product categories (see appendix A.2) as defined by the United Nations University [97]. All products within the WEEE category II, IV and V will be investigated with a couple of exceptions. Unu keys 303 (Laptops) and 307 (Professional IT) will be excluded as these are deemed to high grade, while 501 (Small lighting equipment), 506 (Houshold Luminaires) and 507 (Professional Luminaires) will be ignored due to a lack of PCBs in the products. Furthermore, unu key 2 (PV panels) will also not be taken into account as these are out of scope for the thesis.

1.7. Naming hierarchy

This thesis tackles the topic of WEEE on multiple levels. Therefore, a clear (naming) hierarchy has to be established how all the different levels encompass and interact with each other. This allows aggregated calculations such as precious metal flows on the level of product and their relations.

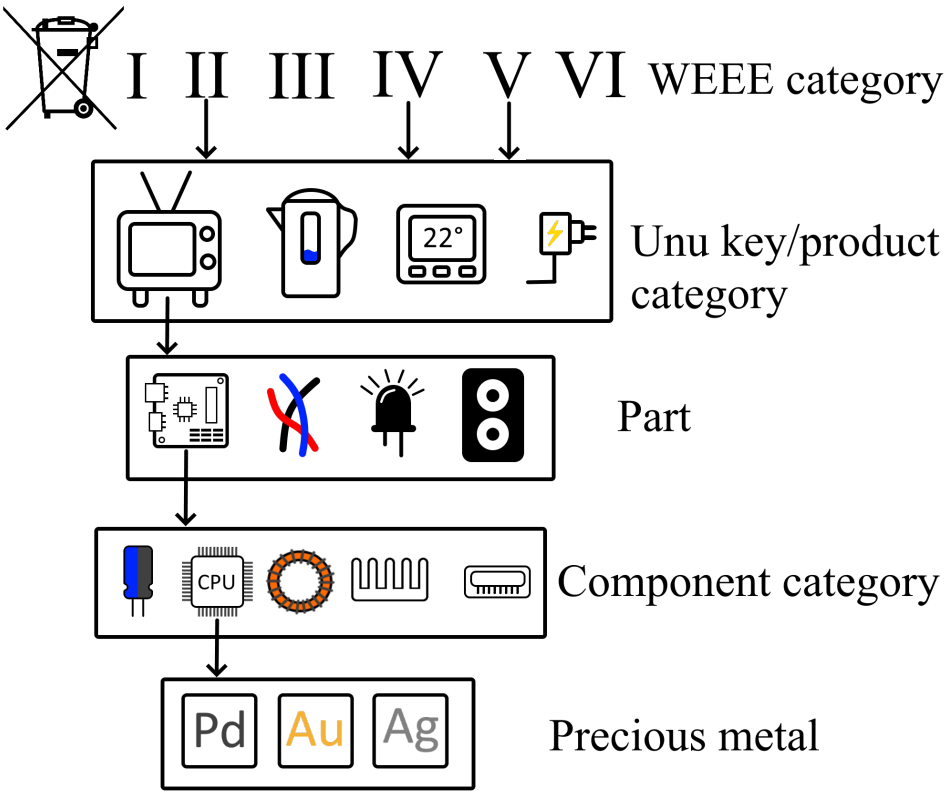

Figure 1.8: The hierarchy of the different parts used in this system.

Out of the six WEEE categories only three will be investigated (II, IV and V). These WEEE categories are composed of multiple product categories (also known as unu keys). These include but are not

limited to CRT TVs, small household electronics and speakers. Each of these products is then broken into different parts of which only one will be further explored (PCBs). The PCB can be further broken down into multiple component categories (20 in total), such as Central Processing Units, Heatsinks and Plastic connectors with pins and others (see table 2.1 in section 2.1.1). Lastly, each of these components is comprised of a mixture of (precious) metals.

1.8. Research questions

As stated in the introduction, this thesis will focus on the urban mining potential of precious and critical materials from low to medium grade PCBs within the EU using Roll Sorting, Magnetic Separation and Magnetic Density Separation under different scenarios. Therefore, the main research question this report seeks to answer is the following:

To what extent can the waste separation technologies Roll Sorting (RS), Magnetic Separation (MS) and Magnetic Density Separation (MDS) improve the sustainability and circularity of precious and critical metals in the European Union (EU) during the recycling of low and medium grade PCBs from E-waste?

This main research question has been broken into several sub-questions:

- *Which components and precious metals can be found in low and medium grade PCBs from WEEE?*
- *How effectively can RS, MS and MDS separate components from low and medium grade PCBs as a feedstock?*
- *How much precious metals can be recovered in the EU from low and medium grade WEEE PCBs in the year 2050 using separation technologies?*
- *How variable are the precious metal flows under different scenarios and due to model sensitivity?*
- *To what degree can the separation system improve the recovery of critical raw materials and what would the impact on their criticality be?*
- *What are the total energy requirements per kg to produce precious metals with the new separation pathway compared to primary production and conventional recycling?*

These research questions will be answered in the sequence set above. Chapter 2 will cover RQ 1 and 2 focusing on the technical aspects of the thesis. In chapter 3 material flow analysis (MFA) will be employed to answer RQ 3 and 4. This is followed by chapter 4 and 5 which will answer RQ 5 and 6, respectively. Lastly, chapter 6 will conclude the research by answering the main research question and providing recommendations for further research.

2

Novel separation technologies

This chapter will tackle the technical aspects of the thesis by employing experimental research to answer the first and second research questions which are:

Which components and precious metals can be found in low and medium grade PCBs from WEEE?

And

How effectively can RS, MS and MDS separate components from low and medium grade PCBs as a feedstock?

These two RQs will be answered in sequence, starting with RQ 1 in the next section followed by RQ 2 . All of the experimental lab work was performed at the Resources & Recycling section at the Civil Engineering and Geosciences faculty of the TU Delft.

2.1. PCB composition

In order to answer the first research question a mixed approach of technical, literature and digital research was performed. From TREEE (a partner in the Peacoc project) the Resources & Recycling group received a batch of 36 Flat panel displays (FDP) and 44 Cathode-ray tube (CRT) PCBs. These PCBs were removed from televisions and monitors gathered in Italy and still had (the vast majority) of their components. However, some of the PCBs were already slightly damaged as can be seen in figure 2.1 and 2.2. Two samples groups, 14 FDP and 3 CRT PCBs, were created from the original batch. Care was taken to make this sample representative in regards to the size and position of the boards in their storage container. This was needed as some smaller PCBs had fallen to the bottom between the bigger boards. More FDP than CRT PCBs were selected as these would later also be used for the separation experiments. Lastly, one extra FDP PCB was dismantled (but not added to the sample) to act as a *Test sample* for determining throughput and testing equipment without contaminating or damaging the actual samples.

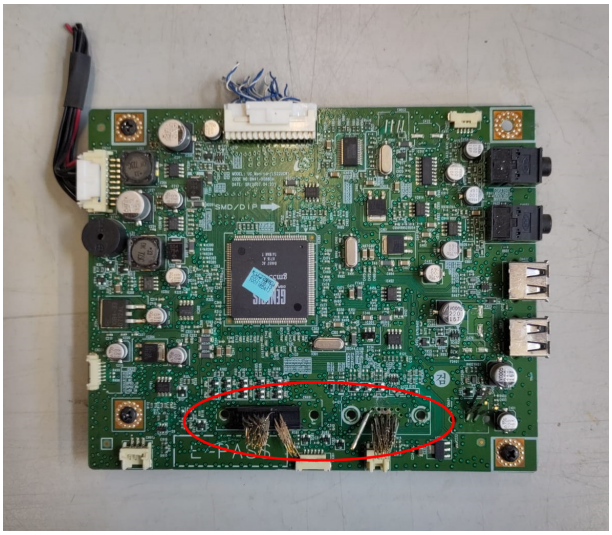

Figure 2.1: An example of a previously damaged FDP PCB where some components were partially removed (red circle).

Figure 2.2: An example of a damaged CRT PCB, direct connection is marked by the red circle.

Component liberation

Three main methods were used to remove the components from the PCBs. These were mechanical (using a screwdriver and wrench pliers), thermal (using a heat gun at 400 - 600°C) and a combination of the two. Whenever possible the lower temperature setting on the heat gun was used to avoid melting the plastics. Furthermore, high temperatures were usually only applied to the bottom of the PCB to just melt the solder and not the component itself. As thermal degradation of the components was still possible, the liberation was performed in a fume hood to avoid potentially inhaling toxic gases. All the components were gathered together in a metal pan (see figure 2.3). Lastly, the fume hood was dusted for any loose components that missed the pan.

Figure 2.3: An example of a filled collection pan from the component removal step.

It should be noted that direct connections (see red circle in figure 2.2), were not removed and have thus not been taken into account for CRT PCBs. This choice was made as they have a negligible weight compared to the components, were hard to remove and do not contain precious metals.

Sorting and weighing of the components

After component liberation, the mixture in the pan was sorted into 20 different categories (see table 2.1). These categories were determined by partners in the Peacoc project based on the function, size and metal concentrations. The components were separately sorted for each sample. If the component could not be confidently identified as one of the categories it would be placed in the *Other* category (e.g. loose pins, screws or stickers). In total 170 trays with components, spread over the 14 FDP samples, were collected for an average of 12.14 component types per FDP board. This was less than the theoretical maximum of 280 trays for FDP as not all component categories were found on every PCB. In the case of the three CRT boards slightly less component types (34 trays) were collected per PCB (11.33). After sorting, the bare PCBs and contents of each tray were individually weighed to determine the weight distribution of the original PCBs. Furthermore, the number of components were also counted to calculate the average weight per component category.

Component composition of all products

As stated in the research questions, one of the goals is to collect data on all low to medium grade PCBs, not only FDPs and CRTs. Therefore, a digital assessment was performed for the other product categories using the FDP or CRT data as a proxy depending on similarity. For each product category three pictures of PCBs were found on the internet and the number of components for each component category was counted (see appendix A.2). This quantity of components was then converted into mass by multiplication with the average weight, resulting in a weight distribution. The specific products within a product category could differ, for instance product category 203 (hot water) included a water kettle and two different types of coffee machines.

Metal composition

The last step was to convert the component distributions to metal distributions. As a part of the Peacoc project one of the partners (ULQ) measured the concentrations of Pd, Au, Ag, Cu, Al and Sn for each component type for FDP PCBs. This data was then used to calculate the precious metal compositions of all the component types. It should be noted that the concentrations of *Large steel and aluminium cases* was set to zero as problems with measurements were noted by the partners in the Peacoc project.

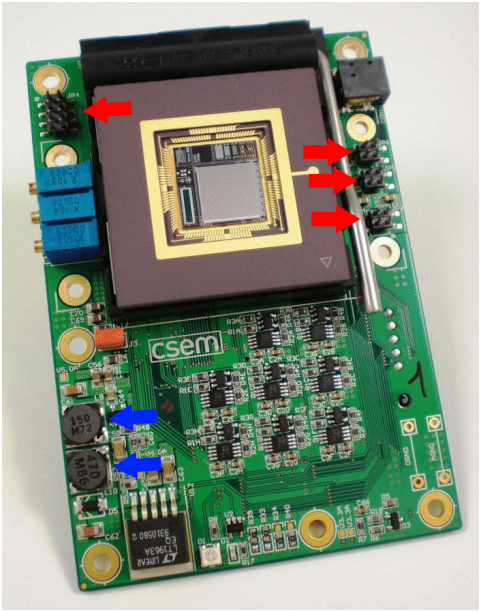

Figure 2.4: An example of counting the components on a camera PCB, with red arrows counting the plastic connectors and blue arrows the inductors. Picture taken from [98].

2.1.1. Results

After processing all the samples (14 FDP and 3 CRT) a couple of general observations about the PCBs could be made. First of all, the FDP PCBs had a large variability in size ranging from 40 to 450 cm^2. This variation was smaller for the CRT samples, which were between 220 and 500 cm^2. Secondly, a difference in (bare) PCB properties was observed between CRT and FDP PCBs. Under heating the CRT PCBs would often ignite/char which was not the case for the FDP PCBs. This is likely due to the introduction of new safety standards (e.g. brominated fire retardants) in electronics to avoid fires [99]. Furthermore, during the mechanical removal of components the CRT PCBs would often break/rip. Lastly, all the CRT boards were beige while the FDP boards had the seemingly standard green colour.

Component composition

As table 2.1 shows, the average weight of FDP components is significantly lower than the ones from CRT PCBs. For example, the average weight of an *IC chips and transistor* from FDP is around half (0.375 grams) compared to the CRT (0.805 grams). This decrease is a direct result of the miniaturisation of PCBs and their components. Due to advances in manufacturing technologies (e.g. CPU wafers), components are smaller in size on the newer FDP PCBs [100, 101]. This change can be observed for almost all categories. Two interesting exceptions are the *MLCC + Ta capactiors* and *Small transistors and small IC chips*, which have not decreased in weight. This is likely due to the fact that these technologies have not inherently changed (nor their weight), but are more prevalent on FDPs compared to CRTs.

In regards to weight distribution, a couple of main observations can be made. First of all, the bare PCB encompasses almost 50 wt% for the FDP PCBs compared to only 27 wt% for CRTs. This is due to two main factors, the average weight for the bare PCBs had a slight increase (from 86 to 106 grams) and the previously mentioned decrease in component weight. Even though there are (usually) more components on the FDP PCBs their total weight is lower, thus increasing the bare PCB weight fraction. It can also be seen that a select number of components comprise the majority of the weight. For instance, *Large steel and aluminium cases* embodies over 11 wt% of the total weight. Furthermore,

a shift in technology is seen. Two old technology components, *Blue capacitors* and *Resistors*, have almost completely disappeared in the (technologically) newer FDP PCBs. These have likely been replaced by the small form factor *MLCC + Ta capacitor* category, which despite the name also includes resistors. Lastly, an increase in connectors (VGA, USB, SCART etc.) shows the increased versatility of the modern FDP technology.

Table 2.1: The weight distribution and average weight per component for FDP and CRT PCBs.

	FDP (14 PCBs)		**CRT (3 PCBs)**	
Component category	**Weight distribution**	**Average weight (g/unit)**	**Weight distribution**	**Average weight (g/unit)**
Bare PCB	48.38 wt%	105.727	27.17 wt%	86.207
Central Processing Units	0.70 wt%	1.653	N.A.	N.A.
IC chips and transistors	3.98 wt%	0.375	3.55 wt%	0.805
MLCC + Ta capacitors	1.63 wt%	0.013	0.28 wt%	0.012
Small transistors and small IC chips	0.29 wt%	0.016	0.09 wt%	0.017
Blue and black rectangular connectors (VGA)	1.40 wt%	8.572	N.A.	N.A.
Rectangular connectors (USB, HDMI etc.)	3.30 wt%	1.713	2.55 wt%	8.077
Golden connectors (RCA)	0.25 wt%	7.530	N.A.	N.A.
Round gray connector (RCA)	2.08 wt%	4.903	N.A.	N.A.
Plastic connectors with pins and others	1.45 wt%	0.425	0.65 wt%	0.779
Large steel and aluminium cases	11.33 wt%	19.261	N.A.	N.A.
Inductors and transformers	5.08 wt%	1.495	34.68 wt%	11.381
Al electrolytic capacitors	4.89 wt%	0.389	15.09 wt%	2.112
Blue capacitors	0.12 wt%	0.305	3.09 wt%	0.841
Resistors	0.17 wt%	0.379	3.37 wt%	0.472
Quartz resonators	0.51 wt%	0.578	0.05 wt%	0.520
Heatsinks	4.60 wt%	10.820	6.80 wt%	12.938
Cables	0.50 wt%	7.600	1.49 wt%	7.075
Connectors of plastic with golden pins	3.02 wt%	6.160	N.A.	N.A.
Connectors of plastic with silver pins (SCART)	3.53 wt%	10.806	N.A.	N.A.
Other	2.77 wt%	Inconsistent	1.13 wt%	Inconsistent

Palladium

As can be seen in figure 2.5, no specific component is dominant in regards to palladium for FDP PCBs. The largest share (21 wt%) is found in *IC chips and transistors*. After this category the share drops and is followed by eight other categories. This result was inconsistent with literature, as multiple papers cited high concentrations (0.05 - 0.95 wt%) of palladium in *MLCCs + Ta capacitors*, which was two orders of magnitude higher than ULQ's results [102–105]. On average a total of 9.27 mg of palladium was found per kg components. Therefore, it can best be concluded that palladium is (roughly) equally distributed amongst the components and no specific target can be found.

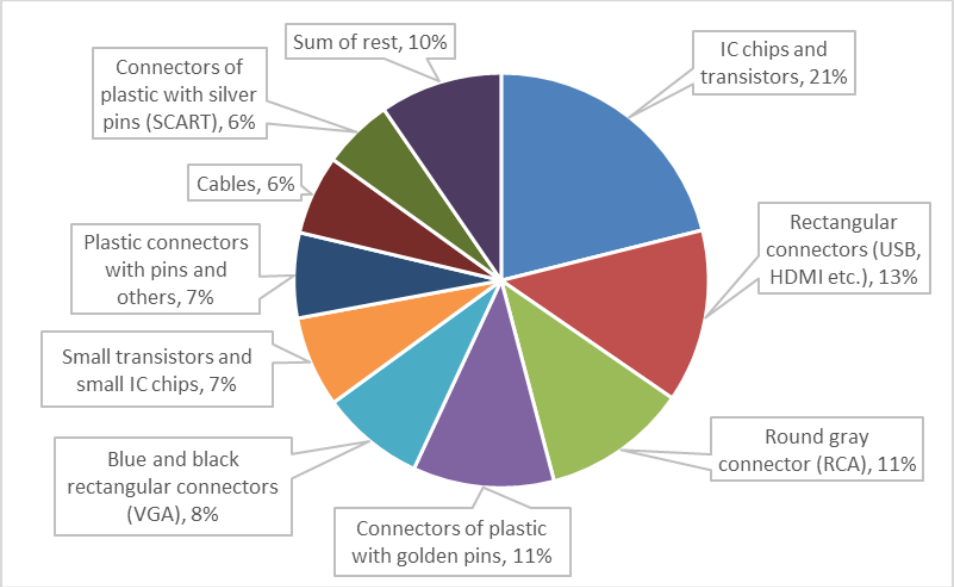

Figure 2.5: The palladium distribution over the different components in FDP PCBs. The categories with less than five wt% have been combined.

Gold

The precedent set by palladium does not hold for gold as can be seen in figure 2.6. By combining just three components (*IC chips and transistors*, *Central processing units* and *Connectors with golden pins*) more than 87 wt% of the gold can be captured. Moreover, almost half of the gold is located in just the *IC chips and transistors*. Thus if the goal is to capture gold, one should focus on these three categories for maximum efficiency. In total an average of 67.48 mg of gold was found per kg of components.

Silver

Silver shows a similar pattern to gold (see figure 2.7). The majority of silver (67 wt%) is located in the *MLCC and Ta capacitors*. Only minor fractions can be found in the other categories such as *IC chips and transistors* (15 wt%), *Central Processing units* (5 wt%) and *Plastic connectors with pins and others* (3 wt%). This once again shows that one should focus on a select number of components to collect all the silver found in the components (489.66 mg per kg components).

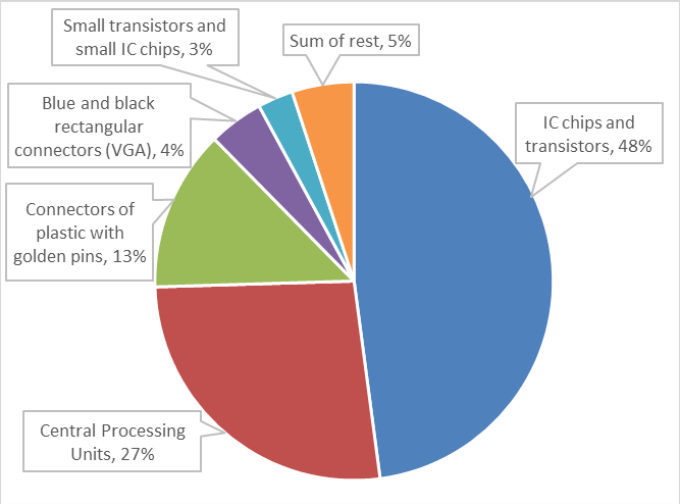

Figure 2.6: The gold distribution over the different components. The categories with less than two wt% have been combined.

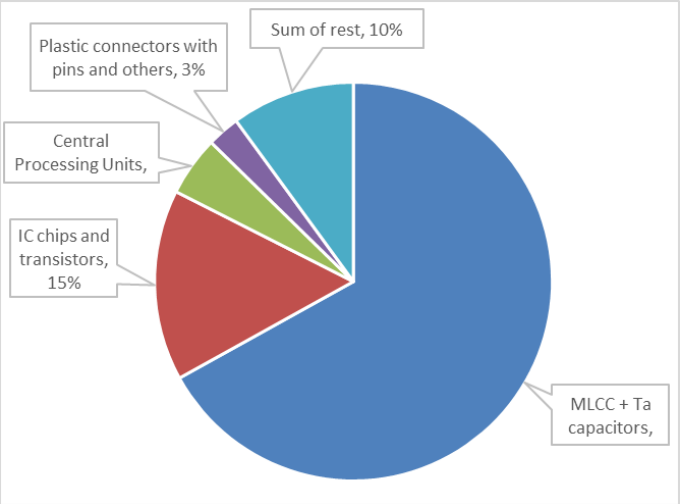

Figure 2.7: The silver distribution over the different components. The categories with less than two wt% have been combined.

Bare PCB

The bare PCB was not taken into account in the previous calculations as it would already be separated during the dismantling step and not join the other components in the separation system. However, this does not mean it is not of interest. According to the data gathered by the Peacoc project, the bare PCB actually possesses more than five times the amount of palladium the components have (82% of total). This provides an explanation for the previous palladium disparity in the *MLCCs + Ta capacitors*. It might be possible that the *MLCC + Ta capacitors* were not correctly removed from the PCB leaving the palladium contacts on the bare PCB. This explanation might also hold for the gold and silver as these were also found in surprisingly high concentrations (13% and 78% of the amount found in the components) on the bare PCB.

2.1.2. Target components

As has been shown in this section, not all components are created equal in regards to precious metals. Some components have no precious metals (e.g. *Inductors and transformers*), while others are rich in a specific precious metal (e.g. *MLCC + Ta capacitors* in silver) or overall valuable (e.g. *IC chips and transistors*). Therefore, the decision was made to focus on only a select number of components (referred to as “Target components”) for the separation technologies:

1. *Central Processing Units (CPUs)*
2. *IC chips and transistors*
3. *MLCC + Ta capacitors*
4. *Small transistors and small IC chips*
5. *Connectors of plastic with golden pins*

By choosing these targets it should be possible to capture 42.97 wt% of the palladium, 90.64 wt% of the gold and 90.93 wt% of the silver from the components. At the same time, they only encompass around 18.66 wt% of the total weight, thus resulting in a significant increase in precious metal concentrations.

2.2. Roll sorter (RS)

The roll sorter (see figure 2.8) is the first novel technology that was investigated in this thesis. As mentioned in 1.1.1, the RS should be able to sort thin objects and is thus expected to effectively sort CPUs and Chips.

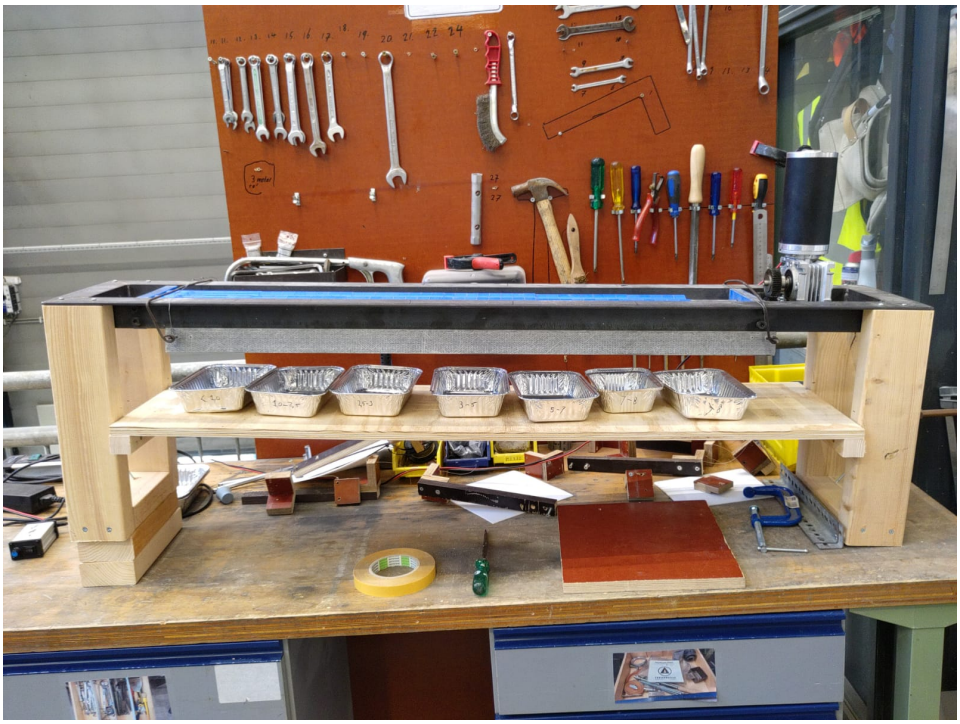

Figure 2.8: The roll sorter used during the experiments.

The roll sorter was custom made for the Resources and Recycling research group for a previous project, but was still suitable for this research. The two rollers are made from PE plastic and are driven by a motor and speed controller from Tandwiel.net. Furthermore, the rollers are made using a modular system where multiple sizes can be slotted on the same roller to provide a multitude of different sieve sizes. On this design the sieve sizes were 1.0, 2.5, 3.0, 5.0, 7.0 and 8.0 millimetres in that sequence. This allowed a total of six size categories to be sieved for (< 1.0, 1.0 - 2.5, 2.5 - 3.0, 3.0 - 5.0, 5.0 - 7.0 and 7.0 - 8.0 mm) and one undetermined (> 8.0 mm). The FDP PCBs were chosen as the waste feed for these experiments as they were deemed more relevant in potential future applications than the CRT PCBs due to their continued production.

Determining the operating conditions

The sorter has two main operating variables which can be changed, the speed and angle of the machine. Two angles were investigated (1.84° and 3.68°) by increasing the left side of the machine using blocks of wood. The higher angle (3.68°) was chosen as observations showed that components would more often get stuck (not moving forwards on the sieve) on the shallow angle without major differences in sorting efficiency.

For the determination of the engine power two speedtests were performed at 60 and 120 RPM. Six large components (transistor, inductor, electrolytic capacitor, plastic connector, USB port and IC chip) were taken from the testing sample and were timed three times on their throughput (see table 2.2). These components were chosen as they are wide and would take the longest to be sorted, thus giving a lower throughput limit. Based on these results the higher speed setting (120 RPM) was chosen.

Table 2.2: The average throughput times from the speedtests.

Component	Sieve size	120 RPM (s)	60 RPM (s)
Transistor	5.0 - 7.0 mm	19.25	31.17
Inductor	> 8.0 mm	20.07	33.50
Capacitor	> 8.0 mm	25.98	49.87
Plastic connector	5.0 - 7.0 mm	16.70	27.21
USB port	> 8.0 mm	24.46	39.11
IC chip	3.0 - 5.0 mm	20.79	13.44

Experiments

After the operating conditions were determined, all the samples were run through the sorter twice. One by one the contents of a tray were emptied and sorted by the sieve. Care was taken to avoid double stacking (a smaller particle being stuck on a large particle) if possible. After all the components from a tray were sieved, each particle size was individually weighed. In the first run the sieved sizes were recombined together for each sample. However, during the second run the resulting sieve sizes were collected separately for later experiments, resulting in an increase from 170 to 397 trays.

2.2.1. Results

As figure 2.9 shows, the majority of components (97%) are captured/sorted by the sieve with only 3 % falling in the > 8.0 mm category. However, the components in the > 8.0 mm category are quite heavy (e.g. 19 grams for *Large steel and aluminium cases*), resulting in only 34 wt% being captured by the machine (see figure 2.10). This points to the fact that this maximum grade size is likely not sufficient and larger sizes should be investigated if the target materials are not properly captured.

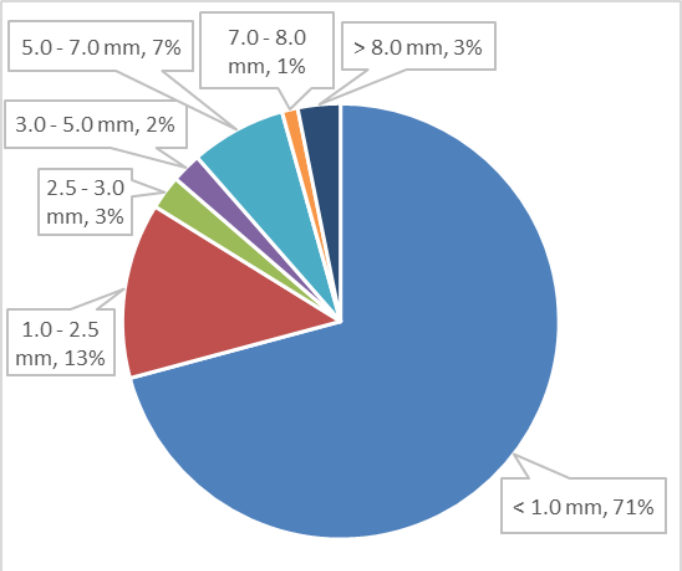

Figure 2.9: The distribution of number of components of the rolling sorter by sieve size (mm).

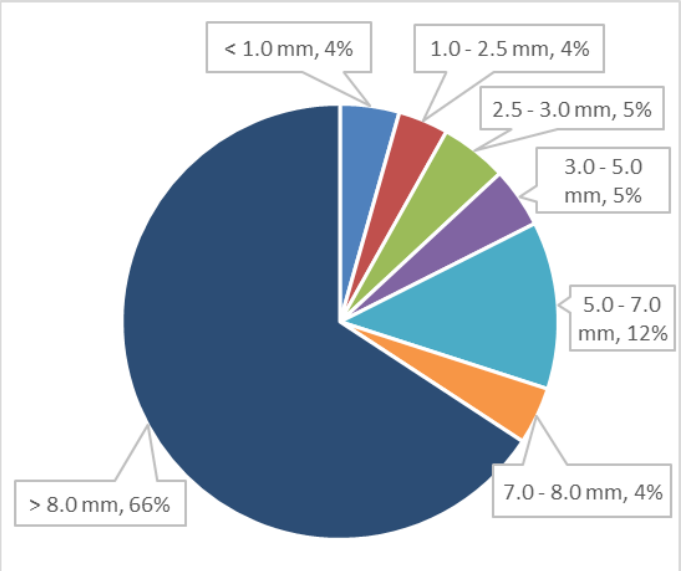

Figure 2.10: The weight distribution of the rolling sorter by sieve size (mm).

Recovery

Complete separation could be achieved for four of the five target components in the sieve sizes below 7.0 mm (see figure 2.11). The two smallest components (*MLCC + Ta capacitors* and *Small transistors and small IC chips*) were predictably found in the smallest sieve sizes, none being larger than 3.0 mm. On the other hand, the *IC chips and transistors* were almost equally distributed (by weight) between the sizes smaller than 7.0 mm. It should be noted that the number of *IC chips and transistors* in the higher category was lower, but each chips was heavier thus achieving the same total weight. Interestingly enough, the *Central Processing Units* had a very tight size category (1.0 - 5.0 mm), with the majority (60 wt%) falling in the 2.5 - 3.0 mm range. It might be possible to completely specify this category by introducing a category from 2.0 - 4.0 mm.

Unlike the previous four categories, it was not possible to sort the *Connectors of plastic with golden pins* as they are too sizeable with an average thickness of 15 mm. This shows that increasing the sieve sizes might offer additional insights. Furthermore, a small amount of this component type (16 wt%) was captured in the 5.0 - 7.0 mm size. However, these comprised plastic pieces that broke of the rest of the connector, which do not contain any of the golden pins and will thus not be counted as targets for the rest of the report.

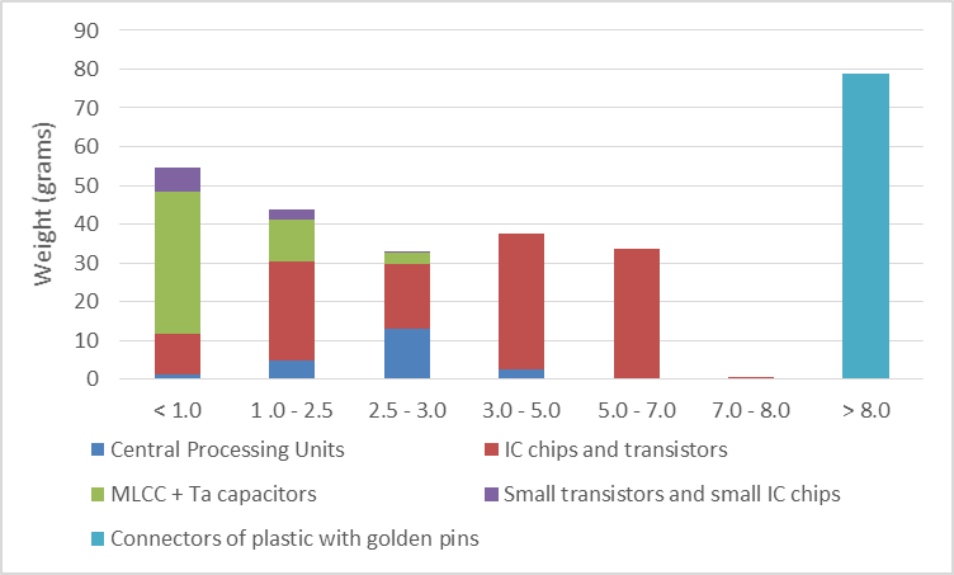

Figure 2.11: The roll sorter's recovery for the target components. Sieve sizes are in mm.

Grade

In regards to grade, the targets once again perform well in the RS, especially below 5.0 mm. As can be seen in figure 2.12, the grade for the targets is high in most sieve sizes, reaching a maximum of 79 wt% for < 1.0 mm. However, the grade does worsen after 2.5 mm due to capturing non-targets. For 2.5 - 3.0 mm this is mostly *Heatsinks* (38 wt%), while 3.0 - 5.0 and 5.0 - 7.0 mm biggest categories are *Al electrolytic capacitors* (9 and 29 wt%, respectively) and *Inductors and transformers* (12 and 11 wt%, respectively). In the case of 5.0 - 7.0 and > 8.0, the grades are bad (17 and 8 wt%, respectively) and need to be improved if possible. Lastly, the grade in 7.0 - 8.0 is negligible as (almost) no targets are recovered at this size and therefore is not of interest.

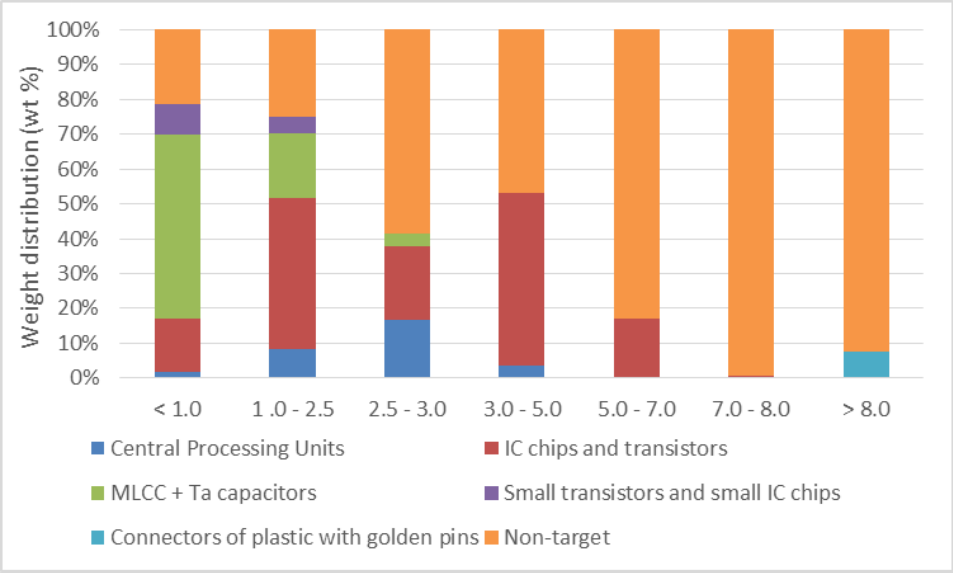

Figure 2.12: The roll sorter's grade at each sieving size. Sieve sizes are in mm.

2.3. Magnetic separation (MS)

The second investigated separation technology was a magnetic separator. This step was required as a pre-processing step to the MDS as magnetic particles cannot be sorted on density in the MDS.

An overbelt magnet owned by the Resources & Recycling group was modified for the experiments (see figure 2.13). A gutter (8 cm wide) was added to the setup in the direction of the magnet at a shallow angle (6°). By placing the gutter at an angle, the distance to the magnet was decreased over distance from 21 to 13 cm thus allowing an increasing magnetic gradient. Furthermore as the magnet consists of two magnets, a (relatively) flat magnetic field exists in the gutter. Lastly, a removable plastic sheet (2 mm) was added to ease the cleaning of small particles.

To determine the components' susceptibility to a magnetic field, each component was sorted into one of three categories (see table 2.3). If the magnetic interaction between component and magnet was strong enough to overcome gravity it would be attracted to the magnetic surface and sorted. The first category (strongly magnetic) was determined by pushing the components through the gutter and collected the strongly magnetic particles. The lightly magnetic components were sorted by holding them at a distance of 6.5 cm from the surface in the middle of the magnet. This placement was chosen as the field is strongest in the middle and some components were close to 5 cm in height. The last category were the non magnetic components which were not picked up by the magnet at any distance.

Table 2.3: The different categories with their minimal and maximum field strength.

Magnetic category	Min. B-field (mT)	Max. B-field (mT)
Strongly magnetic	4.49	33.30
Lightly magnetic	21.70	92.90
non magnetic	N.A.	N.A.

Experiments

All the experiments were performed using the method described above. Furthermore, the previously sorted sieve categories from the roll sorter experiments were used as the feed. This choice was made to observe the combined effectiveness of the Roll sorter and Magnetic separator. Furthermore, it allowed the grades of the targets to be further increased. Once again the sorting categories were separately collected and stored, increasing the number of trays from 397 to 507.

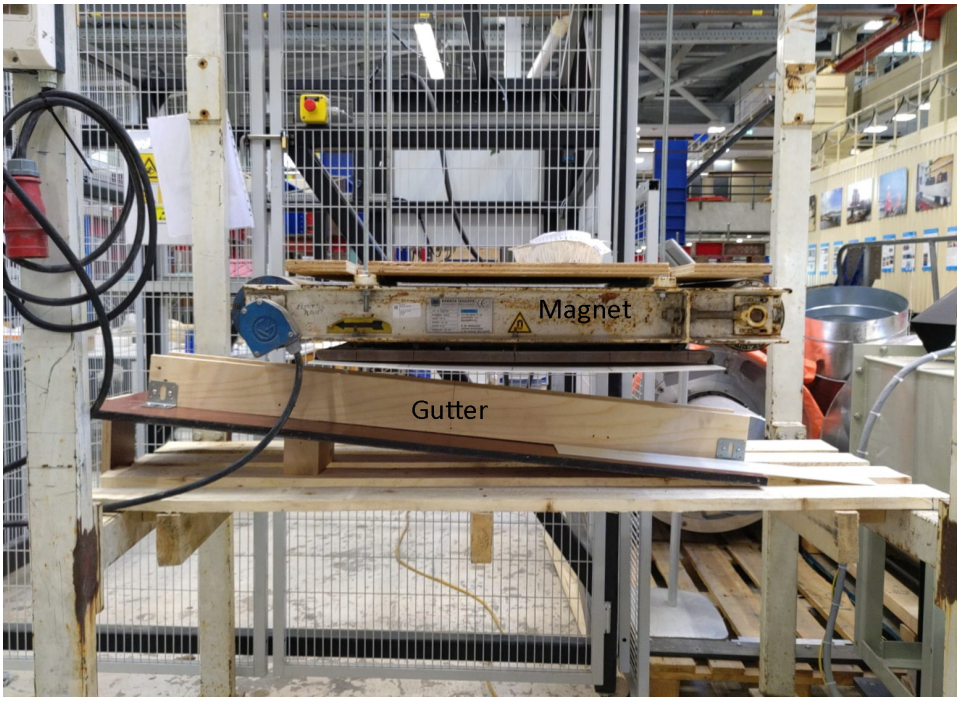

Figure 2.13: The modified overbelt magnet used during the experiments.

2.3.1. Results

As mentioned above, the MS is a continuation of the RS and its results will thus also be presented as such. As can be seen in figure 2.14, the majority (89 wt%) of the targets are non magnetic. However, a sizeable fraction of *MLCC + Ta capacitors* (46 wt%) and *Small transistors and IC chips* (44 wt%) are lightly magnetic and care should be taken to not lose them to achieve maximum recovery. This can best be achieved by collecting both the lightly and non magnetic particles from the smallest sieve sizes (< 1.0, 1.0 - 2.5 and 2.5 - 3.0 mm).

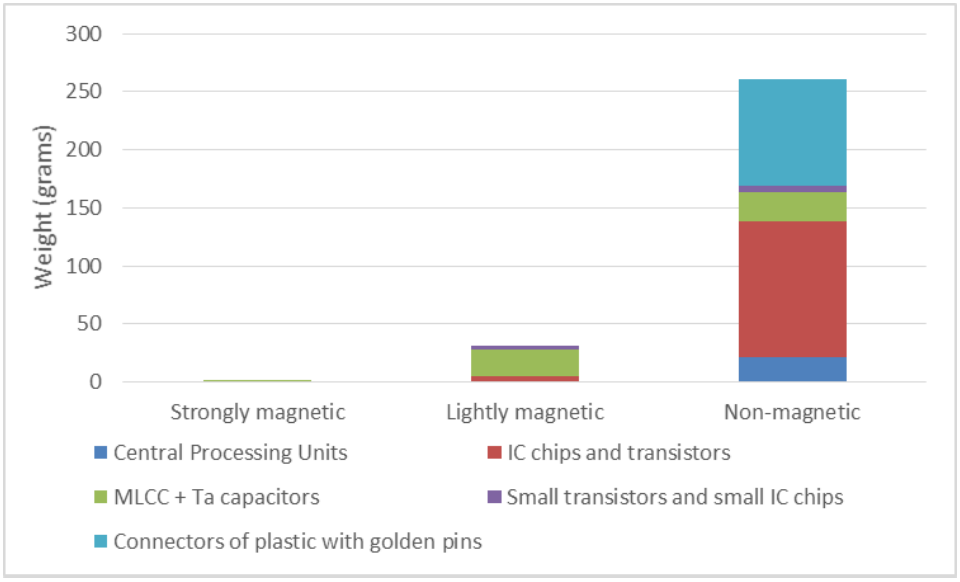

Figure 2.14: The selectivity of the target materials in the magnetic separator.

As can be seen in table 2.4, this problem does not exists for the larger sizes (3.0 - 5.0, 5.0 - 7.0 and > 8.0 mm) where (almost) all targets are non magnetic. By only collecting the non magnetic particles a significant increase in grade should be achievable without decreasing the recovery.

Table 2.4: The weight fraction of target components in each combination of sieve size and level of magnetic susceptibility. N.A. indicates no target components were found in this combination.

Sieve size	Strongly magnetic	Lightly magnetic	non magnetic
< 1.0 mm	76 wt%	95 wt%	72 wt%
1 .0 - 2.5 mm	5 wt%	97 wt%	74 wt%
2.5 - 3.0 mm	N.A.	51 wt%	43 wt%
3.0 - 5.0 mm	N.A.	2 wt%	81 wt%
5.0 - 7.0 mm	N.A.	N.A.	26 wt%
7.0 - 8.0 mm	N.A.	N.A.	2 wt%
> 8.0 mm	N.A.	N.A.	16 wt%

The results from implementing both propositions can be seen in table 2.5. Without a sizeable decrease in recovery (overall recovery is 99 wt%), the grade has either significantly improved (3.0 - 5.0, 5.0 - 7.0 and > 8.0 mm) or stayed similar (< 1.0, 1.0 - 2.5 mm and 2.5 - 3.0 mm). As expected, these increases were especially effective for the larger sieve sizes. No further increases were achieved for the 2.5 - 3.0 mm sieve size as the majority (38 wt%) was composed of non magnetic *Heatsinks* likely made from aluminium.

Table 2.5: The target components' grade improvements after magnetic separation.

Sieve size	Orginal grade	New grade	Share of target components
< 1.0 mm	79 wt%	79 wt%	19 wt%
1 .0 - 2.5 mm	75 wt%	79 wt%	16 wt%
2.5 - 3.0 mm	42 wt%	43 wt%	12 wt%
3.0 - 5.0 mm	53 wt%	81 wt%	13 wt%
5.0 - 7.0 mm	17 wt%	26 wt%	12 wt%
> 8.0 mm	8 wt%	16 wt%	28 wt%

2.4. Magnetic density separation (MDS)

MDS was the last investigated separation technology during this thesis. It is a density based separation technology for non magnetic particles and was used as such (see section 1.2). Similarly to the other machines, an older setup with small modifications was used for the MDS experiments. For previous MDS experiments a three gutter (68 x 11 x 9 cm each) plastic box was created. Previously, the whole gutter had to be drained to determine the results. However, as the components were (relatively) large in size, a (non magnetic) mesh was placed inside the box to ease the removal of components and increase experimental efficiency.

The (level) box is placed on an angled magnet (9°) of 0.6 T at its surface and a wavelength of 0.12 m. Due to the angle, the field strength decreases over the length of the box, thus creating the density gradient. All components are placed into the liquid at the same spot (left side in picture) and will slowly move to the right settling at the correct effective density. Therefore, the components are separated by density over the length of the box.

Experiments

Unlike the previous machines, only one experimental run (one sieve size) was performed, due to time and setup limitations. The 5.0 - 7.0 and > 8.0 mm non magnetic sieve sizes were deemed most interesting. This was due to the fact that they still contained a sizeable share of the *IC chips and transistors*,

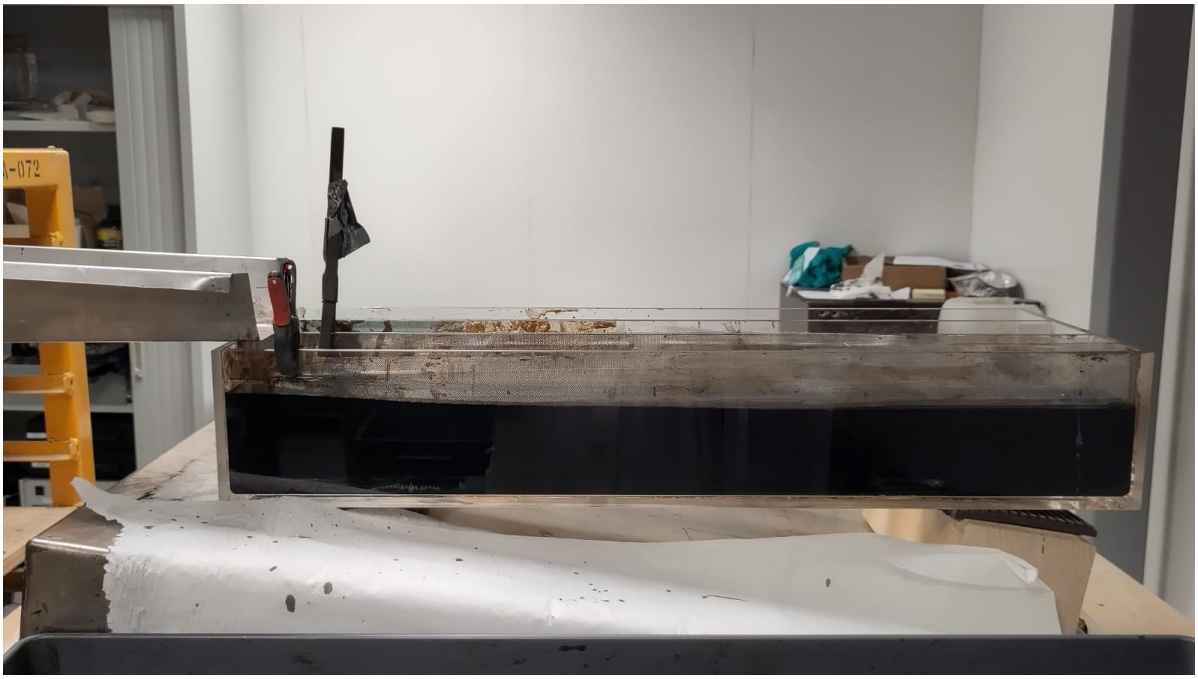

Figure 2.15: The (modified) MDS setup used in the experiments.

and *Connectors of plastic with golden pins*. However, using the current setup for the > 8.0 mm setup was not possible as the majority of components were similar in size to the width of the gutter. This made them unable to freely float and sink at the desired density, making the experiments inconsistent. Lastly, only one magnetic fluid (density of 1.058 kg/m^3 and estimated magnetisation of 4000 A/M) was investigated as it was considered sufficient in creating a separation of the components. This magnetic fluid was a diluted magnetite ferrofluid (1:3) created by Ferrotech.

Several techniques were employed to achieve consistency. As is seen in the figure above, a shaker was used to consistently drop the components from the same height (11.5 cm above the bottom). Secondly, the gutter was always filled to the same level (6.3 cm). This was always measured on the right side of the setup as less ferrofluid would accumulate due to the magnet. Thirdly, all the components were prewetted in boiling water to reduce the effect of air bubbles playing a role in the components' density. Lastly, the experiment was performed twice.

2.4.1. Results

In total nine component categories were investigated in this experiment, of which only one (*IC chips and transistors*) were a target component (see figure 2.16). Therefore, the resulting outflow was determined by the location of this target which resulted in a density range of 5100 to 2700 kg/m^3 (10 to 30 cm in the setup). The MDS significantly increased the grade of the targets from 26 to 58 wt% (see figure 2.17). The increase can best be attributed to the removal of *Al electrolytic capacitors* (31 wt% of the original weight). They were removed in two ways. A part of them were still slightly magnetic, while the rest all settled within the 2300 - 1900 kg/m^3 range (35 - 45 cm in the setup). The magnetic capacitors still had parts of their connectors, which were magnetic in nature. However, these weigh so little that they were not enough for removal during the MS.

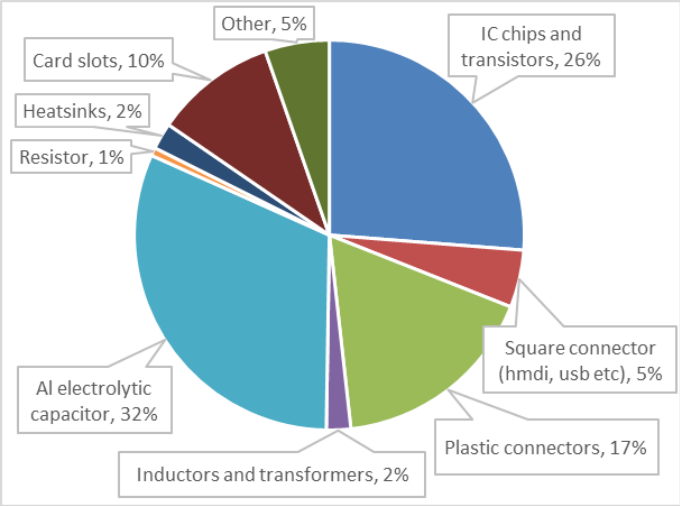

Figure 2.16: The non magnetic 5.0 - 7.0 fractions before MDS.

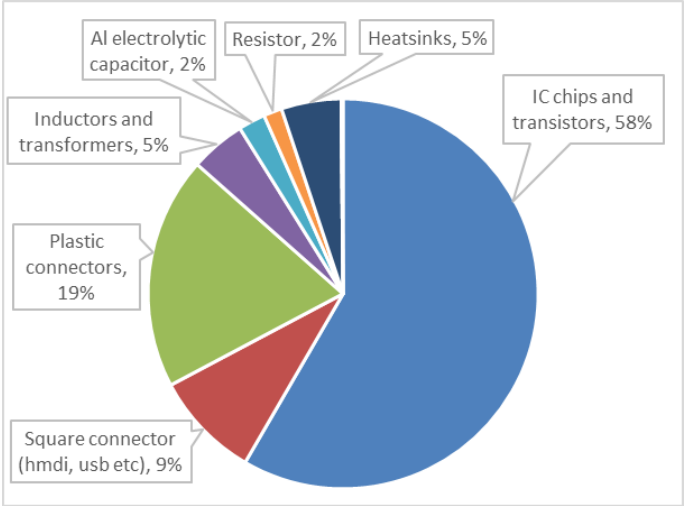

Figure 2.17: The non magnetic 5.0 - 7.0 fractions after MDS, taking only the 3800 to 2200 kg/m^3 density range.

2.5. Proposed separation system

Using the data collected in the previous sections it is possible to propose an optimal separation system for the components taken from FDP PCBs. This flowchart can be seen in figure 2.18 and has been optimised for the recovery of precious metals. The focus on precious metals was taken as this is the main goal of the Peacoc project (see section 1).

By applying this flowchart it should be possible to recover the majority of the target components. In total 303.82 grams left the system in the target flow of which 199.05 grams were target components (65.52%). A full 100% recovery of the *Central Processing Units* and *Small transistors and small IC chips* was achieved. While for *IC chips and transistors* (99%) and *MLCC + Ta capacitors* (97%) recovery was near total. This was not the case for the *Connectors of plastic with golden pins* as they could not be properly isolated in the non magnetic > 8.0 mm sieve size nor upgraded in the MDS for technical reasons (see section 2.4). As the grade for this category was low (28 wt%), the choice was made to not recombine these with the other flows. If this mixing would take place the outflow would more than double to 782.67 while decreasing the target grade to 35.50 wt%.

In regards to the precious metals around 36 wt% of the palladium, 77 wt% of the gold and 88 wt% of the silver was captured by the flowchart (see figure 2.19 for gold). The low recovery of palladium was expected due to the fact that palladium is roughly evenly spread over the components (see section 2.1.1). Unlike palladium, gold was only found in a select number of components resulting in its high recovery. This recovery could be increased by an additional 13 wt% if the *Connectors of plastic with golden pins* were recovered as well. Lastly, it can be seen that the vast majority of silver is indeed captured (around 48.89 mg per PCB).

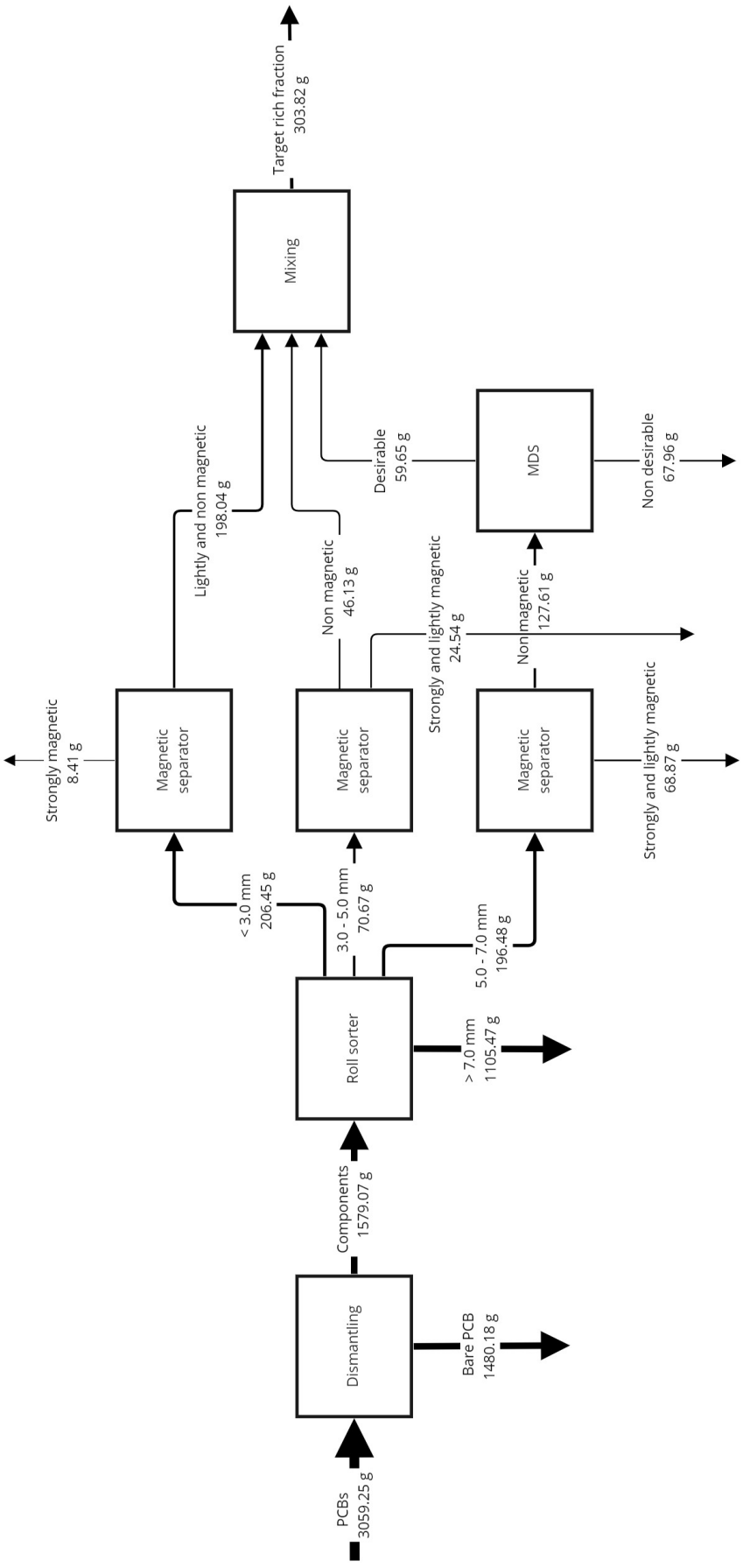

Figure 2.18: The proposed flowchart for the separation of FDP PCBs with the goal of maximising precious metals recovery.

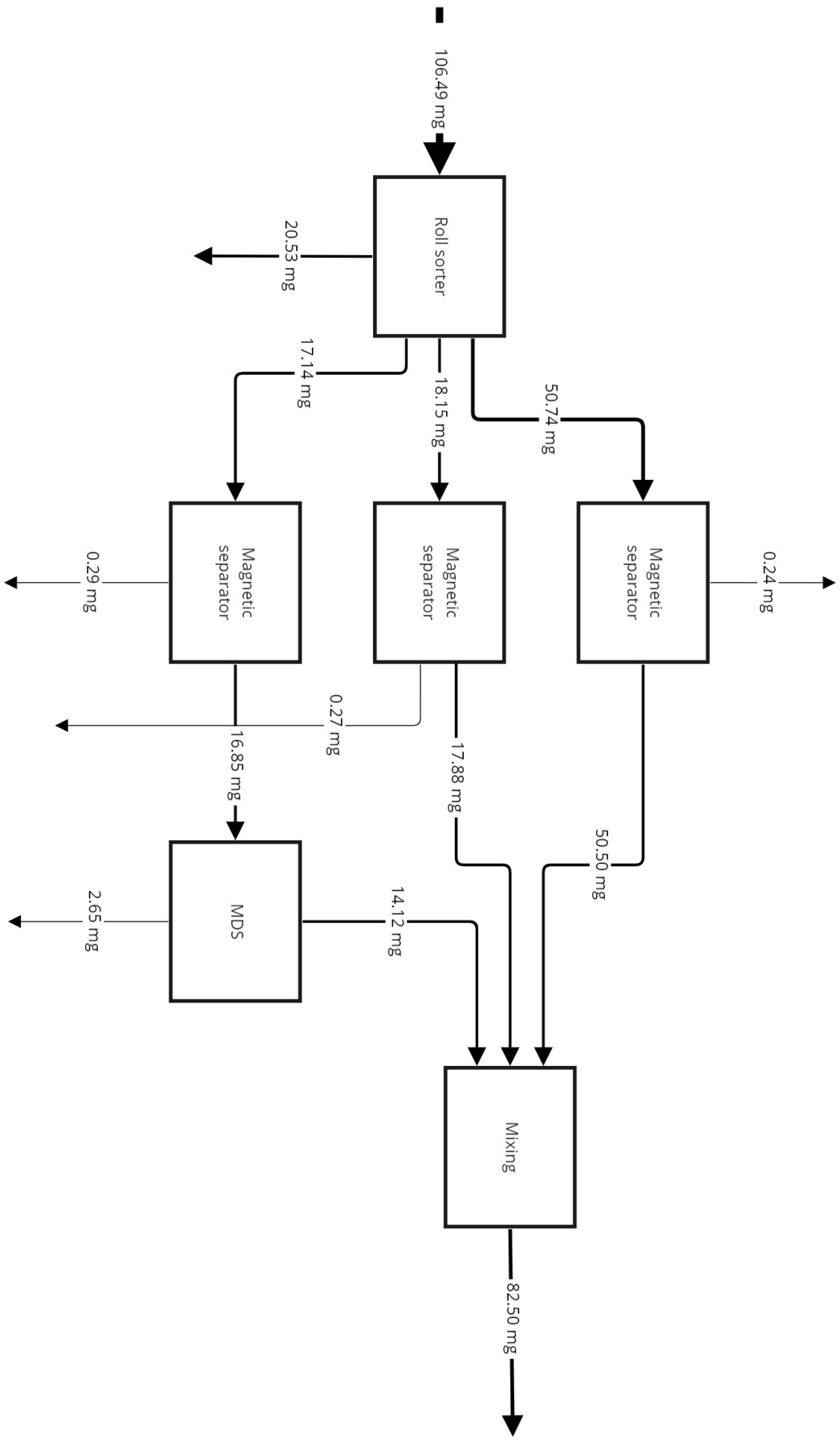

Figure 2.19: The gold flows in the proposed flowchart.

2.6. Conclusion

This chapter had the aim of answering the following research questions:

Which components and precious metals can be found in low and medium grade PCBs from WEEE?

And

How effectively can RS, MS and MDS separate components from low and medium grade PCBs as a feedstock?

As was shown, only a select number of components comprise both the majority of the weight and the gold and silver concentrations. This was not the case for palladium which was equally distributed over more than eight component types. However, the majority of palladium could actually be found on the bare PCBs and not the components. In total, five component types were attributed as target components (*Central processing units*, *IC chips and transistors*, *MLCC + Ta capacitors*, *Small transistors and IC chips* and *Connectors of plastic with golden pins*).

Using the proposed separation setup (see section 2.5), it was possible to collect only a fraction of the palladium (36 wt%) but the majority of gold (77 wt%) and silver (88 wt%) in the components. Yet the total weight of the components was reduced by an order of magnitude, showing significantly higher concentrations. The roll sorter was able to increase the concentration of the targets from 18.66 in the feed to 42.61 wt%. Further increases to 53.69 wt% were achieved using the magnetic separator and finally 66.23 wt% with the magnetic density separator. However, it was not possible to sort the *Connectors of plastic with golden pins* (> 8.0 mm) nor upgrade their concentration as the setup for magnetic density separation did not allow the > 8.0 mm components due to technical limitations.

3

Material flow analysis

The main goal of this chapter is to answer RQ 3 and 4, stated as:

How much precious metals can be recovered in the EU from low and medium grade WEEE PCBs in the year 2050 using separation technologies?

And

How variable are the precious metal flows under different scenarios and due to model sensitivity?

Both research questions employed a material flow analysis using a Python model. RQ 3 will be answered in two steps. First the amount of low and medium grade PCBs in the EU will be calculated. This is then combined with the proposed separation system (see section 2.5) to determine the precious metal flows. The chapter will conclude with two sections to answer RQ 4 focused on different scenarios and model sensitivity.

3.1. WEEE availability

The first step in answering RQ 3 was to calculate the amount of WEEE PCBs using a dynamic MFA in Python (see figure 3.1). This model was run individually for each of the investigated product categories as described in section 1.7.

The geographic boundaries for the MFA are the EU-27 as of the first of January 2022, thus including overseas regions (e.g. French Guiana) and previously independent countries (e.g. German Democratic Republic). However, EU linked countries, such as Norway and the United Kingdom, are excluded from the analysis as data was not always available for them in all sources. Furthermore, the EU is split into four regions (north, east, south and west) in accordance with *Baldé et al.* to better represent the population dynamics, consumption per capita and collection rates [106]. Therefore, the model is run four times (once for each region) and summed for the EU's totals. A map of the different countries can be found in appendix A.1.

The time frame is split into two parts. First a historical period using historical data runs from 1980 until 2020. However, two variables run until 2019 (collection rate) or 2021 (population). This is followed by a period until 2050 for exploration of the future. The year 2050 was taken as the end point of the model as this is often a goal in circularity targets [107, 108].

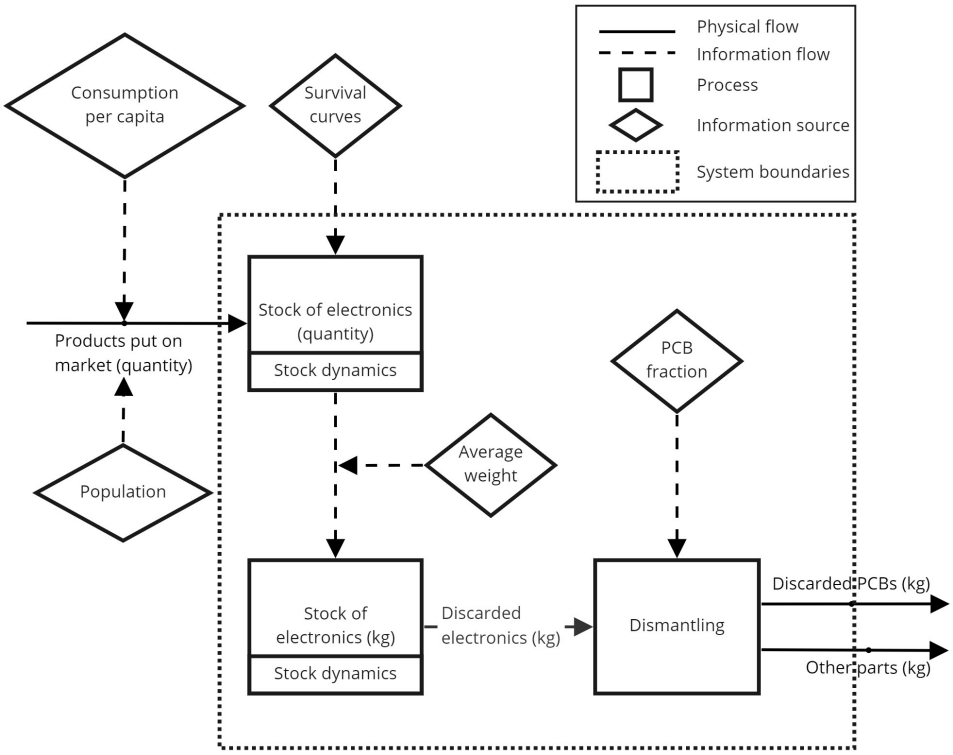

Figure 3.1: The MFA flowchart for the waste availability.

3.1.1. Model

As the time scale is one year it was assumed that only one process (Stock of Electronics) behaves as a dynamic stock and the other processes do not accumulate. This dynamic stock was inflow driven as sales numbers (e.g. PRODCOM) and historical inflow data (e.g. ProSUM) are more easily accessible than data on the stock.

The model has one external inflow, Products put on market (POM), which is a quantity (number of products) based flow. This inflow is calculated using two exogenous variables and the following formula for every cohort (x):

$$POM_{quantity}(x) = population(x) * consumption_{quantity}\ per\ capita(x) \tag{3.1}$$

The stocks are calculated using a cohort based approach as can be seen in table 3.1. The inflow of each year (x) decreases over time (t) due to the effects of a survival curve as can be seen in equation 3.2. The survival curve is a Weibull survival curve with a set shape and scale dependent on the EEE product (see appendix A.2).

$$EEE_{quantity}\ stock_x(t) = POM_{quantity}(x) * survival\ curve(t - x) \tag{3.2}$$

If the yearly total of a stock or outflow is preferred instead of the cohorts this can be achieved by summing row of year t. An example is provided in equation 3.3

$$EEE_{quantity}\ stock(t) = \sum_{t=1980}^{t} EEE_{quantity}\ stock_x(t) \tag{3.3}$$

Table 3.1: An example of the cohort based approach (stock) for Flat Display Panels in Northern Europe.

t ↓ x →	**1980**	**1981**	**1982**	**1983**	**1984**	**1985**	**1986**	**1987**	**1988**	**1989**	**1990**
1980	**1,603**										
1981	1,600	**3,219**									
1982	1,585	3,213	**4,844**								
1983	1,556	3,184	4,834	**6,475**							
1984	1,511	3,126	4,791	6,461	**8,106**						
1985	1,449	3,035	4,703	6,403	8,089	**9,750**					
1986	1,371	2,910	4,567	6,287	8,017	9,730	**11,411**				
1987	1,277	2,752	4,379	6,104	7,871	9,643	11,387	**13,084**			
1988	1,172	2,565	4,142	5,853	7,642	9,467	11,285	13,056	**14,793**		
1989	1,057	2,353	3,860	5,536	7,328	9,192	11,079	12,939	14,763	**16,547**	
1990	937	2,123	3,541	5,159	6,930	8,814	10,757	12,703	14,630	16,512	**18,367**

As the stocks are currently in quantity and the average product weight is not constant, they are converted into mass per cohort using formula 3.4.

$$EEE_{mass}\ stock_x(t) = EEE_{quantity}\ stock_x(t) * average\ weight(x) \tag{3.4}$$

The outflow (Discarded electronics or WEEE) for every year is calculated for each cohort in accordance with formula 3.5. Here the difference in stock between the current and previous is taken. One exception is the first year when the inflow occurs where it is set to zero.

$$WEEE_{mass}\ outflow_x(t) = EEE_{mass}\ stock_x(t-1) - EEE_{mass}\ stock_x(t) \tag{3.5}$$

Similarly to the average weight, the PCB weight fraction of new products changes over time. Therefore, the WEEE mass outflow cohorts are also multiplied by the average PCB fraction for its inflow year.

$$PCB_{mass}\ outflow_x(t) = WEEE_{mass}\ outflow_x(t) * average\ PCBfraction(x) \tag{3.6}$$

As can be seen in the formulas, multiple exogenous informational inflows are used in the model. Therefore, each one of these will now be discussed in further detail.

Consumption per capita

The consumption per capita was mainly gathered from the Waste over Time script (part of ProSUM) by CBS with some small changes to remove outliers (see appendix A.3) [109, 110]. This data provided the total inflow per country in quantity (number of products) and mass from 1980 until 2015. For each region the yearly inflow per capita was calculated by summing the inflows for all relevant countries and dividing by the region's population.

As historical data for ProSUM ended in 2015, data from PRODCOM was used for 2016-2020. However, due to the complexity and confidentiality of the ProSUM project, irreconcilable discrepancies between PRODCOM and ProSUM exist. Therefore, the choice was made to use PRODCOM data as a trend for the 2015 ProSUM data (see appendix A.4 for the correlation between unu keys and PRODCOM codes). For example, if the PRODCOM data showed an increase of 10% in apparent consumption for 2016 compared to 2015, consumption per capita for 2016 would also be 10% higher. However, this method could sometimes be quite erratic in nature due to the yearly timeframe, therefore changes to consumption per capita were limited to ±50% each year. Furthermore, some countries showed negative apparent consumptions and were thus set to zero for these years.

$$apparent\ consumption(t) = inflow(t) - outflow(t) + production(t) \tag{3.7}$$

As no data exists for the period until 2050, these were estimated using some assumptions. For each region and unu key a linear trendline based on historical consumption (per capita) was calculated for the last 40, 20 and 10 years. Then one of these trendlines was proposed if it seemed a good fit (high R2 and followed the current trend well) for all regions. If no trend was deemed satisfactory, the inflow was kept stable at current levels. An overview for each unu key can be found in appendix A.5.

Population

As the population over the period is not stable, historical and predicted population statistics created by Eurostat were used. For the period 1980 to 2021 historical data is used, while the period 2022-2050 is based on estimations of the growth/decline [111, 112]. It should be noted that for the period 1980-1990 Metropolitan France instead of France was used due to lack of data and Germany included the former German Democratic Republic.

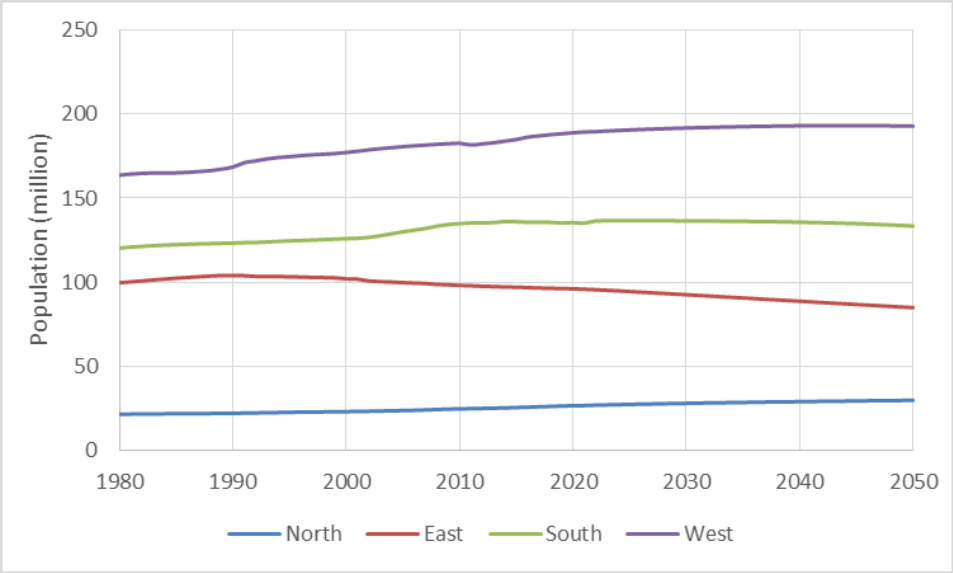

Figure 3.2: The population in the EU-27 from 1980-2050.

Survival curves

The stock dynamics of the model use a survival curve to properly represent how long a product stays in use by consumers. The survival curves take the form of a Weibull distribution curve and were taken from *Forti et al.* with all countries using data for the Netherlands/France [97]. The survival curves are kept the same for the whole period unless stated otherwise.

Average weight

In order to convert the number of products to a mass flow, the average weight per product (unique for each unu key and region) was calculated. This data was also extracted from the Waste over Time script, as it both presented inflows in weight and in quantity [109]. For some of the unu keys, the average weight was not stable and either increased or decreased over time. In order to take this into account the average growth/decline for the period 2010-2015 was calculated and used for extrapolation of the period 2016-2050. However, it should be noted that this growth was limited to ±1% in order to avoid extreme exponential growths or declines over the period.

PCB fraction

The last step was to convert the weight of discarded products to the weight of discarded PCBs. Therefore, data from appendix A28, A29 and A32 by *Wagner et al.* was used to make this conversion [113]. As this data was presented in graphs, the tool WebPlotDigitizer was used to create raw data [114].

Similar to the average weight, the PCB fraction for most products was not stable and tended to decrease over time. Therefore, the same method was applied to the PCB fraction. However, here the growth was limited to ± 2% as they tended to be higher. An overview of all growth rates can be found in appendix A.6.

It should be noted that the average weight and PCB fraction are both applied on the year that the product was originally put on market. Thus the average weight and PCB fraction of a product from the year 2005 does not depend on the year it leaves the economy as WEEE.

3.1.2. Unknown initial stocks

The model does not use an initial stock for any of the products. This choice was deliberate as an initial stock can create adverse effects, such as large outflows in certain years, and was not required. As the inflow data already starts in 1980 there is a 40 year lead up period to 2020. Over this 40 year period almost all of the original inflow from 1980 leaves the system. Therefore, it is possible to ignore inflows from before 1980 to the system. This assumption was also checked using the Weibull data and plotted in figure 3.3 and seems to hold for almost every product. The only product where more than 1% of the original inflow is still in stock by 2020 is 402 (Portable Audio & Video). As this is the only case, this discrepancy was deemed acceptable.

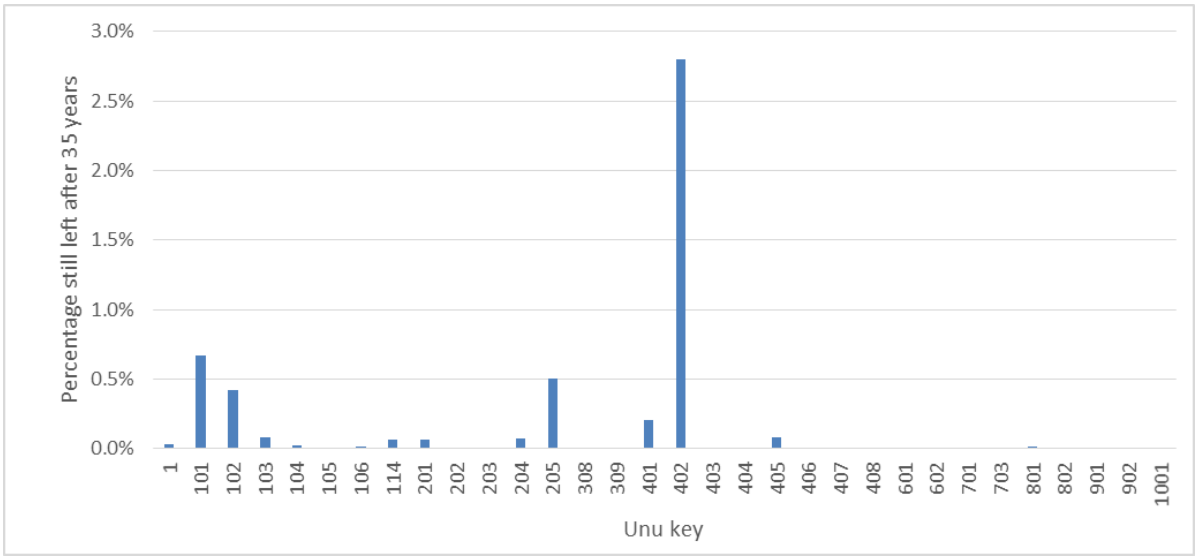

Figure 3.3: The percentage of every Unu key that is still left in 2020 from 1980.

3.1.3. Results

As can be seen in figure 3.4, the inflow (number of products) increases year over year with the outflow and stock following the same trend. This was expected as both population and consumption per capita increase over the years. An exception to this trend can be found between the years 2006-2012, where the inflow stabilises. This is likely a result of decreasing consumption per capita due to the 2008 financial crisis [115].

The same anomaly can also be seen when looking at weight instead of number of products (see figure 3.5). However, during the whole period average weight per product also slightly decreased. Therefore, the effect is not completely the same in both graphs. Lastly, both graphs clearly show that the historical data ends in the year 2020 as afterwards the inflow becomes a straight line due to the previous assumptions made.

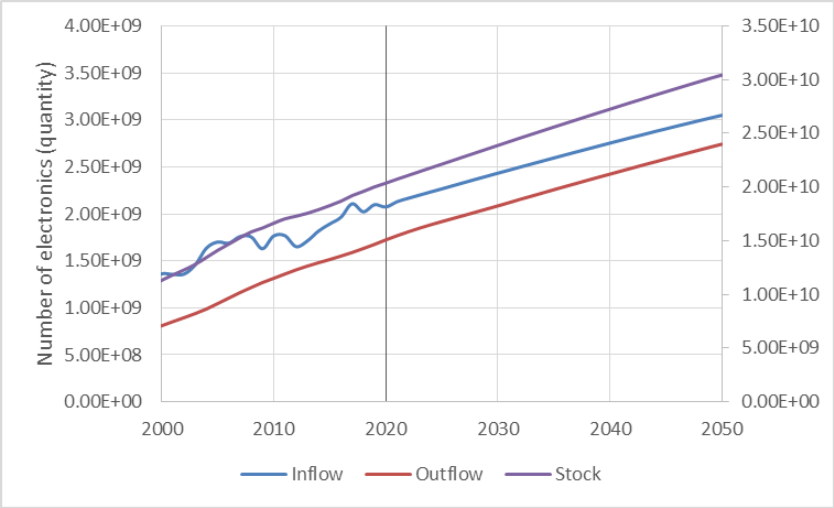

Figure 3.4: The inflow, outflow and stock (right axis) development from 2000-2050 (number of units). The end of the historical data is shown with a vertical line.

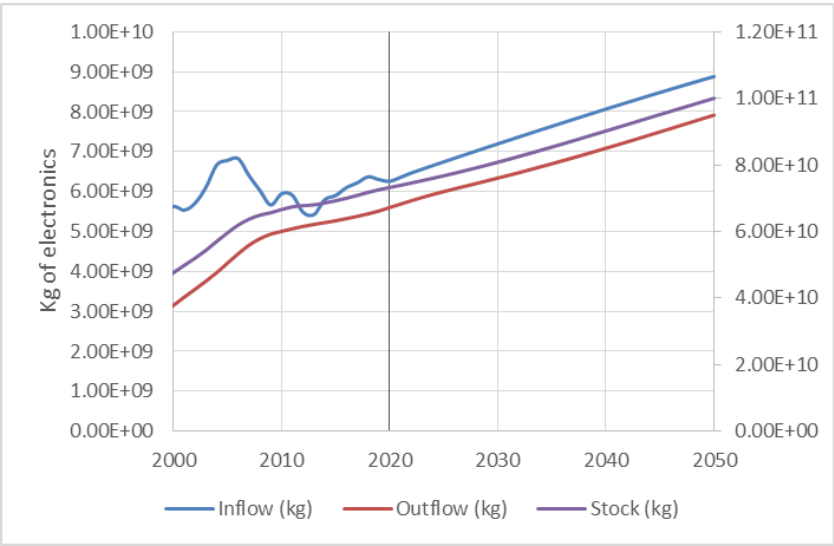

Figure 3.5: The inflow, outflow and stock (right axis) development from 2000-2050 (kg). The end of the historical data is shown with a vertical line.

The story changes when one looks at the mass (kg) of low and medium grade PCBs that flow in and out of the system (see figure 3.6). Around the year 2006 the inflow takes a sharp decline and falls below the yearly outflow, creating a large negative addition to stock ($-4.58 \cdot 10^7$ kg in 2012). As a direct result of this negative addition, the stock decreases sharply in the same period. This decrease in inflow can best be attributed to the miniaturisation of PCBs in electronics. A perfect example is the replacement of CRT TVs and monitors by FDP technology (see figure 3.7). The average CRT monitor in 2000 required 1.78 kg of PCB, while the average FDP in 2010 required only 0.25 kg of PCBs. This observation is also in line with the literature [116, 117].

These trends can also be seen in the outflow compositions. Two examples (2008 and 2050) are shown in figure 3.8 and 3.9. First of all, CRT TVs and monitors are expected to be been completely replaced by FDP TVs and monitors, yet at a lower combined share (28 wt%) than before (47 wt%). Video and Music Instruments remain two of the major categories, but slightly decrease their shares. However, it should be remembered that the actual outflow will decrease (from 131 kton to 57 kton), thus also decreasing the Video and Music Instruments mass outflows. Lastly, the number of categories that crossed a 3 wt% threshold (arbitrarily chosen) has increased from 4 to 11, showing a greater diversification of outflows.

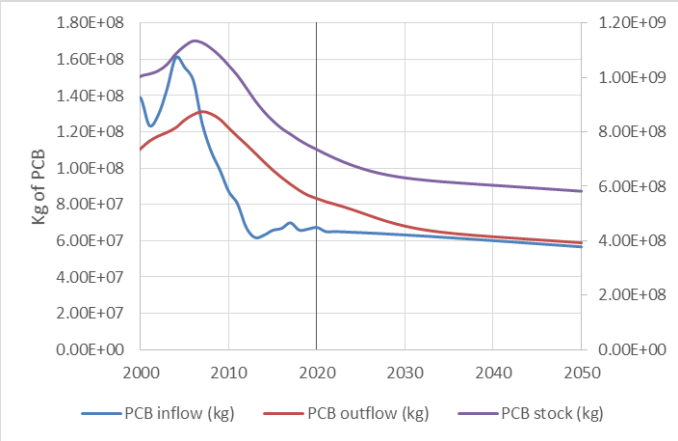

Figure 3.6: The inflow, outflow and stock (right axis) development of PCBs from 2000-2050 (kg). The end of the historical data is shown with a verticle line.

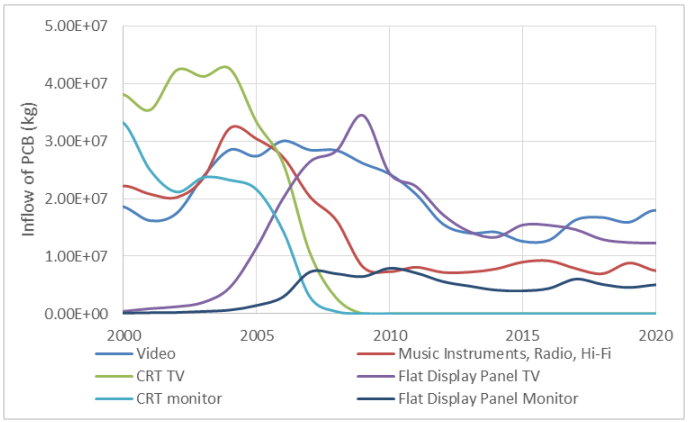

Figure 3.7: The PCB inflow of the most important categories from 2000-2020 (kg).

Once again, this can best be attributed to the previous dominance of CRT technology and to a lesser degree an increased popularity of the other categories. It should also be noted that this fact will likely complicate the waste management systems as the separation processes will have to be applicable to a large number of product categories. However, this diversification also increases the number of potential niches for recyclers to specialise in. For example, a recycler could specialise in recycling Toys due to the increased outflows in 2050 (2,269 tons compared to 822 tons in 2020) and through their familiarity with the products increase efficiency and thus reduce energy demand while increasing profits.

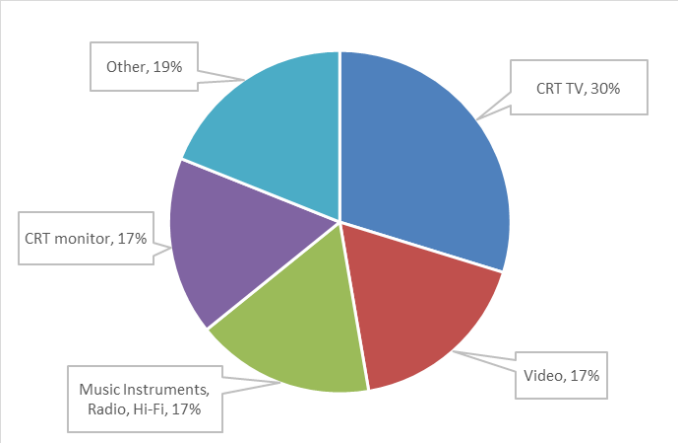

Figure 3.8: The weight distribution of discarded PCBs in 2008 with all categories larger than 3 wt%.

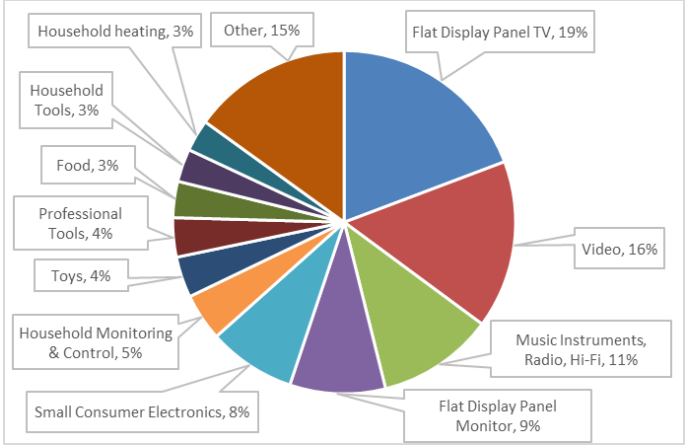

Figure 3.9: The predicted weight distribution of discarded PCBs in 2050 with all categories larger than 3 wt%.

3.2. Precious metal flows

For the calculation of the precious metal flows the previous MFA is continued and now includes the waste management system and recovery (see figure 3.13). First of all, a new variable called collection rate is introduced which models the collection the WEEE/PCBs. After collection the components on the PCBs are liberated using data gathered in chapter 2, resulting in a component and bare PCB stream. The bare PCBs will continue directly to their metallurgical recovery while the component streams will enter the novel separation technologies. These processes will use data gathered for RQ 2 to efficiently separate the components to their individual categories before entering metallurgical recovery. Lastly, during metallurgical recovery the precious metals will be recovered from the different streams.

Two main results were calculated, the maximum potential recovery and the recycling recovery. The former assumes that all PCBs are collected and all components enter metallurgical recovery, which operates at 100% efficiency. Thus, showing the upper limit of precious metals which can be extracted. However, the recycling recovery shows the predicted recovery by the proposed system of RQ 2 and is therefore more interesting. Here the collection rates, separation and metallurgical efficiency are taken into account. Furthermore, this second result will be evaluated using the scenarios and Monte-Carlo sensitivity analysis of RQ 4.

Three indicators were used to present the results. The first indicator is the amount (weight) of recovered precious metals that is achieved. The second indicator shows the ratio between this new secondary flow and the EU's overall raw consumption of the metal (see equation 3.8). To show the specific impact on the sector the third indicator calculates the ratio between the inflow and the EU's raw consumption for electronics production (see equation 3.9). These inflows are taken from the 2020 CRM analysis factsheets and are assumed to stay at 2020 levels for the evaluated period [7, 8].

$$Ratio_{all\ products} = \frac{secondary\ inflow}{EU's\ raw\ consumption\ (all\ products)} \tag{3.8}$$

$$Ratio_{electronics} = \frac{secondary\ inflow}{EU's\ raw\ consumption\ (electronics)} \tag{3.9}$$

Collection

Quite often collection rates are calculated using by assuming the products placed on market in the three preceding years are the current year's outflow (see equation 3.10). To give a more accurate view of the problem formula 3.11 was used instead as this presents the actual fraction of outflow which gets collected by the waste management system. For each country in the EU-27 the collection rate was individually calculated for each of the three investigated WEEE categories (II, IV and V). It should be noted that the excluded products categories (Laptops, Professional IT, Small lighting equipment, Household Luminaires and Professional luminaires) were included in these calculations. These collection rates were then averaged for each of the regions. This does mean that small but effective nations (e.g. Croatia at 100) are able to compensate for large yet ineffective countries (e.g. Spain). For the period after 2019 it was assumed that the 2019 collection rates would be kept (see table 3.2) as the main model assumes business as usual.

$$collection\ rate(t) = \frac{collected\ WEEE(t)}{POM(t-3,\ t-2\ and\ t-1)} \tag{3.10}$$

$$collection\ rate(t) = \frac{collected\ WEEE(t)}{generated\ WEEE(t)} \tag{3.11}$$

Table 3.2: The collection rates for 2019 and onwards. For all years see appendix A.7

Region	II	IV	V
North	86%	81%	30%
East	76%	74%	34%
South	72%	43%	21%
West	73%	70%	35%

Data regarding collected WEEE flows were collected in several ways. First of all, for the period 2010-2015 data was taken from the ProSUM project (collected and reported) [110]. For the year 2019 (and 2018 for Bulgaria, Hungary, Lithuania, Poland and Portugal) it was possible to take data (Waste collected from households) from Eurostat's new WEEE database which was published earlier this year

[118]. However, the Eurostat database does not have reporting for the six (new) WEEE categories for the period before 2019 as it previously used the old ten WEEE categories [119]. Therefore, it was assumed that in these years the collected WEEE flows linearly increased/decreased to 2019 levels.

In order to determine the generated WEEE flows the MFA model from the previous section was employed. Instead of running the model on a regional level it was run for each individual country. This was possible as the EEE inflows from ProSUM and Eurostat were on the national level as well.

Finally, a couple of points should be noted. First of all, no data was gathered for the period before 2010 as this report aims for the application of future technologies and does not focus on historical behaviour. Secondly, the collection rates for each country was limited to 100% to avoid skewing the numbers as some collected more than they generated (e.g. Finland and Sweden). For category IV (Large Equipment and PV panels), any data regarding the PV panels was excluded as this was considered out of scope for this report. Lastly, four countries (Cyprus, Greece, Malta and Romania) were not yet in the Eurostat database. Therefore the decision was made to exclude them from the averages to avoid using old (2015) data.

Metallurgical recovery

In the last step of the recycling system the metals are extracted from the feed. Many technologies are employed in this regard including mineral acids (e.g. HCl), cyanide or Acidic thiourea [120]. The Peacoc project advances the work of the Platirus project using a two step metallurgical recovery process developed by VITO [25, 121]. The metals are leached from the substrate at a temperature of 150°C using 6M HCl and H_2O_2 for 10 minutes. The metals are then recovered using gas diffusion electrocrystallization (GDEx) where a gas (e.g. O_2) is reduced leaving the metals [122]. The process is already able to capture over 95% of platinum groups metals (PGMs), which includes palladium, in autocatalysts and is in active development for WEEE [92]. Therefore, a recovery of 90% will be assumed as it is also in line with other hydro metallurgical recoveries (90-99%) [123–125].

3.2.1. Results

Maximum potential recovery

The maximum potential recovery for all three precious metals (gold, silver and palladium) can be seen in figure 3.10. This graph shows how much precious metals would be recovered if no losses in collection, separation or metallurgical recovery take place.

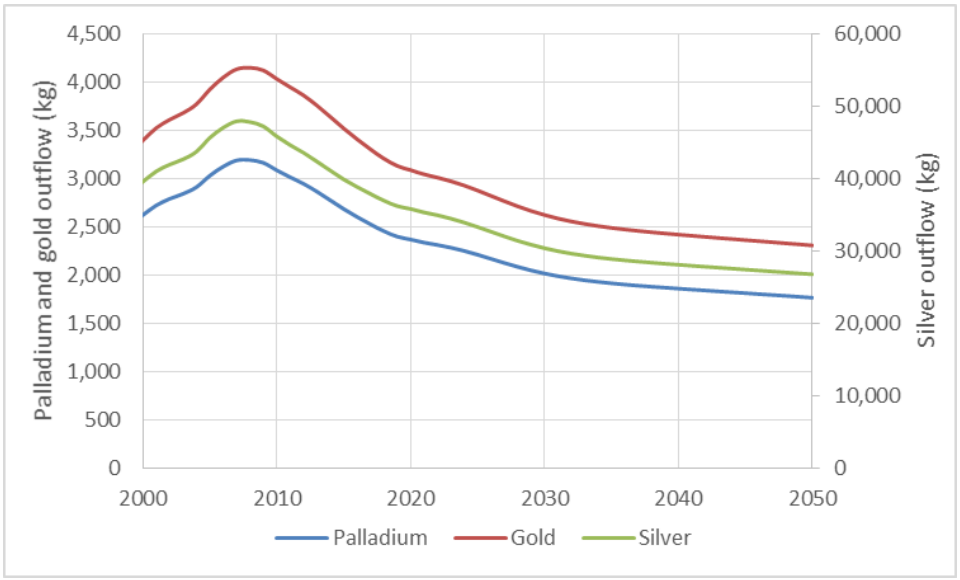

Figure 3.10: The maximum potential recovery (kg) of palladium, gold and silver.

All the flows follow a very similar pattern to the previously established PCB outflows (see figure 3.6). In the early years they rise, reaching their zenith in 2008, after which they slowly decrease over the years. Silver is by far most prevalent (an order of magnitude higher) of the three precious metals. This was expected due to the very high concentrations in the MLCC + Ta capacitors, as established in section 2.1.1.

The estimated flows are significantly lower than the Peacoc projects cites as their goal (30 ton gold, 10 ton palladium and 100 ton silver) [25]. This is likely the result of multiple factors. First of all, this thesis only focuses on low and medium grade PCBs. So precious metal rich EoL PCBs from laptops or phones are not included. Secondly, due to problems with the data any flows from Large steel and aluminium cases were ignored. If this data is included precious metal flows increase significantly, 11% for palladium, 40% for gold and 36% for silver. Lastly, it is also possible that the Peacoc proposal overestimated the amount of precious metals available. For instance, ProSUM calculated around 2.7 tons of palladium, 13.1 tons of gold and 68 tons of silver for the investigated WEEE categories (II, IV and V) for 2020. Although it should be noted that ProSUM also includes laptops and professional IT (both high grade PCBs).

As can be seen in table 3.3, only a small part (less than 5%) of the current (2020) demand can be supplied from PCB outflows. This even worsens in the future due to the previously mentioned decreasing flows where only around 3% of demand can be supplied from this secondary source. Furthermore, the actual supply will likely be far lower as this is the maximum potential outflow.

Table 3.3: The maximum outflow, current consumption and their ratio of precious metals in the EU-27 for 2020 and 2050

	Pd		Au		Ag	
	2020	2050	2020	2050	2020	2050
Raw consumption all products (ton)	2.37	1.77	3.09	2.31	35.85	26.80
Raw consumption (all products) (ton)	59		73		849	
Ratio all products	4.02%	3.00%	4.23%	3.16%	4.22%	3.16%

Recycling recovery

As mentioned before, this section shows the expected metal recovery for the proposed separation system where (household) collection rates, separation efficiency and metallurgical recovery also play a role.

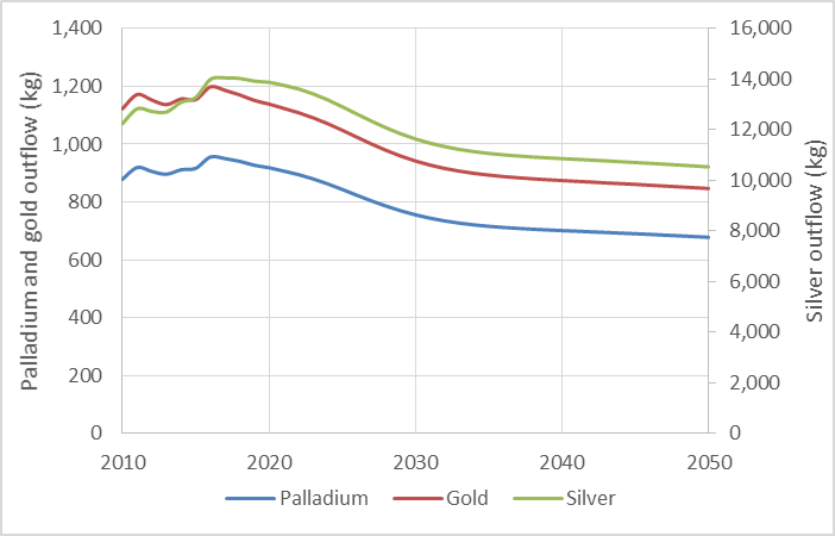

Figure 3.11: The effective recovery (kg) of palladium, gold and silver (right axis).

A couple of interesting observations can be made. First of all, the historical fluctuations and their

later smoothing for collection rates can be observed in the early years (2010-2019). Secondly, after 2020 the recovered metal flow goes down. This was expected as the maximum potential outflows was previously shown to decrease as well (see figure 3.10). In reality recovery would likely go up or stay at similar levels due to increases in collection rates, thus compensating for the lower potential. These increases in collection rates were not modelled for this system as the Eurostat database only provided one data point (2019) for the majority of nations complicating trend extrapolation. Lastly, it can once again be seen that the potential for silver is an order of magnitude higher than for gold and palladium. However, it should be noted that the majority of the monetary value is still located in the gold (46.21%) and palladium (46.45%) instead of the silver (7.34%).

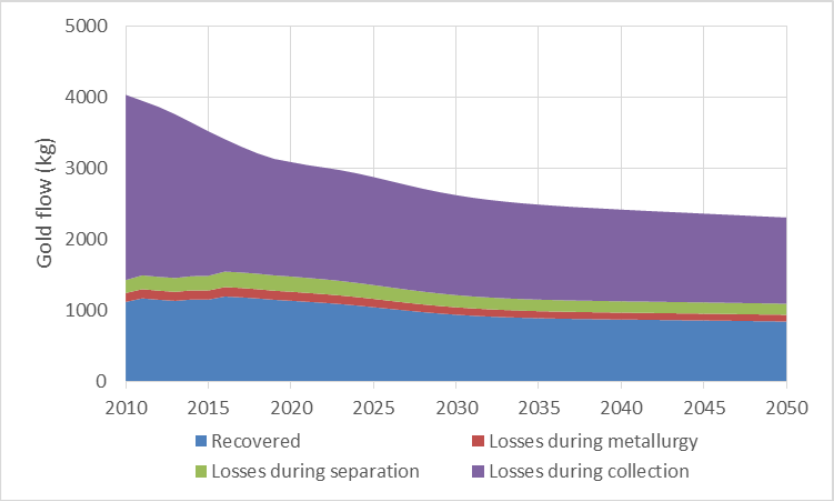

Figure 3.12: An overview of where the loses take place (gold).

As can be seen in figure 3.12, only between around 40% of the potential is currently exploited by the proposed system. However, this gap is not due to failure of the sorting system, but due to the previously mentioned low collection rates (see section 3.2). Here the collection step loses around 52.50 wt% of all the gold, while the separation system and metallurgical recovery only lose 6.75 and 4.07 wt%, respectively, for 2050. This shows that even with an efficient separation system, proper recovery cannot be achieved if the initial collection from households remains low. The flowcharts for gold can be seen in figure 3.14 while palladium and silver can be found in appendix A.8.

In a similar vein, the supply to the economy also roughly halved with the system only able to supply around 1.6% of the required input for 2020. Furthermore, this also drops again for 2050 with all three metals being below 1.3% as the maximum potential decreases.

Table 3.4: The recovered outflow, current consumption and their ratio of precious metals in the EU-27 for 2020 and 2050

	Pd		Au		Ag	
	2020	2050	2020	2050	2020	2050
Recovered outflow (ton)	1.02	0.75	1.27	0.94	15.42	11.71
Raw consumption all products (ton)	59		73		849	
Ratio all products	1.56%	1.15%	1.56%	1.16%	1.63%	1.24%
Raw consumption electronics (ton)	2.36		8.03		110.37	
Ratio electronics	38.94%	28.74%	14.19%	10.55%	12.58%	9.55%

The story changes when looking at metal consumption for electronics production. This consumption is only a fraction of the total demand (4% for palladium, 11% for gold and 13% for silver) and secondary production could thus significantly increase circularity and the End-of-life recycling input rate. In all

three cases this amounts to over 10% of demand can be satisfied with the current collection rates. This is possible due to the fact that the majority of electronics are produced outside of the EU and thus do not count in the raw consumption.

Therefore it can be stated that the implementation of this recycling system will only have a small effect on the overall circularity of the EU, yet could provide significant yields for the electronics sector.

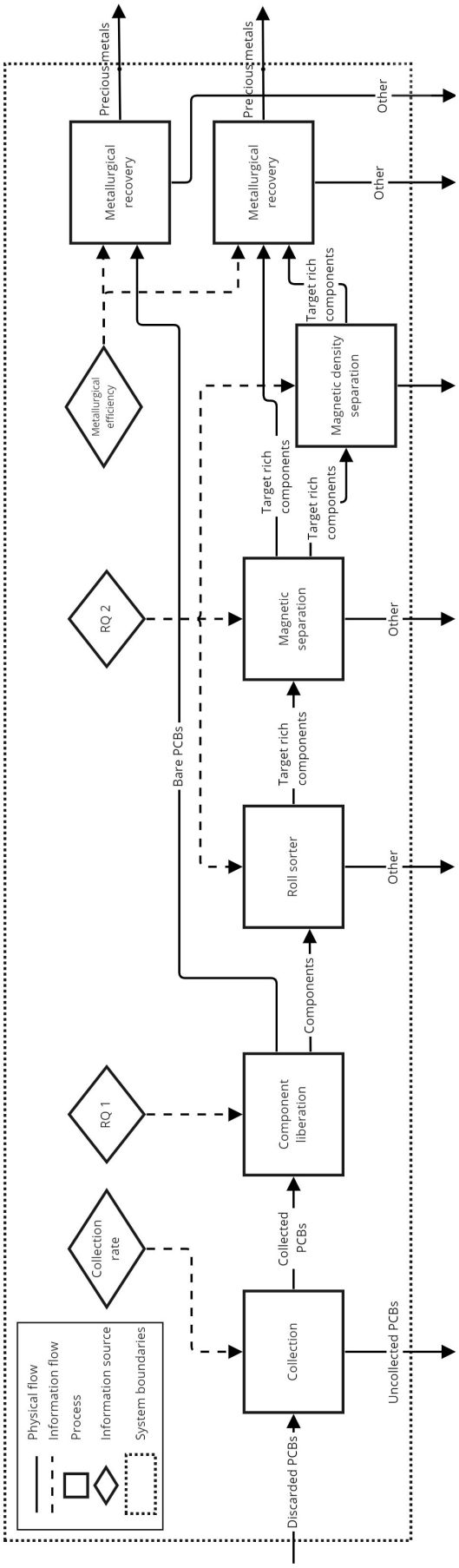

Figure 3.13: The MFA flowchart for the recycling system.

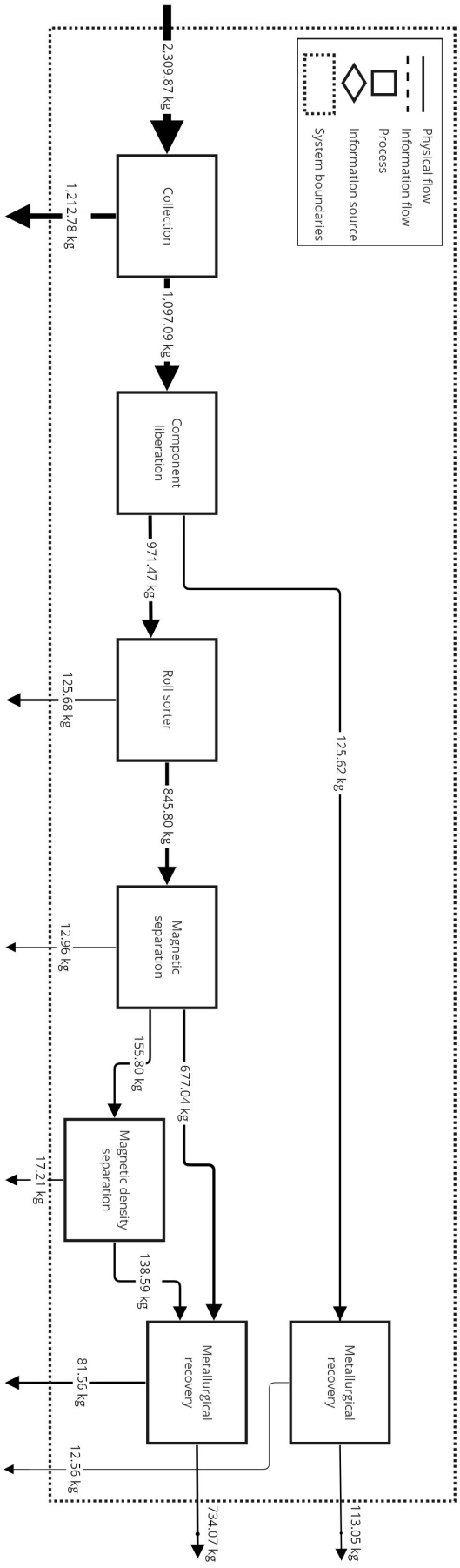

Figure 3.14: The gold flows within the recycling system for 2050.

3.3. Scenarios

As mentioned in the research questions (section 1.8), RQ 4 will explore several scenarios of potential future pathways. The main input parameters for these scenarios are population growth, consumption per capita, WEEE collection rate, product lifespan and miniaturisation (see table 3.5). All scenarios will start in the year 2021 and will usually take until 2030 to take full effect. Any changes compared to Business As Usual (BAU) are made used a linear growth model. Thus, if a variable increases a total of 20% over 10 years, a 2% (cumulative) increase on yearly basis is calculated. First the results for WEEE availability will be given followed by the precious metal flows.

Table 3.5: The different scenarios and their impact on the exogenous variables.

Scenario	Population growth	Consumption	Collection rate	Product lifespans	Miniaturisation	Repurpose
BAU	Follows trend	Follows trend	Follows trend	Follows trend	Follows trend	N.A.
Goals	Follows trend	10% decrease	Directive target	20% increase	Follows trend	N.A.
CE	Follows trend	20% decrease	Reaches 95%	50% increase	20% decrease	Reaches 50%
Decline	Depends on region	Stabilises	Follows trend	Follows trend	Stabilises	N.A.
Consumption	Follows trend	50% increase	Follows trend	20% decrease	20% increase	N.A.

Business As Usual (BAU)
The first scenario will be a Business As Usual (BAU) scenario. Here, current trends (e.g. population growth) will be assumed to continue on their current trajectories, while potential pitfalls (e.g. an economic crisis) and/or unexpected benefits (e.g. new technologies) are ignored. Therefore, this can best be seen as a “realistic” or “conservative” scenario and a baseline for the rest. All variables will follow the calculations as previously written.

Goals
The first scenario will be followed by the Goals scenario. In this potential future the European Union (both the governmental body, its citizens and companies) will all act towards sustainability. Through widespread campaigns, the awareness of the population on the topic of E-waste has increased. This results in sizeable improvements of WEEE collection and the EU reaches its goals by the year 2030 [126]. Furthermore, the population also puts pressure on the electronics producers through governmental legislation. New initiatives such as right to repair laws will be implemented, which in turn increases the lifespan of newly produced products up to 20% by the year 2030. Lastly, as products stay longer in use the demand for new products slightly decreases by 10%.

Circular Economy (CE)
In the third scenario called Circular Economy (CE) the campaigns of the second scenario exceed all expectations. The EU has one mind, which is to solve the WEEE problem. By the year 2030 collection rates for all categories reach 95%, greatly exceeding anybody’s dream. Furthermore, in addition to the previously stated legislation new business models, such as product as a service, are adopted by industry. This combination makes new products last for 50% longer, while reducing consumption by 20% compared to BAU by 2030. This new market also creates new opportunities. For instance, electronics producers recognise the outflow of cheap, clean yet usable PCBs and decide to use these to reduce manufacturing costs. Higher grade PCBs (e.g. from FDP TVs and monitors) are repurposed in newly manufactured equipment such as washing machines and dryers. About 50% of these higher grade PCBs are used for this purpose closing the loop at an even earlier stage than recycling. However, this innovation also means that old/obsolete PCBs are used in new products instead of newly designed PCBs, slightly slowing down development. This in turn means that the rate of miniaturisation (weight per product and PCB fraction) is decreased by 20%.

Decline

In order to provide some contrast, the fourth scenario will be a negative scenario called Decline. In this scenario Europe's economy will grind to a halt causing public upheaval and an EU stuck in political gridlock. Due to stagnating income and wealth, consumption will no longer increase and stabilise at current levels. Furthermore, as nations are more focused on internal matters migration between EU members will cease as well. This will result in a decrease in population growth for northern and western Europe, while increasing growth in southern and eastern Europe compared to the growth in BAU (see appendix A.9). Lastly, as the economy has stagnated, product development has not improved either, leading to a halt of the miniaturisation process.

Consumption

The last potential future that will be explored is called Consumption. Through careful planning and luck, new R&D breakthroughs are achieved and product innovation is greatly increased. These improvements allow smaller and better products to be made, resulting in increases to the miniaturisation process of 10%. At the same time consumerism increases as well because people want the newest and best products available. Therefore, the consumption per capita by the year 2030 is expected to increase by 50% compared to BAU, while decreasing product lifespans by 20%.

3.3.1. WEEE availability

As expected all scenarios remain very similar for the first five years and only start to diverge after the year 2025 (see figure 3.15). The first is the consumption scenarios, which increases sharply only to slow down around 2035. The sharp increase can be explained by the overall increased consumption per capita, while the latter slowdown is due to the shorter lifetimes. The extra consumption already flows out again, thus reducing total stocks. Around the year 2030 the next divergence of the Decline scenario can be seen. This falls in line with the expectations as the consumption slows down in the Decline scenario, reaching full stability in 2030. The Goals and CE scenario both diverge in 2035 and behave very similar with slightly increased stocks for CE. This shows the importance of lifetimes (increased by 50%) on stocks as CE's stock increases even though consumption decreased by 20%. In 2050 Decline has (almost) completely stabilised (82% of BAU), while Consumption achieves the highest stock (119% of BAU) with Goals (106% of BAU) and CE (113% of BAU) in between Consumption and BAU.

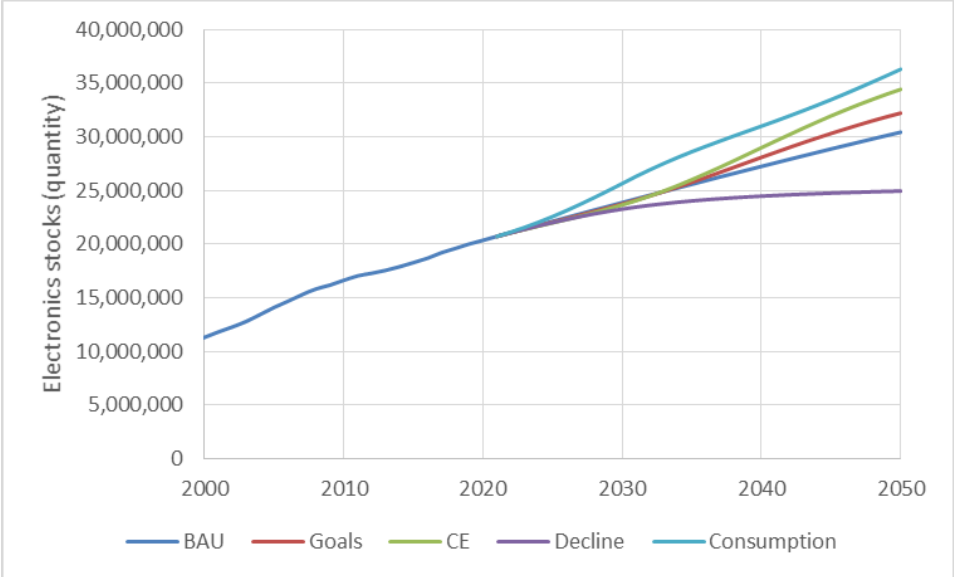

Figure 3.15: The stock of electronics for each scenario.

The previously established conclusions do not hold in regards to the PCB outflows (see figure 3.16). Here it can clearly be seen that the Consumption scenario produces the highest outflows (138% of

BAU), while Goals (90% of BAU) and CE (82% of BAU) produce less waste. This should not come as a surprise as Consumption focuses on high, short-term consumption, while CE does the exact opposite with a strong focus on increased product lifespans. It is also interesting to note that after the year 2040 these two scenarios actually start to convergence once again. This is likely due to the effects of miniaturisation (increased in Consumption and decreased in CE) catching up with the product lifetimes. It should be noted that miniaturisation is a part of all scenarios (including BAU) and is only accelerated or slowed down by the scenarios unlike the survival curves.

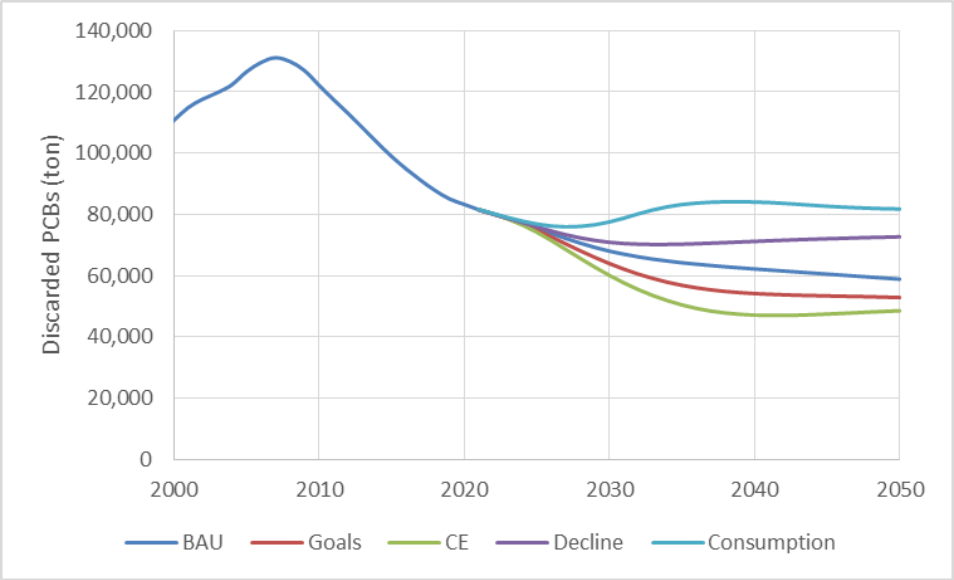

Figure 3.16: The produced waste PCBs produced by the five scenarios.

3.3.2. Precious metal flows

The story once again changes when looking at the recovered precious metal flows (see figure 3.17). Initially the Goals and CE scenario show the highest recovered outflows as their collection rates have increased. However, both start to decrease in later years, CE after 2026 and Goals after 2030, due to several factors. First of all, both decrease due to the preciously stated general decline (see section 3.2.1). Secondly, their increases in recovery were due to increases in collection rate, which stabilises in 2030. Thirdly, both have decreased PCB outflows due to the increases in lifetimes. Lastly, the CE scenario recovery decreases as repurposing PCBs reaches its full potential in 2030 (50% of collected PCBs). Therefore, these PCBs are no longer available for precious metal recovery through the recycling system.

On the other hand, the Consumption and Decline scenarios increase their metal recovery as more PCBs are discarded (see figure 3.16). As mentioned before for the Consumption scenario, this is due to increased per capita consumption and lowered lifetimes, while Decline increases due to the halting of the miniaturisation process. It should also be noted that even though Goals and Consumption recover a similar amount of gold, the Goals scenario should be the preferred outcome as it does it more efficiently by using 40% less product outflows.

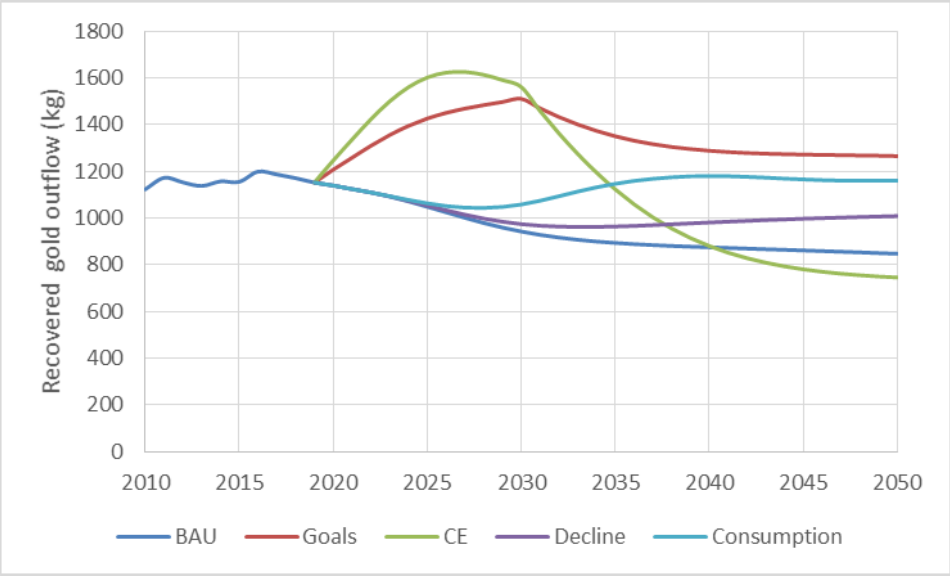

Figure 3.17: The recovered outflow of gold in different scenarios.

3.4. Uncertainty and sensitivity analysis

In order to evaluate potential pitfalls with the MFA model and data, an uncertainty and sensitivity analysis were performed using Monte-Carlo uncertainty analysis and parameter sensitivity analysis. The former showed the uncertainty in the data and their results for the overall model, while the latter provides the effect of each input variable. For the sake of conciseness gold will be the only precious metal that will be explored. This was deemed acceptable as no major differences between the three metal flows exist.

3.4.1. Uncertainty analysis

In total 1.000 runs were performed for the Monte-Carlo uncertainty analysis. During a run the flows of all product types in each region were individually run with randomised variables. Therefore, achieving complete randomness during every run. All variables used a normal distribution with the mean being the original data point and the standard deviation (differed per variable) a percentage of this point. To avoid extreme outliers and errors, the random variable had a minimum of 0.0001 and a maximum of two times its original value. Furthermore, for the variables in the form of fractions (PCB fraction, collection rate, component weight distribution, component separation and metallurgical recovery) care was taken to keep the fractions between 0 and 100%.

Consumption per capita

For the consumption per capita a standard deviation of 10% was assumed for the historical period (1980-2020). This was increased to 20% for the predicted period (2021-2050).

Population

For population it was assumed that historical data was accurate and thus not randomised. However, uncertainty was introduced in the 2022-2050 period. As population is determined using the predicted growth, this growth was randomised using a standard deviation of 10%.

Survival curves

In the case of survival curves, both the shape and scale were randomised. As the same survival curve is used for the whole period, no variability in curve was introduced between different years. For the shape and scale a standard deviation of 10% and 20% were used, respectively.

Table 3.6: All the input variables to the model and their uncertainty.

Variable	1980-2020	2021-2050	Notes
Consumption per capita	5%	20%	N.A.
Population growth	0%	10%	Second period starts in 2022
Shape (survival curve)	10%		N.A.
Scale (survival curve)	20%		N.A.
Average product weight	10%	25%	Second period starts in 2016
PCB fraction	10%	25%	Second period starts in 2016
Collection rate	10%		N.A.
Component weight distribution	10 or 20%		Non CRT or FDP is 20%
Metal concentration	10 or 20%		FDP data is 10%, CRT 20%
Component separation	10%		N.A.
Metallurgical recovery	10%		N.A.

Product weight and PCB fraction

For the average weight per product and PCB weight fraction a similar approach was taken. Both had a standard deviation of 10% during the historical ProSUM period (1980-2015), but 25% from 2016 onwards. This choice was made to reflect the potential of newly produced products which currently do not exist.

Collection rate

The collection rates were randomized with a standard deviation of 10% as their calculation methods were not always clear and consistent.

Component weight distribution

In regard to the component fractions two ranges were used. As the components for the CRT TV/monitors and FDP TV/monitors were gathered from laboratory work, these had a low standard deviation of only 10%. This was not the case for the other products. As these were taken from a select number of (online) sources and used CRT/FDP proxies (see section 2.1 and appendix A.2), they had an standard deviation of 20% to reflect this data uncertainty.

Metal concentrations

The metal concentrations had a base standard deviation of 10%, which was increased by an additional 10% if the product used the CRT data as a proxy. This choice was made as the metal concentrations for CRTs were not experimentally determined but based on the FDP data and thus less precise.

Component separation

As data for component separation is taken from experimental lab work, a low standard deviation of 10% was implemented. This was the same for all types of products and no differentiation was made between FDP or CRT proxies.

Metallurgical recovery

For metallurgical recovery a standard deviation of 10% is used. This choice was made as the original efficiency (90%) was based on an assumption, but neither significantly higher or lower values were found in literature.

Results

As mentioned before, overall model sensitivity was first explored with randomisation for all variables and its results can be seen in figure 3.18. As the period 1980-2020 was based on historical data, the uncertainty for this period is low as well. After 2020 the consumption per capita data becomes uncertain resulting in a sharp increase of uncertainty. However, this increase in uncertainty does not yield immediate effects on the outflow (see figure 3.19) as the uncertain inflows have a time delay before they flow out again.

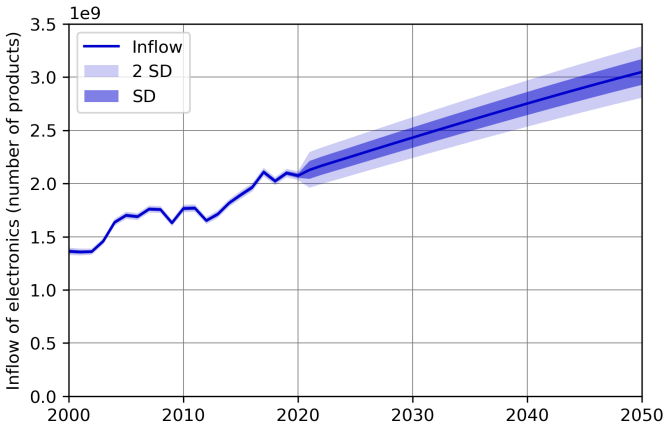

Figure 3.18: The uncertainty of the inflow of electronics.

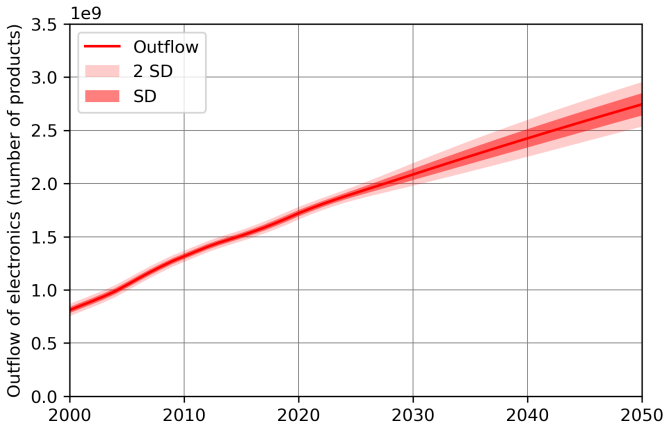

Figure 3.19: The uncertainty of the outflow of electronics.

PCB weight

The results differ after conversion to PCB mass. First of all, the uncertainty in the inflow and outflow for the historical period is slightly wider than before due to the additional uncertain variables. Interestingly enough, the standard deviation for the outflows (figure 3.21) stays at a very similar level throughout the whole period even though individual parameter uncertainty was increased after 2020. This lack of increase is likely the result of the miniaturisation process (decrease in product weight and especially PCB fraction in the product) compensating for the increased uncertainty for each variable.

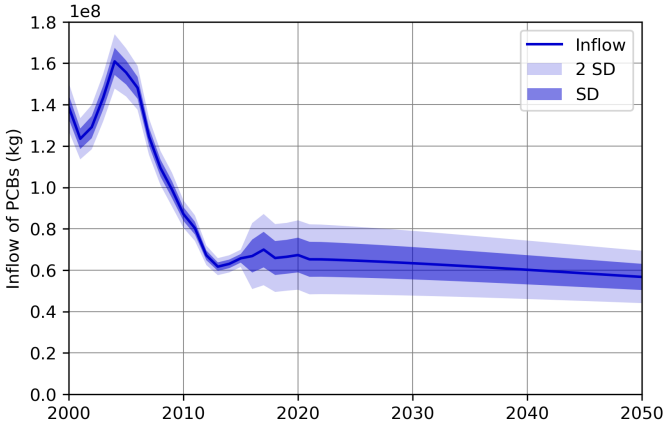

Figure 3.20: The uncertainty of the inflow of PCBs.

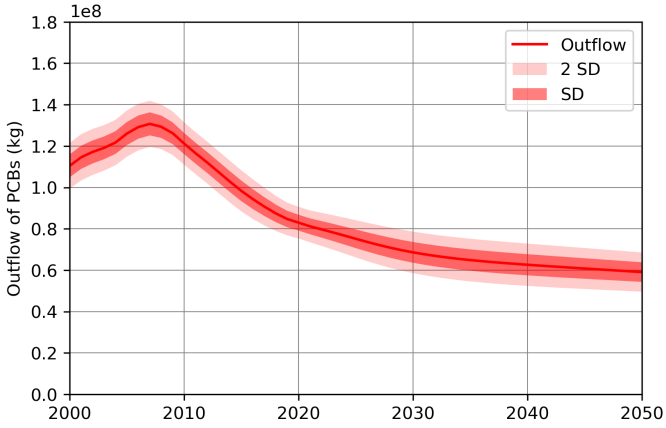

Figure 3.21: The uncertainty of the outflow of PCBs.

Precious metal flows

As can be seen in figure 3.22, the maximum precious metal flow follows a very similar trend to the PCB weights from figure 3.21. It starts high with a maximum of 4,133.38 kg in 2008 and decreases over the years. Furthermore, the standard deviation stays very similar over the years with SD being 10.69% of the mean for 2008 and 10.64% for 2050. This shows that the relative uncertainty stays similar even thought the absolute flows do decrease.

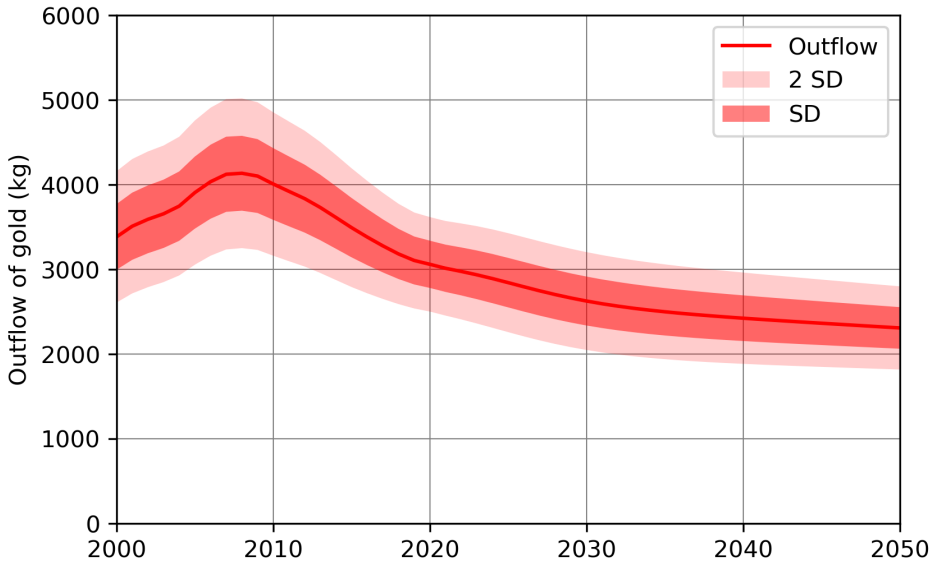

Figure 3.22: The uncertainty in the gold outflow.

As figure 3.10 shows, the recovered gold shows a very similar trend to the maximum gold outflow. However, due to the introduction of more variables (collection rate, separation and metallurgical efficiency) the uncertainty in the results has slightly increased to 12.29% for 2050. This once again shows that additional input variables increase the uncertainty of the overall model.

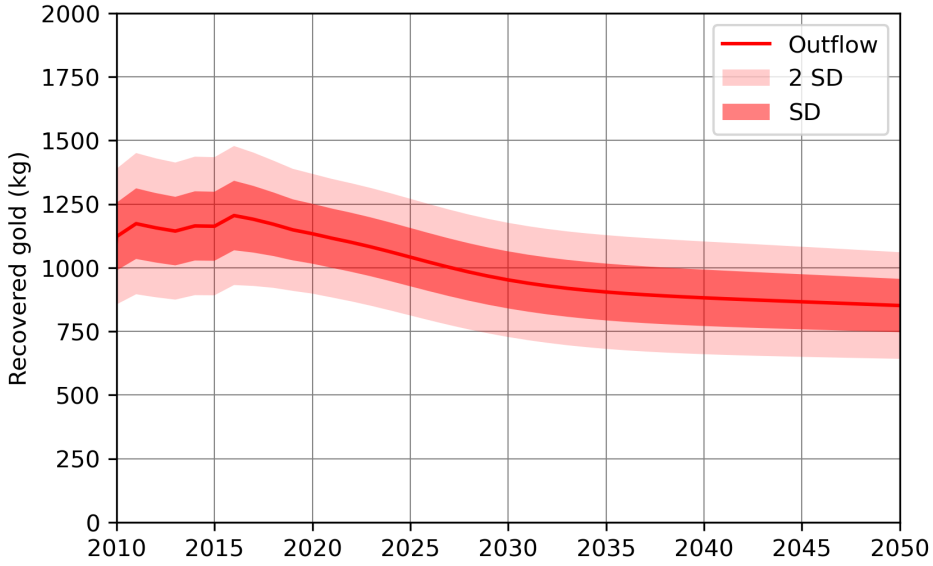

Figure 3.23: The uncertainty in the gold outflow of the recycling system.

3.4.2. Sensitivity analysis

In order to evaluate the robustness of the model multiple sensitivity analyses were performed. Each evaluated a different part of the model and its underlying assumptions. In all cases the recovered gold over the years was taken as the final indicator.

Non-limited multiplying factors

Several of the input variables behaved in a similar manner to changes (+25%) in their input, as can be seen in figure 3.24. This was the case for the overall population, inflow per capita, product weight, PCB fraction and metal concentration. Each of these variables is a direct non-limited multiplication in the model. Therefore, it there is no specific difference between final outflows between these variables.

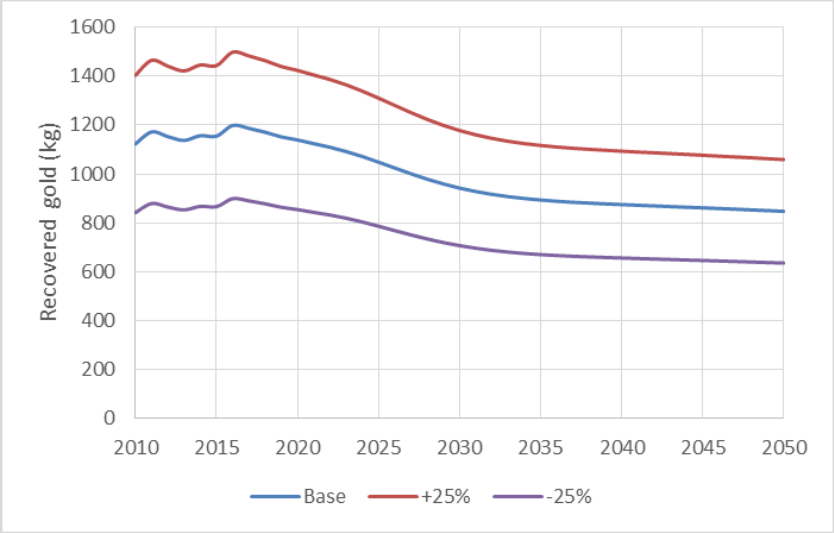

Figure 3.24: The model's sensitivity to changes of the non-limited multiplying factors.

Limited multiplying factors

This was not the case for the limited multiplying factors collection rate and metallurgical efficiency. When increasing (+25%) their inputs some of the values went over 100% and were thus limited. This in turn resulted in a less than 25% increase in the final recovered outflow. It should also be noted that this could be the case for the PCB fraction (currently non-limited) as well, yet it should increase 500% to be the case.

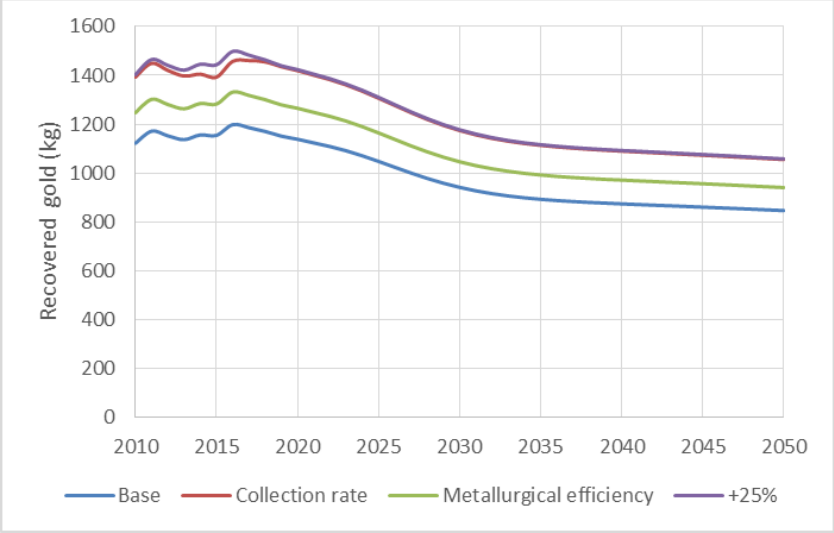

Figure 3.25: The model's sensitivity to changes of the limited multiplying factors.

Survival curves

As can be seen in figure 3.26, increasing the shape or scale has quite a strong effect on the short and medium term. In the case of the shape a higher outflow is found (as the median lifetime decreases), while slightly lowering the flow around 2030. The opposite happens when increasing the scale, which stretches the survival curve and thus lifetime, which results in more outflows on the medium term. However, in both cases there is a negligible difference on the long term (2050). This is likely the result of the smooth inflow due to the linear assumptions.

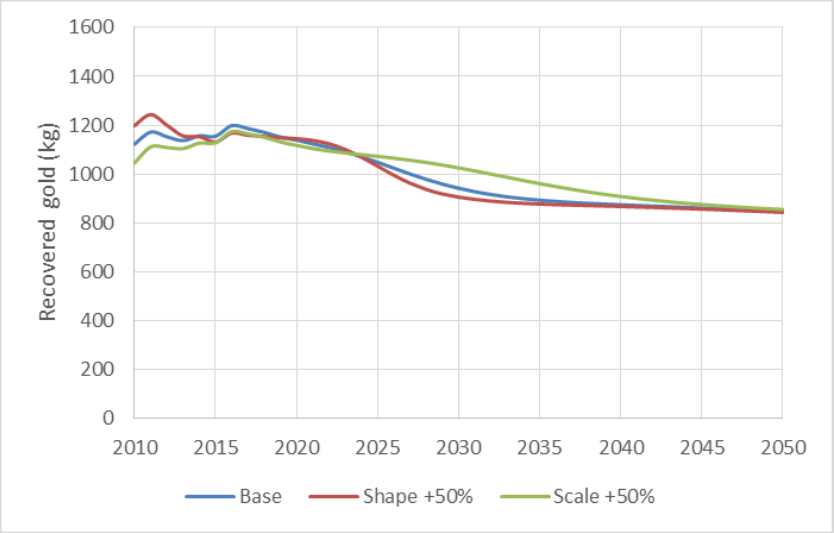

Figure 3.26: The model's sensitivity to the shape and scale of the survival curves.

Inflow per capita

As the linear inflow assumptions create such a strong effect on the long term, these were also evaluated. In the original model a mixture of linear trendlines (no trend, last 10 years, last 20 years and last 40 years) were used depending on the product category. If one of these assumptions is applied to all products categories a strong effect on the final outflow can be found (see figure 3.27). The lowest recovery is expected if no linear assumptions are made at all and the current consumption per capita is continued (Current value). The strong overlap between the base model and the long term trend (last 40 years) are due to the fact that over halve of the product categories currently uses this assumption. This in turn also means that the product categories that use the other assumptions produce a trivial amount of recoverable gold.

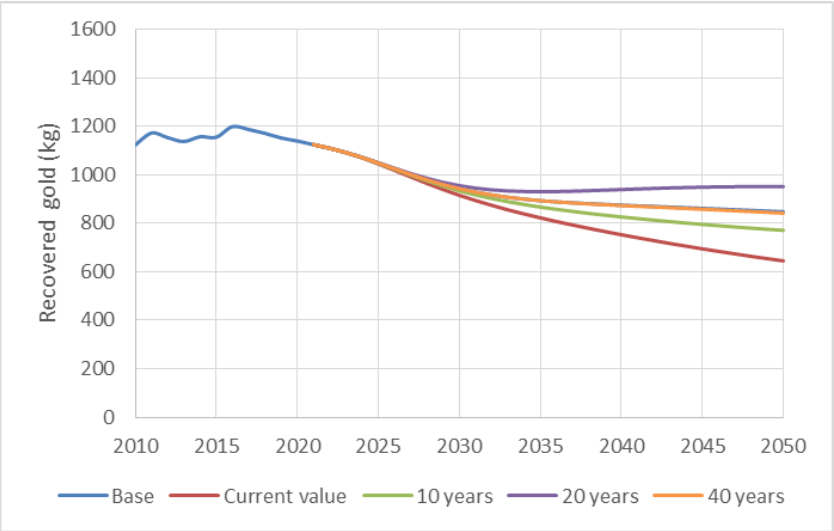

Figure 3.27: The model's sensitivity to the assumption of the inflows.

WEEE categories

Lastly the model's sensitivity to the three different WEEE categories was investigated. As can be seen in figure 3.28, increases to category IV have a trivial effect on the final recovered gold while category II and V have similar effects. This once again shows that category IV products are not of great importance to gold recovery. This is also in line with the previous section as many category IV products do not use long term inflow trends, but use stable inflows per capita. Yet it was slightly unexpected as collection rates and product weights for category IV are high (e.g. 81% in northern europe and 43.3 kg for product 102).

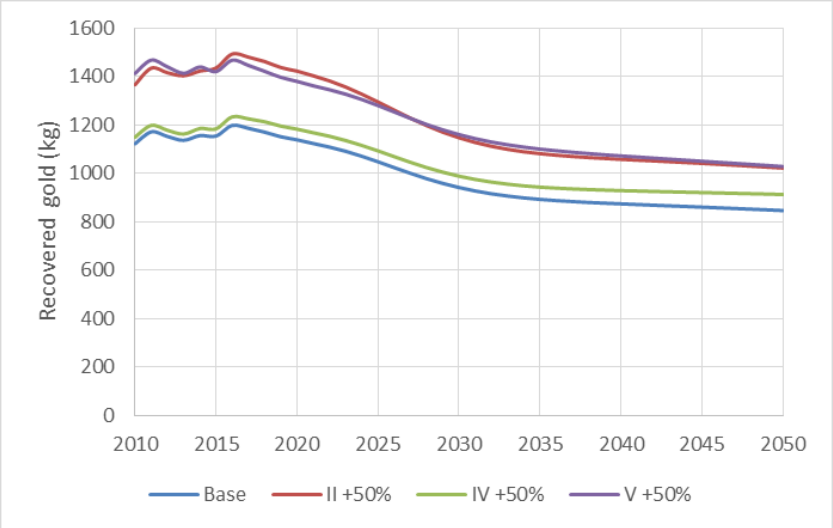

Figure 3.28: The model's sensitivity to the three different WEEE categories.

3.5. Conclusion

This chapter analysed the third and fourth research questions of the thesis:

How much precious metals can be recovered in the EU from low and medium grade WEEE PCBs in the year 2050 using separation technologies?

How variable are the precious metal flows under different scenarios and due to model sensitivity?

It was shown that only a small fraction of the EU's demand for precious metals (4.02% for palladium, 4.23% for gold and 4.22% for silver) can be satisfied using secondary production from low to medium grade WEEE. However, these fractions are likely lower due to significant losses during collection (52.50 wt%), component separation (6.75 wt%) and metallurgical recovery (4.07 wt%) for an effective recovery of 36.68 wt%. Thus it can be stated that a stronger emphasis should be placed upon collection. Yet the effects on the electronics sector itself can be quite significant with potentials of over 10% with incomplete collection.

This chapter also discussed different potential futures using scenarios and the model's uncertainty and sensitivity using Monte-Carlo simulations. It was once again shown that collection rates play an important role combined with consumption per capita and product lifespan. By increasing the products' lifespan less consumption is required, which in turn increases the systems effectiveness (as demand decreases). However, this also means that recovered outflows will decrease. Additionally, it was shown that the uncertainty in the outflows is relatively small with a maximum standard deviation of 12.29% of the mean in 2050. Lastly the model shows a strong degree of convergence on the longer term for a lot of variables. However, some parts are more impactful (e.g. assumptions about inflow correlations) than other (e.g. survival curves).

4

Critical raw materials

This chapter aims to tackle the fifth research question of this report:

To what degree can the separation system improve the recovery of critical raw materials and what would the impact on their criticality be?

In total eight different CRMs were evaluated in this thesis: barium, beryllium, cobalt, magnesium, antimony, titanium, vanadium, platinum and palladium. All were evaluated on their material flows and three on their criticality as well.

4.1. Raw material flows

The material flows were evaluated using the previously established MFA system for precious metals. This system was developed with (metal) modularity in mind and could thus easily be adapted. The only change that had to be made were the addition of the metal concentrations for the CRMs. A paper by *Huang et al.* provided data on multiple metals including the critical raw materials Ba, Be, Co, Mg, Sb, Ti, V and Pt in different types of components [127]. However, their component categories did not align with the Peacoc component categories and were thus converted (see appendix A.10).

For the bare PCBs multiple papers were used to determine the CRM concentrations (see appendix A.11). However, no concentrations were found for titanium or vanadium. Furthermore, as not all papers looked at the same grade PCBs (e.g. populated or bare), the results were also shown for both the boards and components separately. Data for Pd was taken from the previous chapter.

For the calculation of the criticality score a number of assumptions were made. First, the introduction of a new recycling pathway will generate a new secondary raw material flow. It was assumed that the collection rate is 100% and metallurgical efficiency is 90%, while the separation efficiency depended on the proposed setup. This secondary flow will in turn increase the EoL-RIR, where it was assumed that primary consumption goes down due to the increase of secondary production to keep total input constant. For the raw material inflows of the EU, the CRM-factsheets were used [8]. In accordance to the EU's CRM methodology, secondary production is a risk free SR dampener but does not impact the Import Ratio or HHI [87]. Lastly, EI is not impacted/changed as EoL recycling does not directly impact this axis.

4.1.1. Results

An overview of all outflows and their ratios compared to the EU's total input for 2020 can be seen in table 4.1. Here it can be seen that only four CRMs (beryllium, antimony, platinum and palladium) have any potential for supplying a part of the current consumption (defined as more than 1.0%). However, when only looking at the electronics sector two others (cobalt and vanadium) should also be able to have a significant impact. The consumption for the electronics sector also included batteries and magnets if those were used for electronics [8].

Table 4.1: The maximum potential flows in 2020 for all the CRMs and their ratio compared to current (2020) consumption.

Metal	Ba	Be	Co	Mg	Sb	Ti	V	Pt	Pd
Maximum outflow in bare PCBs (ton)	13.45	1.25	107.75	40.78	191.15	N.A.	N.A.	0.81	1.94
Maximum outflow in components (ton)	217.81	2.17	67.70	529.04	222.15	407.07	16.93	0.03	0.43
Maximum outflow both (ton)	231.26	3.43	175.45	569.81	413.30	407.07	16.93	0.84	2.37
Raw consumption all products (ton)	506,000	37.5	36,203	113,000	17,023	1,509,000	12,717	63.9	59.0
Ratio all products	0.05%	9.13%	0.48%	0.50%	1.58%	0.03%	0.13%	1.32%	4.02%
Raw consumption electronics (ton)	N.A.	15.75	3,258.27	N.A.	11,261.70	90,540	127.17	2.56	2.36
Ratio electronics	N.A.	21.75%	5.38%	N.A.	3.67%	0.45%	13.31%	32.91%	100.45%

4.2. Beryllium

Beryllium is one the CRMs that currently has no primary or secondary production in the EU and is thus a supply risk to the EU (SR is 2.29 for 2020). At the moment the majority (55%) of beryllium is imported from the USA and the metal is mainly used in the production of Electronics and telecommunications (42%), and Transport and Defense (44%) [8]. No production of beryllium alloys, metal or oxides currently takes place within the EU, thus creating an import reliance of 100%.

According to the SCRREEN project, beryllium recycling from post-consumer scrap is currently not taking place. The main reasons cited are the low concentrations and dilution (2 ppm) in its most common form (alloyed copper) [128]. Furthermore, the low price of beryllium (500 USD/kg) makes recovery currently not economically viable [8]. Therefore, any beryllium recovery will have to find other ways to be achieved, such as quotas or subsidies.

4.2.1. Concentration

As can be seen in figure on the right, only a very limited amount of components contain the beryllium. Furthermore, there is a strong overlap in components that contain precious metals and beryllium. This is advantageous as the same separation setup for precious metals can likely be employed with some small modifications. These modifications are needed to capture the *Blue capacitors* as well. The *Blue capacitors* can all be found in the lightly magnetic 2.5 - 3.0, 3.0 - 5.0 and 5.0 - 7.0 mm sieve sizes. The 2.5 - 3.0 mm sieve size is already captured with the precious metals and can thus be ignored. However, the grades for the 3.0 - 5.0

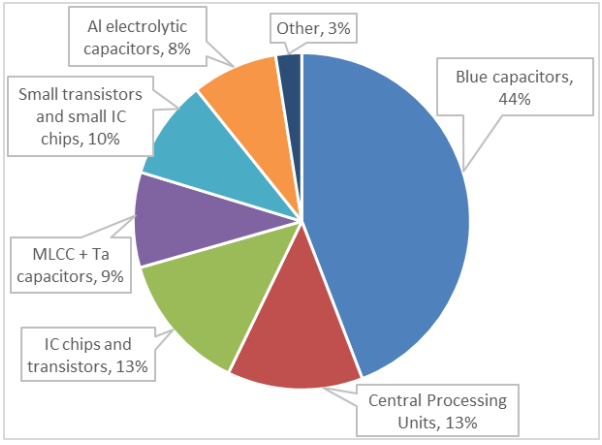

Figure 4.1: The weight distribution of beryllium.

and 5.0 - 7.0 are quite low at 21 and 4 wt%. Therefore, further upgrading will likely have to take place.

In both cases the major contaminants are *AI electrolytic capacitors* and *Inductors and transformers*, which if removed would increase the grade to 51 wt% (3.0 - 5.0 mm) and 85 wt% (5.0 - 7.0 mm). This could be achieved through shape separation as both *AI electrolytic capacitors* and *Inductors* are cylindrical in shape while *Blue capacitors* are not. Heavy liquid density separation might also be possible if a density based method is preferred. MDS is not an option as all components are too magnetic in nature. If these additional separation steps are achieved 89.45 wt% of all beryllium from components can be captured for an average concentration of 53.09 ppm in the final mixture.

As it can be seen as an additional step to the precious metal recovery a synergy could be developed. For instance if the removal method chosen for the precious metals also dissolves beryllium, the costs for beryllium recovery can be decreased. This will likely also further increase concentrations, further closing the gap to financial viability.

4.2.2. EoL-RIR and Criticality

As mentioned above, the maximum outflow for 2020 was 3.43 tons of which 2.88 tons would be recovered using the proposed separation system (89.45 wt% of beryllium in components and all in the PCBs). This will in turn result in an EoL-RIR of 7.67% assuming consumption stays at the same level. As this recycling rate is still very low it will only reduce the SR score from 2.29 to 2.11, thus it remains a critical material.

As mentioned before, only a small amount of beryllium is used as a pure metal (5.6 tons per year) [8]. Thus if this 2.88 tons of secondary beryllium is used in this niche an EoL-RIR of 51.37% could be achieved, significantly reducing this application's criticality.

4.3. Cobalt

Cobalt is one of the most contentious CRMs due to its human rights issues and conflicts during the mining stage [129]. This can also be seen in its SR score of 2.54 for the mining stage even though there is an EoL-RIR of 22%.

4.3.1. Concentration

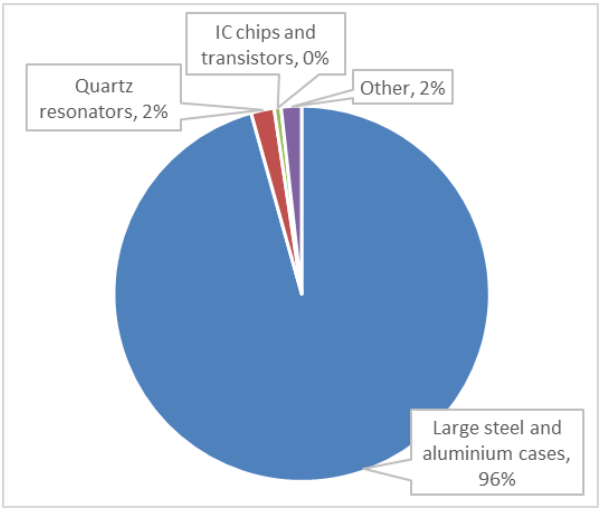

Figure 4.2: The weight distribution of cobalt.

As can be seen in figure 4.2, over 95 wt% of the cobalt is located in the *Large steel and aluminium cases*. Therefore, one should focus on collecting these separately from the other components. This can easily be achieved as 95% of all the *Large steel and aluminium cases* are both larger than 8.0 mm and magnetic at a grade of 64%. This can likely be further upgraded by sieving or visual separation as they are both larger than other components and have a metallic colour. However, it should be noted that this is a very one sided result for the components and that more cobalt can be found in the bare PCB than the components.

4.3.2. EoL-RIR and criticality

As mentioned before, only very little cobalt can be recovered compared to the EU's overall consumption. Therefore, its effect on the EoL-RIR and criticality score are negligible. However, when specifically looking at the electronics sector it could supply around 5.15 wt% of the required input, showing significant yields.

4.4. Antimony

Antimony is an interesting CRM due to several factors. First of all, it has no production during the extraction stage within the EU, yielding an extraction SR of 2.01. However, the EU does play a major role during antimony refining, as can be seen in figure 4.3, resulting in a refining SR of 0.99 (not critical). Furthermore, recycling rates are (relatively) high in the EU at 28% due to functional recycling of lead-acid batteries [128]. However, almost none of this recycling yields the original metal and thus an interesting niche could be found.

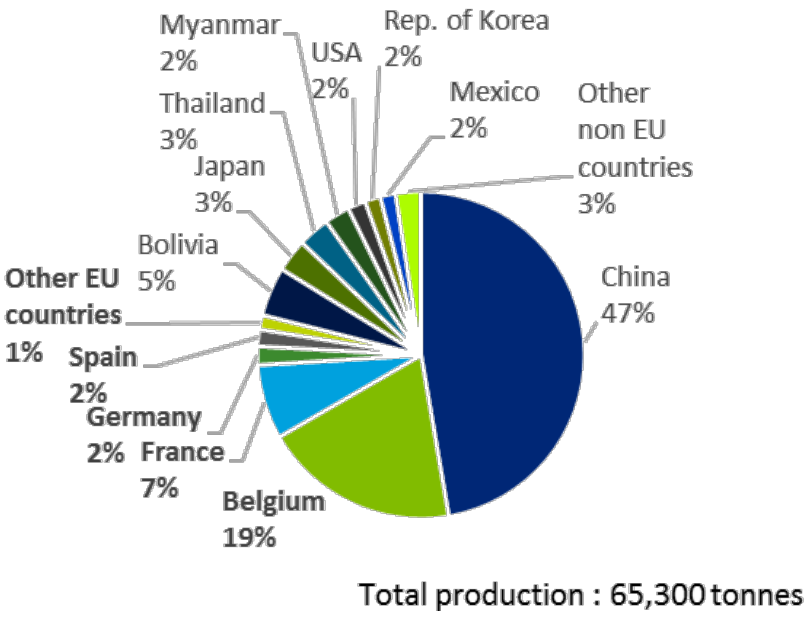

Figure 4.3: The worldwide shares of antimony trioxide production, taken from [8].

4.4.1. Concentration

Unlike beryllium only a small part (12.12 wt%) of the antimony can be found in the target components. The vast majority (48.78 wt%) is found in the *Large steel and aluminium cases*. Less is found in the *Connectors of plastic with silver pins (SCART)* (8.61 wt%) and *Rectangular connectors (USB, HDMI etc.)* (8.09 wt%). However, this might actually prove to be an advantage for the recovery of antimony as the majority of these components are found in the currently non exploited > 8.0 sieve category. If all the > 8.0 mm sieve sizes were used for antimony extraction, it should be possible to recover 74.08 wt% of the available antimony. However, further concentrating the feed using the magnetic separator is not possible as the components are both magnetic (e.g. *Large steel and aluminium cases*) and non magnetic (e.g. *Connectors of plastic with silver pins (SCART)*) Therefore, it will be advantageous to redirect the > 8.0 mm components directly to a metallurgical antimony recovery facility.

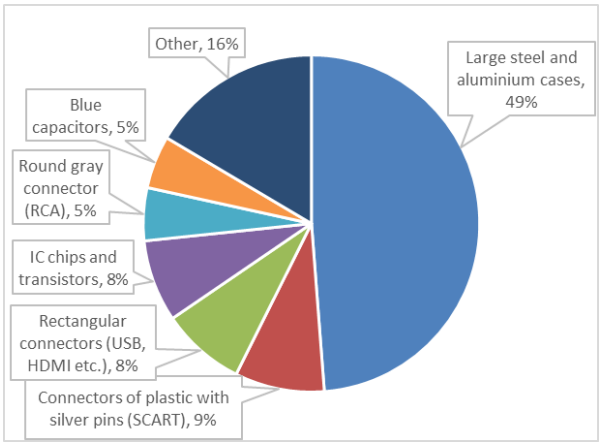

Figure 4.4: The weight distribution of antimony.

4.4.2. EoL-RIR and criticality

In total 413.30 tons of antimony are available for capture. If the bare PCBs and > 8.0 mm sieve size are properly exploited, this should result in a recovery of 320.15 tons for 2020. When comparing this to the EU's input an additional end-of-life recycling input rate of only 1.22% can be achieved. If this is added to the current 28%, the SR will decrease from 2.01 to 1.98. Once again the effects on the supply risk are minimal as the EoL-RIR only decreases marginally.

4.5. Vanadium

Vanadium might be the least interesting CRM of all discussed in this section as only very little (around 1%) is consumed by the EU's electronics sector. Furthermore, its SR is low at 1.69 for the refining stage as around 53% gets produced within the EU. Nevertheless, it should still be looked at as its EoL-RIR is currently very low at 2% and can thus be easily improved.

4.5.1. Concentration

As can be seen on the right, around 90 wt% of the vanadium is located in just two components (*Large steel and aluminium cases* and *Heatsinks*) and should thus be the focus. In the case of the *Large steel and aluminium cases* a similar approach to the extraction of cobalt can be performed. *Heatsinks* are harder to collect as only around 63 wt% of is located in one sorting category (> 8.0 mm non-magnetic). Furthermore, the grade in this category is low at 19 wt%, thus further upgrading with MDS would be required. This should be achievable as the majority of the *Heatsinks* weight is composed of aluminium and thus has a very specific density.

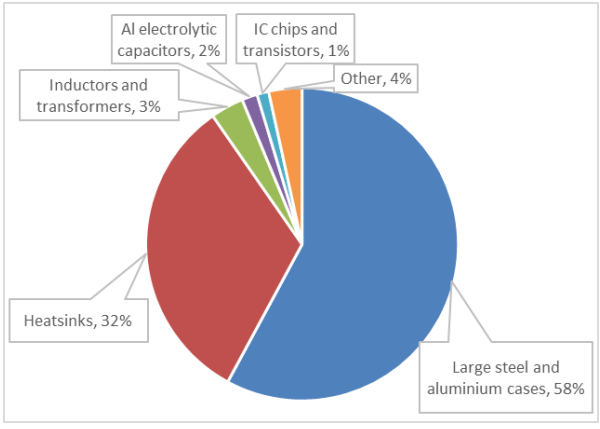

Figure 4.5: The weight distribution of vanadium.

4.5.2. EoL-RIR and criticality

Similar to cobalt, the effects on the overall EoL-RIR and criticality are inconsequential, due to the small flows (12.87 tons using the above mentioned system). However, for the electronics sector (production of batteries) it is able to supply around 10.11 wt% and can therefore have a significant impact.

4.6. Platinum and palladium

Like all PGMs (platinum group metals) platinum and palladium are critical raw materials (SR of 1.84 and 1.27). Both are mainly used as a catalyst in the exhausts of fossil fuelled vehicles (74 and 87% of consumption), therefore demand is expected to decrease over time. However, at the moment demand is still high (63.9 and 59 tons per year for the EU) and supply is limited to a few countries. South Africa (71%) and Russia (13%) are currently the worldwide leaders for platinum and palladium (Russia 40% and South Africa 37%). The EU on the other hand only produces around 1.0 tons of platinum and palladium per year in Finland and Poland [8]. Therefore, the Import Reliance is very high in both cases at 98 and 93%.

Due to the fact that almost all platinum and palladium is located in catalytic converters and their high price (28,000 and 65,000 EUR/kg) EoL recycling is already taking place with 60-70% of old scrap being recycled. However, this results in only an EoL-RIR of 25 and 28%.

4.6.1. Concentration

As palladium was already a target material for the original proposed system and the amount of platinum in the components is negligible, the setup will not be changed. Furthermore, as mentioned in section 2.1.1, the majority (82 wt%) of palladium is located in the bare PCBs and thus optimising the component separation would yield minimal results. Thus only 35.70 wt% of palladium from the components gets recovered due to the separation but 100% of the bare PCBs.

4.6.2. EoL-RIR and criticality

Around 0.75 tons of platinum is expected to be regained. Slightly more palladium gets recovered (1.88 tons) using the proposed separation system. This results in an additional EoL-RIR of 1.17 and 2.96%, respectively. Similar to the previous CRMs, the effects on the SR are again minimal. The SR decreases from 1.84 to 1.81 for platinum and 1.27 to 1.22 for palladium, leaving the metals critical. However, unlike the previous two CRMs economical viability is within reach e.g. the Peacoc and Platirus projects [25, 121]. Furthermore, both can supply a significant fraction of the demand (29.30 and 79.66 wt% respectively) that the EU's electronics sector demands.

4.7. Conclusion

This chapter aimed to answer the following research question:

To what degree can the separation system improve the recovery of critical raw materials and what would the impact on their criticality be?

Similarly to the precious metals of chapter 3, it was shown that only very little of the overall demand for critical raw materials can be met by secondary production. Only four metals (beryllium, antimony, platinum and palladium) were able to supply more than 1.00% of the demand. However in all cases, the secondary supply was again limited due to the previously stated collection rates and thus only a very limited impact on their criticality was observed. Yet, it is possible to supply a sizeable fraction of the demand in the electronic sectors in all cases (including cobalt and vanadium).

It was also shown that it is possible to concentrate the CRMs in the components. For beryllium one should aim to capture the *Blue capacitors* which are located in the lightly magnetic 2.5 - 3.0, 3.0 - 5.0 and 5.0 - 7.0 sieve sizes. Antimony on the other hand can best be found in the large components (> 8.0 mm), but was not specifically found in magnetic or non magnetic components. Both cobalt and vanadium could best be found in the *Large steel and aluminium cases*, while *Heatsinks* also held a sizebale part of the vanadium.

5

Energy requirements

This chapter tackles the last research questions as stated in the introduction:

What are the total energy requirements per kg to produce precious metals with the new separation pathway compared to primary production and conventional recycling?

To answer this question the operational energy consumption of the proposed recycling system was analysed. Each of the individual processes was separately evaluated on both the specific energy (kJ/kg input) and its actual consumption (kJ) which also took their inputs into account. This was then compared to primary production and conventional WEEE recycling methods. As the aim of this chapter is to compare the energy consumption of the recycling process, the intermediate steps (e.g. collection and transport) are excluded.

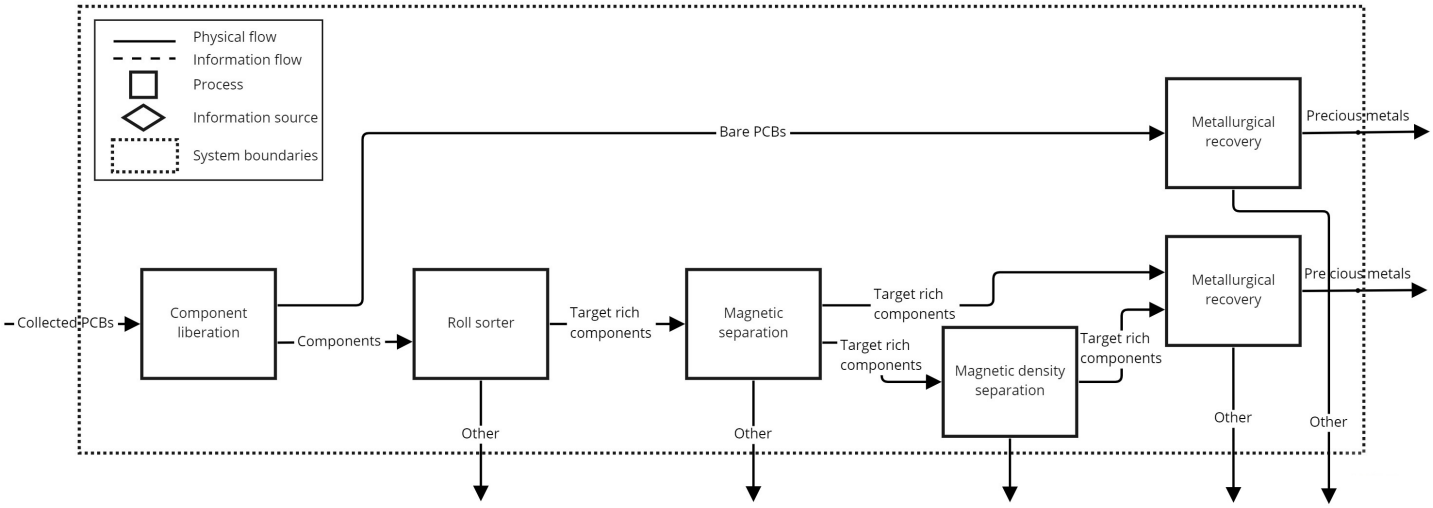

Figure 5.1: The flowchart used for the energy calculations.

It should be noted that this analysis is not a life cycle assessment and thus does not include the complete life cycle of the products or machinery. Therefore, it also does not include factors such as transport, collection or the environmental footprint of manufacturing the machines. Furthermore, the RQ will be answered using energy (Joules) and not CO_2-equivalent or use a form of impact analysis.

5.1. Required energy for every process

Component liberation

There are multiple papers discussing the removal of components from PCBs using automated machinery [130, 131]. However, none specify the actual energy requirements of these machines. Therefore, the embodied energy for this process will be estimated using data for shredding PCBs. This choice was deemed acceptable as the machinery for dismantling and shredding is similar and it is likely that shredding will still be used during metallurgical recovery to increase surface area. However, it might be an overestimation as not all components will be shredded.

In total three sources (two commercial producers and one paper) that presented energy requirements were found, as can be seen in table 5.1. The three different sources present quite a range in embodied energy and have thus been averaged to 84.51 kJ/kg input.

Table 5.1: The energy requirements per kg input for shredding PCBs.

Max capacity (kg/hr)	Power (kW)	Embodied energy (kJ/kg)	Source
500	11	80.54	[132]
3000	30	36.00	[133]
Literature		137.00	[24]
Average		**84.51**	

Roll sorter

The energy requirements for the roll sorter were determined by its power draw and throughput. Using a multimeter it was possible to measure the voltage (12 V) and current (2.56 - 2.84 A), resulting in the setups required power (W). As the rollers are rotating outwards (thus not crushing the feed) it was assumed that the size/weight of the feed did not increase the power consumption. The power draw was between 30.72 and 34.08 W for an average of 32.40 W.

In order to calculate the throughput of the device a throughput test was performed. The components from the *Test sample* were mixed together and run through the roll sorter while being timed. As the weight of the *Test sample* (112.27 g) has less than 1% deviation from the average weight of all 14 main samples (113.37 g), it was deemed representative. To further reduce variability the test was repeated five times and the average was taken.

The *Test sample* took an average of 104.6 seconds (table 5.2) to be completely processed by the roll sorter. This results in a throughput of 1.073 grams per second (3.86 kg/hr). If this is combined with the power draw an average power consumption of 30.20 kJ/kg is achieved. This energy consumption can likely be improved by increasing the speed of the components through an increased angle or roller speed.

Table 5.2: The time the *Test sample* required to pass through the roll sorter.

Run	1	2	3	4	5	**Average**
Time (s)	115	100	107	102	99	**104.6**

Magnetic separation

The energy consumption of the overbelt magnetic separator was estimated using the power consumption of a conveyor taken from Engineering Toolbox (extracted using WebPlotDigitizer) [114, 134]. This is the only operational energy that the separator requires as the magnet was a permanent magnet (as opposed to an electrical magnet).

The lowest capacity (100 t/hr) conveyor at the shortest length (7.62 m) was chosen from Engineering Toolbox [134]. This resulted in a power consumption of 1453.88 W per belt, as there are two (one feed and one on the magnet), this is doubled to 2907.76 W. Therefore, the total consumption per kg is 0.10 kJ/kg.

Magnetic density separation

The MDS requires (operational) energy in two separate steps. The feed has to be wetted in (near) boiling water and the components have to be moved through the magnetic liquid.

The energy requirements for moving the feed through the liquid using a belt were calculated by repeating the calculations for magnetic separation. However, in this case only one belt is required reducing the embodied energy to 0.05 kJ/kg.

For the calculation of the wetting a couple of assumptions and estimations had to be made. First of all, the average surface area of all the components that enter the MDS (5.0 - 7.0 mm non magnetic) were measured. These surface areas were rough estimations and depended on their shape (cylindrical or a (hollow) rectangular cuboid) as can be seen in table 5.3. This was followed by the assumption that a thin layer of 1.0 mm thick and 100°C water was deposited on the surface area. This resulted in 0.91 ml water being used for every gram of MDS feed. Lastly, it was assumed that the temperature increases 80°C (from 20 to 100°C) and stays in liquid form. Therefore, a total of 365.62 kJ/kg input is required for the wetting process.

Table 5.3: The shape and surface area of the different components entering the MDS.

Component	Number of components	Shape	Average surface area per component (mm^2)
IC chips and transistors	15	Rectangular cuboid	1242.64
Rectangular connectors (USB, HDMI etc.)	9	Hollow rectangular cuboid	1310.71
Plastic connectors with pins and others	58	Rectangular cuboid	575.46
Large steel and aluminium cases	1	Rectangular cuboid	1310.71
Inductors and transformers	3	Cylinder	223.78
Al electrolytic capacitors	150	Cylinder	223.78
Resistors	1	Cylinder	251.99
Heatsinks	1	Rectangular cuboid	1192.06
Connectors of plastic with golden pins	2	Rectangular cuboid	1310.71
Other	10	Rectangular cuboid	1310.71

Metallurgical recovery

As mentioned in 3.2, two separate steps (leaching and precipitation) are employed during metallurgical recovery and were calculated separately.

For the microwave assisted leaching, a lixiviant acid mixture (6M HCl and H_2O_2) of 150°C was used. During the Platirus project 50 ml lixiviant for every 5 grams of input was required [122]. However, as this method continued development during Peacoc it was assumed that this amount could be halved. Furthermore, due to internal recycling of the lixiviant is was assumed that heating only took place from 90°C instead of room temperature. Lastly, as microwave assisted heating is a volume based heating technology, any heating inefficiencies were ignored. This resulted in an energy requirement of 1,257.11 kJ/kg of input.

The metals are recovered during the GDEx step. Here the paper by *Nicol et al.* is once again used. It is stated that the GDEx process requires 2-6 kWh (7,200-21,600 kJ) per kg of product [122]. Using 6 kWh as the worst-case scenario this would result in 10.13 kJ per kg of bare PCB feed and 55.70 kJ per kg of components. As these are different it should be noted that the bare PCBs and components were separately calculated.

5.2. System's energy requirements

As can be seen in table 5.4, the two metallurgical steps (bare PCBs and components) are the most energy intensive of all the processes due to fact that water is heated 70°C in this process during leaching. This is also the reason that the MDS wetting process has a relatively high energy requirement. However, as the MDS feed is low this does not actually create a high energy demand. Lastly, it is once again important to note that only operational energy was calculated and any indirect emissions (e.g. production of REE's in the magnet) are not taken into account.

Table 5.4: An overview of the energy requirements of every separation step for the dismantled PCBs from chapter 2

Processing step	Energy requirements (kJ/kg)	Feed (kg)	Energy (kJ)
Component liberation	84.51	3.06	258.54
Rolling sorter	30.19	1.57	47.36
Magnetic separation	0.10	0.46	0.05
MDS wetting	365.62	0.13	46.66
MDS band	0.05	0.13	0.01
Metallurgy PCB	1267.25	1.48	1875.75
Metallurgy components	1311.91	0.30	398.58
Total			**2,626.96**

In total the whole recycling process requires around 858.69 kJ/kg of feed. As can be seen in figure 5.2, 71% of this energy is used during the metallurgical recycling of the bare PCB and only 3.58% is used during the mechanical separation steps (Rolling sorter, MDS wetting, Magnetic separation and MDS band). Therefore, it could be interesting to employ more separation steps and technologies to further increase the component grades and thus decrease the metallurgical energy requirements (as less matter enters metallurgy).

If metallurgical recycling of the bare PCB is ignored, the energy requirements decrease to 245.55 kJ/kg feed (see figure 5.3). However, this does also mean that the majority of palladium (84 wt%), silver (44 wt%) and a small amount of gold (12 wt%) is lost.

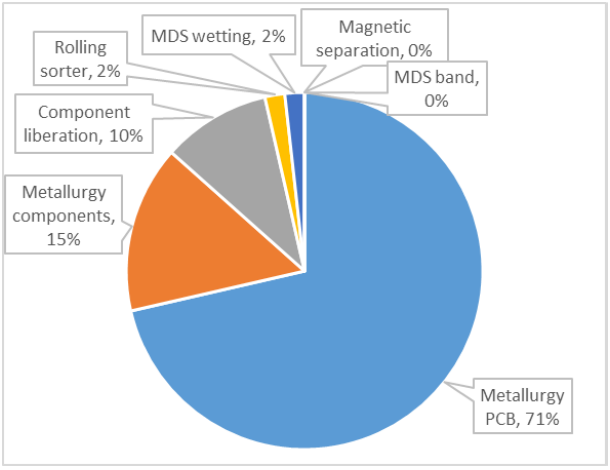

Figure 5.2: The energy distribution of the whole process (858.69 kJ/kg feed).

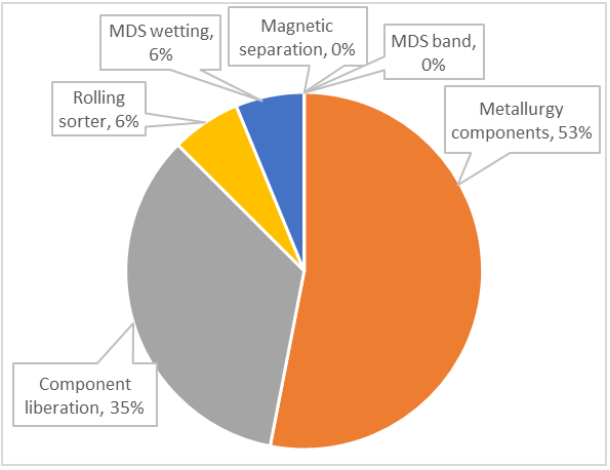

Figure 5.3: The energy distribution of the whole process excluding bare PCBs (245.55 kJ/kg feed).

5.3. Energy requirements per metal

In order to compare the energy requirements to primary production and conventional recycling, the required energy per kg of precious metal was calculated. As value is currently the main driving factor in the recycling sector, it was decided to determine allocation of the energy by monetary value of the metals (see table 5.5). As different amounts of metal were recovered and metallurgical recovery is only 90%, this energy allocation was converted to MJ per kg of the recovered precious metal.

Table 5.5: The energy requirements of the three precious metals per kg.

Metal	Recovered (g)	Value fraction	Energy allocated (kJ)	MJ per kg product
Pd	0.075	47.7%	1,253.95	**16,796**
Au	0.087	44.7%	1,174.32	**13,514**
Ag	1.157	7.6%	198.68	**172**

It can be seen that palladium and gold encompass the majority of the allocated energy, as they also represent the majority of the value. Furthermore, as their concentrations were significantly lower, the required energy to produce 1 kg of product is also significantly higher than silver.

5.4. Comparison to primary production

The first step in the comparison was to determine the energy requirements of primary production. This was achieved by calculating the embodied energy from multiple sources and averaging them out (see table 5.6). If materials were used for heating (coal and natural gas) they were converted to energy using their average heat value [135]. Furthermore, not all sources provided data for each individual metal but gave multiple together. Therefore, the total energy requirements were calculated and allocated based on the value of the metals. An example can be found in the production of silver from the ecoinvent database as “gold-silver mine operation with refinery” (Global). A total of 125,348 MJ is consumed in the production of 1.00 kg of gold and 0.48 kg silver. This was allocated to 124,588 MJ/kg for gold and 1,583 MJ/kg silver.

Table 5.6: The energy requirements for primary production from 5 different sources, all values in MJ/kg.

Metal	[24]	[136]	[89]	[137]	[138]	Average (MJ/kg)	Peacoc (MJ/kg)
Pd	167,600	-	-	55,116	308,329	**177,015**	**16,796**
Au	34,228	127,000	240,000	148,413	103,539	**130,636**	**13,514**
Ag	1,155	-	1,400	605	1,583	**1,186**	**172**

As the table shows, the energy requirements for Peacoc is around 10% of primary production for all three metals. This in turn means that significant reductions in energy consumption should be achievable compared to the current situation (assuming consumption stays the same). As mentioned in 3.2.1, around 2,371 kg palladium, 3,091 kg gold and 35,851 kg silver were available in 2020 from low-medium grade PCBs. Thus, if properly exploited a reduction of 778,200 GJ could have been achieved. This shows that secondary production is significantly more energy efficient compared to primary production.

5.5. Comparison to conventional recycling

Even though the results from the previous section prove the concept of Peacoc, they were expected as secondary production is regularly cited as more energy efficient. Therefore, a comparison to other methods of secondary production was also performed. A similar approach to primary production was taken (energy allocation based on value). For a proper comparison both pyro and hydrometallurgical methods were used. Furthermore, it should be noted that the majority of papers were focused on high-grade PCBs. Lastly, the heat value (incineration) of PCBs for the Umicore methods were ignored.

Table 5.7: The energy requirements for precious metal production from several WEEE recycling pathways, all values in MJ/kg.

	[139]	**[91]**	**[24]**		**[140]**	**[141]**			**Average**	**Peacoc**
Pd	64,406	6,554	64,120	-	9,729	-	-	-	**36,202**	**16,796**
Au	51,821	5,274	19,322	18,765	7,828	10,323	40,390	4,075	**19,725**	**13,514**
Ag	658	67	-	980	99	-	-	-	**451**	**172**
Grade	Medium	High	High	High	Medium	High	High	High		**Low-medium**
Metallurgical pathway	Pyro	Pyro	Pyro	Hydro	Hydro	Hydro	Pyro	Electro-chemical		**Hydro**

As can be seen, the proposed Peaecoc method consumes a very similar amount of energy compared to other hydrometallurgical pathways, but significantly less than pyrometallurgy. This was expected as pyrometallurgy is known to be energy intensive due to the extreme temperatures (> 1,000°C). However, it is interesting to see that Peacoc performs similar to other hydrometallurgical methods that use high grade PCBs, while using low to medium grade PCBs. A good example of the impact of grade can be seen in the first two columns. Both use Umicore's pyrometallurgical pathway (market leader in the BeNeLux), but a different feedstock (LCDs for medium grade and mobile phones for high grade) and an order of magnitude difference can be observed. Therefore it can be stated that the Peacoc method performs similar, if not better, than conventional recycling methods.

5.6. Conclusion

This chapter compared the energy requirements of Peacoc's secondary production pathway in order to answer the last research question:

What are the total energy requirements per kg to produce precious metals with the new separation pathway compared to primary production and conventional recycling?

As could be seen in figure 5.2, the vast majority of energy is spent during metallurgical recovery instead of component liberation or separation. In total every kg of feed required 858.69 kJ to be processed. This translated to 16,796 MJ/kg palladium, 13,514 MJ/kg gold and 172 MJ/kg silver. These energy requirements were significantly lower (one order of magnitude) compared to primary production of these metals. If all available precious metals from low to medium grade PCBs from the EU were captured a reduction of 778,200 GJ could be achieved which is similar to the energy requirements of the municipality of Wageningen (see appendix A.12). Lastly, the chapter also discussed other WEEE recycling methods. Here it was shown that Peacoc's method requires less energy than conventional pyrometallurgical processes but similar to hydrometallurgy.

6

Conclusion

The goal of this thesis was to present both a birds eye and in-depth view on the topic of precious and critical metal recovery from low to medium grade PCBs in order to answer the main research question:

To what extent can the waste separation technologies Roll Sorting (RS), Magnetic Separation (MS) and Magnetic Density Separation (MDS) improve the sustainability and circularity of precious and critical metals in the European Union (EU) during the recycling of low and medium grade PCBs from E-waste?

This main research question was subdivided into six sub-questions that were answered in sequence either through practical means, modelling or literature.

RQ 1: ***Which components and precious metals can be found in low and medium grade PCBs from WEEE?***

Section 2.1 of the technical case study showed the different types of components that can be found in FDP and CRT PCBs. Both types had different technological and compositional characteristics. First of all, the CRT PCBs were less heat resistant and more brittle than the FDP PCBs. Secondly, the FDP PCBs used (on average) smaller/lighter components than the CRT PCBs, showing technological advancements in miniaturisation. Furthermore, the FDP PCBs used newer types of components such as *Central Processing Units* and more *USB ports*. It was also shown that for FDP PCBs the precious metals gold and silver are located in only a limited number of component types, known as the target components (*Central Processing Units*, *Chips and transistors*, *Small transistors and small IC chips*, *Connectors with golden pins* and *MLCC + Ta capacitors*). Palladium on the other hand was concentrated in the bare PCBs with only a small amount (18 wt%) being equally distributed over nine different components.

RQ 2: ***How effectively can RS, MS and MDS separate components from low and medium grade PCBs as a feedstock?***

Chapter 2 also discussed three separation technologies (RS, MS and MDS) and their effectiveness in separating the mixture of components from FDP PCBs. It was shown that the roll sorter (RS) was especially effective in separating small (e.g. *MLCC + Ta capacitors*) and thin (e.g. *Central Processing Units*) components. All target components, except *Connectors with golden pins*, could be concentrated with negligible losses to recovery by sieving to a size of < 3.0, 3.0 - 5.0 and 5.0 - 7.0 mm at grades of 63.43, 52.91 and 17.04 wt%, respectively.

These grades could be further improved by applying a magnetic separation (MS) to the sieved components. The magnetic separator removed strongly and lightly magnetic components from the feed. A stationary overbelt magnet was employed to remove the strongly and lightly magnetic particles, requiring a maximum field strength of 33.30 and 92.90 mT magnetic field, respectively. This process removed undesirable components such as *Quartz resonators*, *Inductors and transformers* and *Blue capacitors*. The majority of target components were non magnetic, except for a small fraction in the < 3.0 mm sieve size which were lightly magnetic. Therefore, only the strongly magnetic particles were removed in the < 3.0 mm sieve sizes. The grades of the target components improved to 65.12 (< 3.0 mm), 80.58 (3.0 - 5.0 mm) and 26.24 (5.0 - 7.0 mm) wt%.

As the grade for non magnetic 5.0 - 7.0 mm sieve size was still low (26.24 wt%), this was further upgraded using magnetic density separation (MDS). Using a magnet, this allowed the removal of non-desirable components (e.g. *Al electrolytic capacitors*) and increased the grade to 58.38 wt%. MDS should also be the preferred method for upgrading the > 8.0 mm sieve size, but this was not possible due to setup limitations.

RQ 3: ***How much precious metals can be recovered in the EU from low and medium grade WEEE PCBs in the year 2050 using separation technologies?***

Using a dynamic material flow analysis (MFA) chapter 3 showed that only a small amount of precious metals can be recovered from low and medium grade WEEE in the EU. For example, in the year 2020 the expected gold recovery can only cover 1.73% of the EU's demand for gold. This is due to several factors. First, low and medium grade PCBs possess low concentrations of precious metals. Secondly, only half of the maximum potential can currently be exploited due to mediocre collection rates around 50%. The separation system and metallurgical recovery lose a small amount of the precious metals as they are within the non-target components. However, the effects on the electronics sector are significant (over 10% of raw consumption) as a lot of electronics are imported from outside the EU. Lastly, the potential is expected to decrease over the years due to changes in product demand and the miniaturisation of electronics.

RQ 4: ***How variable are the precious metal flows under different scenarios and due to model sensitivity?***

The MFA model was evaluated under five different scenarios and a Monte-Carlo sensitivity analysis. The scenarios ranged from Business as Usual, sustainability focused (Goals and CE), economic decline (Decline) and extreme consumerism (Consumption). These scenarios once again showed the importance of collection rate and the miniaturisation process on the final recovered gold. For example, the Goals (higher collection rate) and Consumption (higher consumption) scenarios performed relatively similar in final recovered gold even though their storylines differed significantly. The Monte-Carlo uncertainty analysis showed that the model had a stable uncertainty over the whole period with a standard deviation of 10.69% of the mean. It also showed that the model is more sensitive to uncertainty to some variables than others such as the different product categories and their assumptions about continued inflows.

RQ 5: ***To what degree can the separation system improve the recovery of critical raw materials and what would the impact on their criticality be?***

As chapter 4 showed, a multitude of CRMs could be recovered from low to medium grade PCBs. However, for the majority of CRMs a negligible amount compared to the EU's demand could be recovered. Only in the case of beryllium (9.13%), antimony (1.58%), platinum (1.32%) and palladium (4.02%) more than 1% of overall demand could be supplied. A more sizeable fraction could be recovered for the electronics sector with cobalt and vanadium also being relevant. For beryllium it is suggested to gather and further upgrade the *Blue capacitors* located in the lightly magnetic 3.0 - 5.0 and 5.0 - 7.0 mm sieve fractions. For antimony, platinum and palladium a large fraction could be found in the bare PCBs with the > 8.0 mm size of components also containing the a sizeable amount of antimony. However, in all three cases the final effects on the supply risk (SR) of the CRMs were low, a decrease of 7.67, 1.70,

1.56 and 4.10% for each respectively.

RQ 6: ***What are the total energy requirements per kg to produce precious metals with the new separation pathway compared to primary production and conventional recycling?***

In the last chapter (5) the energy requirements of the proposed Peacoc recovery process was compared to primary production and current recycling methods. It was shown that metallurgical recovery of the components and the bare PCB were the most energy intensive steps of the process at 15 and 71%, respectively. However, the energy requirements (16,796 MJ/kg for gold, 13,514 MJ/kg for palladium and 172 MJ/kg for silver) were still an order of magnitude lower compared to primary production for all three metals. Compared to conventional pyrometallurgical recycling methods less energy was required, but performed similar or slightly worse to other hydrometallurgical pathways. Yet in most other cases higher grade PCBs were used in these methods compared to Peacoc.

Main RQ: *To what extent can the waste separation technologies Roll Sorting (RS), Magnetic Separation (MS) and Magnetic Density Separation (MDS) improve the sustainability and circularity of precious and critical metals in the European Union (EU) during the recycling of low and medium grade PCBs from E-waste?*

It can be stated that the three waste separation technologies were effective in concentrating components containing the precious and critical metals. Furthermore, the expected primary energy demand per kg is significantly lower compared to primary production and similar to other recycling methods. However, the material flow analysis showed that the effect of recycling low to medium grade discarded PCBs will be minimal on the scale of the EU as it cannot properly satisfy demand for any of the metals (precious or critical). Therefore it can be stated that this pathway cannot solve the EU's dependency on primary production and its associated emissions, but could be a part of the overall solution.

6.1. Limitations and recommendations

The methods employed in this thesis had a number of limitations with regards to data collection, modelling and the experiments. Therefore these will be shortly discussed. Additionally, recommendations for further research will given.

6.1.1. Component liberation

The first research question had a couple of limitations. First of all, only a small number of PCBs were investigated (14 FDP and 3 CRT), which were all removed from visual displays, this limited the research for all other product categories. Consequently, assumptions with regards to the other categories had to be made using FDP and CRT data as a proxy. Therefore it is recommended to explore more low to medium grade PCBs from other product categories, such as Dishwashers or Household medical. The same holds for the precious metal concentrations for each component category, which was more limited as only FDP PCBs were analysed. This also had a strong impact on the data accuracy of the MFA model as was shown in section 3.4. Lastly, the metal concentrations for *Large steel and aluminium cases* were uncertain, therefore these were removed from the calculations.

6.1.2. Roll sorter

Several limitations were found for the roll sorter. First of all, a large weight fraction (66 wt%) of the components could not be sorted as they were too wide for the sieve sizes (maximum of 8.0 mm).

Secondly, the rollers' diameter was too narrow for some components to stay between them and should thus be increased. This effect was especially pronounced for some of the larger *IC chips*, which would tip over the rollers due to their length (see figure 6.1). Lastly, the roll sorter cannot be scaled-up to increase capacity as all the particles have to go single file through the machine. Therefore, it is not possible to increase capacity by increasing the size of the machine and instead multiple parallel roll sorters are required.

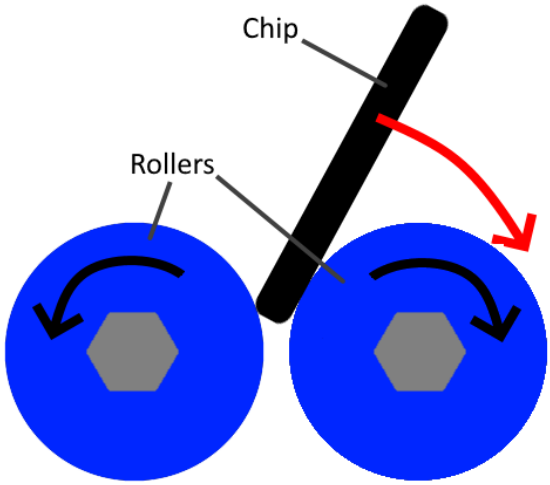

Figure 6.1: An example of how large (in length) particles, such as IC chips, tip over the rollers.

6.1.3. Magnetic separation

The main limitation of the magnetic separator was the strength of the magnetic field on the components. As mentioned in 2.4.1, some slightly magnetic components were found during the MDS experiments. This shows that the magnetic separator was not sufficient for removing all the magnetic components. Furthermore, the setup used was not automated as the belts were removed due to age. This might limit the data's applicability to large scale magnetic separators.

6.1.4. Magnetic density separation

As mentioned before, the major flaw with the MDS setup was the size of the gutters. As these were too narrow the larger sieve size (> 8.0 mm) components could not be run through the setup. Furthermore, the magnetisation of the liquid was unclear. According to the supplier (Ferrotech) the magnetisation should be around 5000 A/m, yet from tests based on the liquid's density it should be around 4000 A/m. However, this new magnetisation did not seem to align with observations for the aluminium *Heatsinks* which point to a magnetization of 2700 A/m.

6.1.5. Material flow analysis

One of the main limitations of the model was the aggregation of the EU-27 into four regions. Even though the countries in each region behaved similar, it did remove specificity and simplified the model. Secondly, the model heavily relied on the ProSUM project. This over-reliance might have impacted objectivity to the project and give a one-sided view of the WEEE problem at hand.

Consumption per capita

One of the other major limitations were the assumptions about the consumption per capita. In all cases these were modelled as linear correlations of (recent) trends or kept at the levels of current years. Initially, it was tried to couple consumption to other exogenous factors such as income, GDP per capita

(purchasing power parity) or heating days as strong correlations have previously been found for WEEE [142–144]. However, these correlations were not found for the majority of product categories and should thus be further explored using methods such as system dynamics. Furthermore, as the author's background knowledge of economics and consumer behaviour was not deemed strong enough, it was decided to simplify the consumption to the linear correlations. A second limitation was the discrepancies between ProSUM and PRODCOm data as previously discussed.

Population growth

As was shown in 3.4, the population growth had an almost negligible effect on the sensitivity of the model. This is likely unrealistic as population is one of the driving forces in total consumption (eq 3.10). Therefore it is recommended to further investigate the population variable instead of the population growth.

Survival curves

Two main limitations for the survival curves could be found. First, all the curves stayed unchanged in the model (not changing in later years) and were the same for all countries. This could be resolved by a deeper investigation in the topic and the use of different curves for the different regions. Secondly, the impact of the shape variable was significantly lower than expected and was possibly chosen too conservative.

Collection rate

As previously discussed, the collection rate for WEEE category II (Screens) was likely an overestimation of the actual value as many countries (7 out the 27 for 2015) had a collection rate over 100%. Furthermore, not all countries had data available for 2019 (Cyprus, Greece, Malta and Romania) and these were therefore not included in the dataset. This could have skewed the collection rates, as their collection rates were lower than the average for the 2010-2015 period. Lastly, the collection rates were measured per WEEE category instead of product category. The data, on product category level, was requested from Stichting OPEN (Dutch WEEE consortium), but access was denied. Therefore it is recommended to find alternative pathways for collecting this information.

Metallurgical recovery

The main limitation of metallurgical recovery is that the method is currently in active development within the Peacoc project. Therefore, accurate data could not be found and the assumption based on Platirus and similar processes had to be made.

6.1.6. Critical raw materials

The biggest limitations for the CRMs were the different sources for CRM concentrations. First of all, a conversion between the components by the paper of *Huang et al.* and the Peacoc component types had to be made. Not all Peacoc component types were available in the paper (e.g. *cables*) or were merged (all ports/connectors). Secondly, it was not possible to find sources in regards to bare PCBs for titanium, vanadium and platinum, thus reducing their yields. These problems could be navigated by measuring the concentrations using a method such as X-ray fluorescence or Inductively coupled plasma atomic emission spectroscopy.

6.1.7. Energy requirements

The limitations in the calculation of the energy requirements were again due to active development of Peacoc. First of all, as the PCBs of RQ 1 were manually dismantled no energy consumption could be calculated for PCB depopulation and a proxy (shredding) had to be used. At the moment ULI (Peacoc partner) is working on an automated depopulation method which is not yet completed. The same holds for the metallurgical step in development by VITO. Therefore, this topic should be reevaluated upon their completion. Lastly, the energy attribution was based on value, resulting in favourable results for silver at the cost of gold and palladium. If another measure, such as mass distribution, was chosen this would likely significantly worsen the result for silver while favouring the other two.

A

Appendix

A.1. Map of the European Union and its four regions

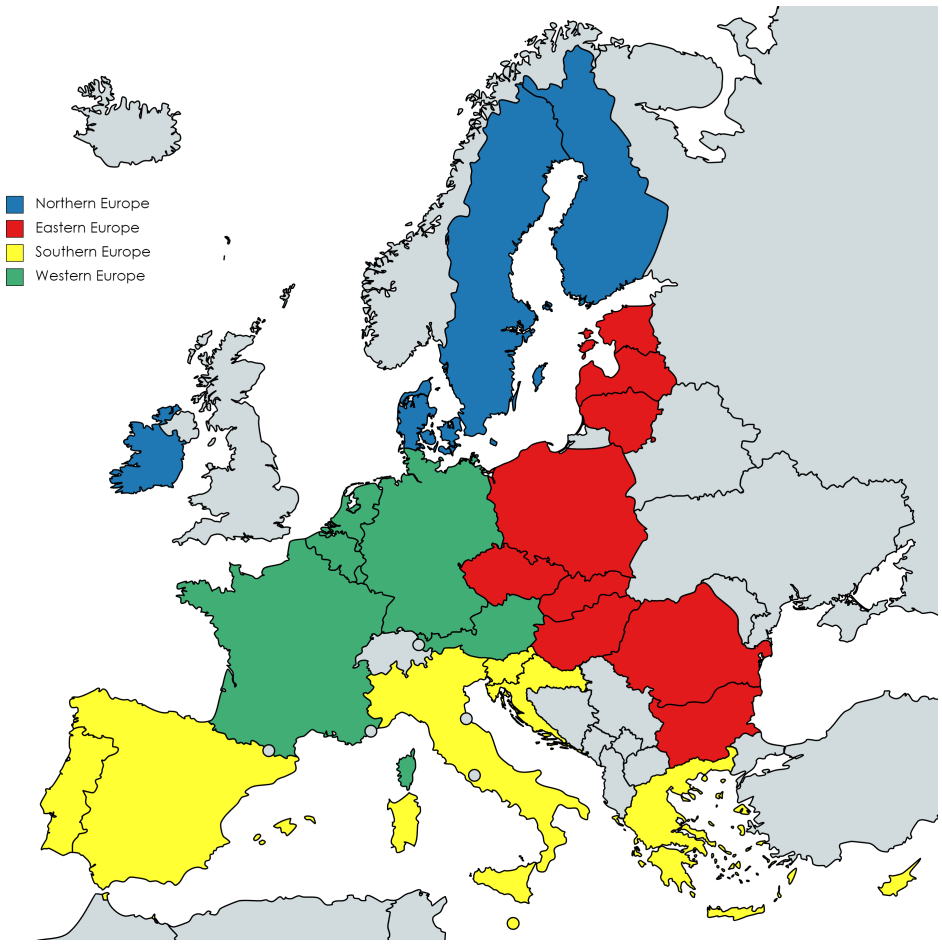

Figure A.1: A map of Europe with the EU-27 in their respective regions.

A.2. All product categories with the three PCB reference pictures

Table A.1: An overview of all product categories.

Unu key	WEEE cat.	Product category (taken from [97]
1	IV	Central heating
101	IV	Professional Heating & Ventilation (excl. cooling equipment)
102	IV	Dishwashers
103	IV	Kitchen (f.i. large furnaces, ovens, cooking equipment)
104	IV	Washing Machines (incl. combined dryers)
105	IV	Dryers (was dryers, centrifuges)
106	IV	Household Heating & Ventilation (f.i. hoods, ventilators, space heaters)
114	V	Microwaves (incl. combined, excl grills)
201	V	Other Small Household (f.i. small ventilators, irons, clocks, adapters)
202	V	Food (f.i. toaster, grills, food processing, frying pans)
203	V	Hot Water (f.i. coffee, tea, water cookers)
204	V	Vacuum Cleaners (excl. professional)
205	V	Personal Care (f.i. tooth brushes, hair dryers, razors)
308	II	Cathode Ray Tube Monitors
309	II	Flat Display Panel Monitors (LCD, LED)
401	V	Small Consumer Electronics (f.i. headphones, remote controls)
402	V	Portable Audio & Video (f.i. MP3, e-readers, car navigation)
403	V	Music Instruments, Radio, HiFi (incl. audio sets)
404	V	Video (f.i. Video recorders, DVD, Blue Ray, set-top boxes)
405	V	Speakers
406	V	Cameras (f.i. camcorders, foto & digital still cameras)
407	II	Cathode Ray Tube TVs
408	II	Flat Display Panel TVs (LCD, LED, Plasma)
601	V	Household Tools (f.i. drills, saws, high pressure cleaners, lawn mowers)
602	IV	Professional Tools (f.i. for welding, soldering, milling)
701	V	Toys (f.i. car racing sets, electric trains, music toys, biking computers)
703	IV	Leisure (f.i. large exercise, sports equipment)
801	V	Household Medical (f.i. thermometers, blood pressure meters)
802	IV	Professional Medical (f.i. hospital, dentist, diagnostics)
901	V	Household Monitoring & Control (alarm, heat, smoke, excl screens)
902	IV	Professional Monitoring & Control (f.i. laboratory, control panels)
1001	IV	Non Cooled Dispensers (f.i. for vending, hot drinks, tickets, money)

Table A.2: An overview of all product categories, including the three different pictures used (available as of 16-06-2022) and their lifespans (taken from [97]

Unu key	Proxy	PCB 1	PCB 2	PCB 3	Median lifespan (years)	Shape	Scale
1	LCD	Link	Link	Link	11.8	2.00	14.21
101	LCD	Same as unu 1			13.3	1.95	17.52
102	LCD	Link	Link	Link	14.5	1.64	14.20
103	LCD	Link	Link	Link	15.5	2.47	18.04
104	CRT	Link	Link	Link	12.9	2.20	15.16
105	CRT	Link	Link	Link	13.7	2.58	15.73
106	LCD	Same as unu 1			13.1	2.00	13.47
114	CRT	Link	Link	Link	11.7	1.90	14.07
201	LCD	Link	Link	Link	6.1	1.25	8.17
202	CRT	Link	Link	Link	9.2	2.06	11.22
203	CRT	Link	Link	Link	6.3	1.73	7.80
204	LCD	Link	Link	Link	7.8	1.45	10.25
205	LCD	Link	Link	Link	7.9	1.26	10.67
308	CRT	From RQ 1			10.7	2.41	12.53
309	LCD	From RQ 1			6.3	2.33	7.39
401	LCD	Link	Link	Link	7.5	1.30	9.87
402	LCD	Link	Link	Link	4.0	0.79	7.97
403	LCD	Link	Link	Link	4.7	2.09	5.54
404	LCD	Link	Link	Link	8.4	1.67	10.47
405	LCD	Link	Link	Link	8.5	1.49	10.78
406	LCD	Link	Link	Link	6.3	1.41	8.12
407	CRT	From RQ 1			10.4	2.49	12.08
408	LCD	From RQ 1			9.8	2.01	11.75
601	LCD	Link	Link	Link	12.2	1.82	11.28
602	LCD	Same as unu 601			13.4	2.50	15.50
701	LCD	Link	Link	Link	3.5	1.43	4.56
703	CRT	Link	Link	Link	9.9	2.40	11.56
801	LCD	Link	Link	Link	11.2	1.99	13.46
802	LCD	Link	Link	Link	11.6	2.41	13.52
901	LCD	Link	Link	Link	4.7	1.55	5.89
902	LCD	Same as unu 901			9.6	1.92	11.56
1001	CRT	Link	Link	Link	8.4	2.00	10.06

A.3. Changes made to the data from the Waste over Time script

Multiple changes were made to the data gathered from the Waste over Time script by CBS [109]. This was done in order to remove outliers in regards to average weight per product and products per capita. Overall this smoothed the inflow. The factors in the quantity and weight columns are multiplications of the original data.

Table A.3: Changes made to the data from the Waste over Time script.

Unu key	Country	Years	Quantity	Weight
1	Sweden	2015	200	200
101	Denmark	2015	10	10
	Ireland	2015		2
	Sweden	2015		2
202	Spain	2002-2007		10
	Italy	2005	5	2
		2006-2007	2	
203	Romania	2015	2	
308	Ireland	2000-2005	All years 10x data from 2004	
		1996-1999	Data extrapolated	
402	Estonia	2005	10	10
	Malta	2015	10	10
405	Romania	2006	Averaged to 2007-2011	
408	Latvia	2015	Data taken from 2014	
601	Bulgaria	2001	Data extrapolated	
	Czechia	2014-2015	2	
	Latvia	2006, 2008	2	
		2007	4	
602	Bulgaria	2000-2007, 2009-2013	0.167	
	Italy	2003-2005		2
	Malta	1980-2013	10	10
	Romania	2000-2001	Data extrapolated	
701	Austria	2014	2	
		2015	4	
	Lithuania	2003	2	2
802	Austria	2009	10	
	Denmark	2009	10	
		2010-2011	0.1	
		2012	0.5	
	Germany	2009	10	
	Finland	2009, 2015	10	
		2011-2012	0.5	
		2008-2015		10
	Ireland	2008-2009	10	10
		2010-2015	0.01	
901	Bulgaria	2013-2014	3	
	Finland	2000-2007	0.25	0.25
	Slovenia	2000	4	
		2001-2003	10	
		2004	2	
	Slovakia	2000	100	100
		2001	1000	1000
1001	Bulgaria	2014	10	10
	Spain	2000-2004	0.1	0.1
	Estonia	2014-2015	0.1	0.1
	Croatia	2003-2004	0.1	0.1
	Malta	2002-2002	0.1	0.1
	Portugal	2002-2005	0.1	0.1

A.4. Correlation between unu keys, CN and PRODCOM codes

Table A.4: The relations between the unu keys, CN and PRODCOM codes

Unu key	CN	PRODCOM
1	84031010	25211200
101	84513000	28942130
	84511000	28942250
102	84221100	27511200
103	85166010	27512810
	85166080	27512870
104	84501111	27511300
	84502000	28942230
105	84512100	27511300
	84512900	28942270
	84211200	28942300
106	84146000	27511580
	85162100	27512630
	85162910	27512650
	85162999	27512690
114	85165000	27512700
201	91011100	26521100
	91021100	26521200
	91059100	26521400
	91081100	26522110
	91070000	26522470
	63011000	27511400
	84145100	27511530
	85098000	27512190
	85164000	27512370
	84231010	28293200
	84521019	28944000
202	85094000	27512170
	85167200	27512450
	85167920	27512490
	85166050	27512830
	85166070	27512850
	85166090	27512890
203	85167100	27512430
	85161011	27512530
	85161080	27512560
204	85081100	27512123
	85081900	27512125
	85086000	27512410
205	85101000	27512200
	85163100	27512310
	85163200	27512330
	85163300	27512350
309	85285980	26403400
	85312040	27902020
	85312020	27902050
401	85181030	26404100
	85183020	26404270
402	85279900	26401100
403	85176200	26302320
	85272120	26401270
	85272900	26401290
	85198111	26403100
	85184080	26404355
	85185000	26404370
	84721000	28232110
	92071010	32201400
	85192010	399900Z8
404	85256000	26301100
	85258011	26301300
	90071000	26701500
	90072000	26701650
	90066100	26701910
405	85182100	26404235
	85182200	26404237
406	85258030	26701300
408	85287299	26402090
601	84331110	28304010
602	85151100	27903109
	85151900	27903118
	85152100	27903145
	85153100	27903154
	84672110	28241113
	84672191	28241115
	84672199	28241117
	84672920	28241120
	84672210	28241123
	84672230	28241125
602	84672290	282241127
	84672951	28241150
	84672980	28241180
	84672985	28241185
701	95030030	32402000
	95030081	32403900
	95049010	32404250
703	85437050	27904570
801	90214000	26601433
802	90181100	26601230
	90181200	26601280
	90184100	32501130
901	85311095	26305020
	85311030	26305080
	90173000	26513300
	90303310	26514300
	90251920	26515135
	90258040	26515175
	90258080	26515179
	90261021	26515235
	90261029	26515239
	90262020	26515271
	90268020	26515283
	90271010	26515313
	90248011	26516200
	90318032	26516690
	90321020	26517015
	85437060	27901150
	85318020	27902080
902	90151010	26702420
1001	84762900	28294350

A.5. Consumption trends 2021-2050

Table A.5: The chosen trends for the period 2021-2050 for each unu key.

Unu key	Trend	Unu key	Trend
1	N.A.	402	N.A.
101	N.A.	403	N.A.
102	40 years	404	N.A.
103	40 years	405	40 years
104	10 N.A.	406	10 years
105	N.A.	407	N.A.
106	40 years	408	40 years
114	40 years	601	40 years
201	N.A.	602	10 years
202	40 years	701	N.A.
203	40 years	703	N.A.
204	40 years	801	40 years
205	40 years	802	N.A.
308	N.A.	901	40 years
309	40 years	902	40 years
401	40 years	1001	N.A.

A.6. Average weight and PCB growth

308 (CRT monitor) and 407 (CRT TV) did not have data available as there were no inflows during the period of 2010-2015.

Table A.6: The average weight and PCB growth/decline for each unu key over the period 2010-2015.

Unu key	Average weight growth	Average PCB fraction growth
1	0.00%	0.00%
101	-4.53%	0.00%
102	-0.01%	-2.29%
103	0.00%	-18.78%
104	0.02%	-9.66%
105	0.00%	-5.08%
106	0.42%	10.69%
114	0.01%	-11.17%
201	-0.14%	0.15%
202	-0.87%	-8.98%
203	1.54%	-6.01%
204	0.04%	-6.16%
205	-0.03%	-5.16%
308	N.A.	N.A.
309	0.01%	-6.02%
401	0.00%	-5.08%
402	0.24%	-7.06%
403	0.90%	-2.55%
404	0.00%	-5.36%
405	0.82%	-5.73%
406	0.09%	-10.17%
407	N.A.	N.A.
408	-6.33%	-2.70%
601	0.07%	-6.96%
602	1.00%	-0.26%
701	-0.02%	9.52%
703	0.00%	0.48%
801	0.00%	-5.63%
802	8.31%	-0.31%
901	0.52%	-6.98%
902	0.00%	-1.18%
1001	0.00%	-2.05%

A.7. Collection rates

Table A.7: The collection rates for WEEE category II (Screens).

Region	2010	2011	2012	2013	2014	2015	2016	2017	2018	2019
North	92%	100%	100%	100%	100%	100%	98%	95%	92%	86%
East	32%	37%	42%	44%	41%	47%	57%	63%	68%	76%
South	38%	45%	44%	50%	49%	56%	66%	68%	70%	72%
West	67%	76%	81%	82%	86%	88%	86%	82%	78%	73%

Table A.8: The collection rates for WEEE category IV (Large equipment).

Region	2010	2011	2012	2013	2014	2015	2016	2017	2018	2019
North	71%	66%	62%	63%	66%	64%	69%	73%	77%	81%
East	38%	39%	38%	37%	47%	48%	59%	64%	67%	74%
South	29%	29%	25%	25%	29%	32%	39%	44%	48%	43%
West	43%	42%	41%	41%	45%	46%	53%	60%	66%	70%

Table A.9: The collection rates for WEEE category V (Small equipment).

Region	2010	2011	2012	2013	2014	2015	2016	2017	2018	2019
North	45%	45%	41%	42%	37%	36%	34%	33%	31%	30%
East	27%	28%	27%	26%	31%	33%	33%	31%	29%	34%
South	15%	15%	14%	13%	18%	17%	22%	23%	24%	21%
West	30%	31%	31%	32%	32%	31%	32%	33%	34%	35%

A.8. Palladium and silver flowcharts

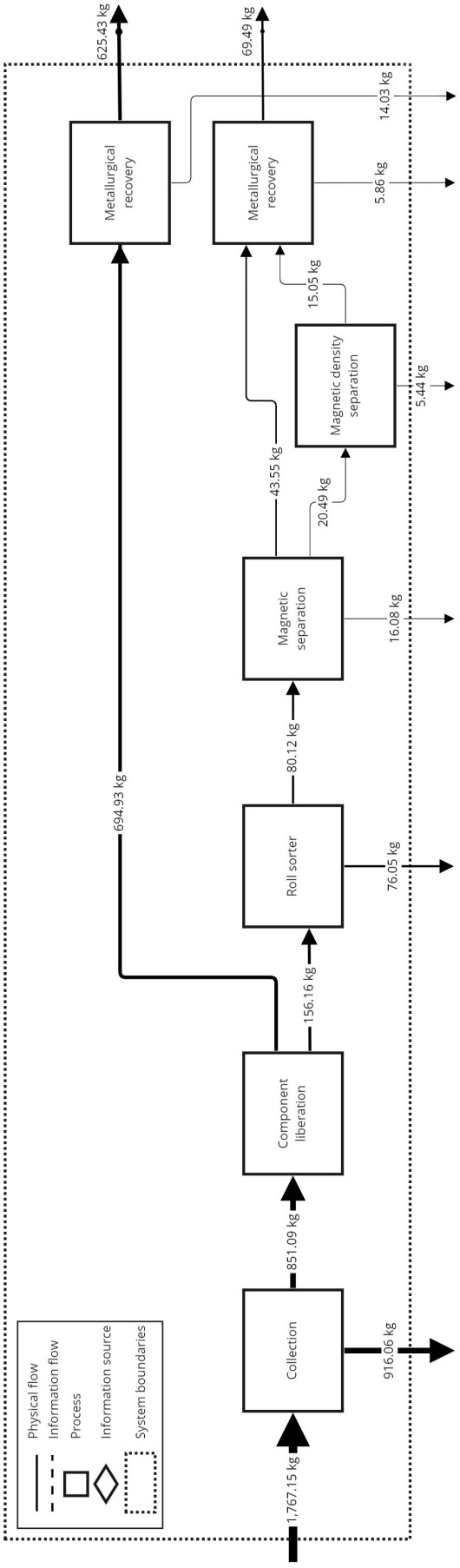

Figure A.2: The palladium flows within the recycling system for 2050.

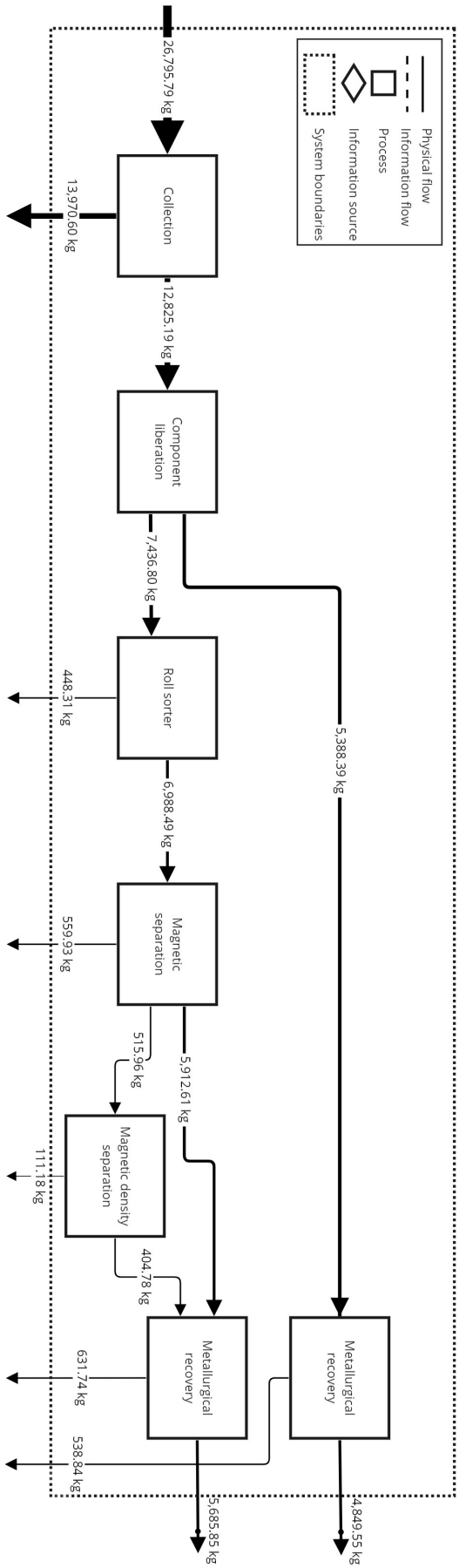

Figure A.3: The silver flows within the recycling system for 2050.

A.9. Population growth and migration

In order to measure the effect of a decrease in migration, historical migration data from Eurostat was used. The databases Immigration by age group, sex and citizenship and Emigration by age group, sex and country of next usual residence were used to determine the patterns [145, 146]. Table A.10 shows the net migration for each region. It was assumed that this migration would halve in the scenario, thus impacting the population growth in each region. For northern and western Europe growth was decreased by 0.50% and 0.29% respectively, while in eastern and southern Europe growth increased by 0.21% and 0.08%. These changes in growth were added or subtracted from the predicted growths as predicted by Eurostat [112]. Therefore, over the set period (2021-2050) this resulted in an decrease in population of 13.89% and 8.25% for northern and western Europe and an increase of 6.44% and 2.53% for eastern and southern Europe compared to BAU.

Table A.10: Net migration of the four EU regions.

	2015	**2016**	**2017**	**2018**	**2019**
North	36,599	38,123	34,602	30,644	26,506
East	-204,884	-194,714	-199,255	-196,037	-206,767
South	-29,407	-38,204	-36,862	-31,277	-27,051
West	197,692	194,795	201,515	196,670	207,312

A.10. Component reconciliation between *Huang et al.* and the Peacoc categories

Table A.11: The conversion table between the Peacoc component categories and *Huang et al.* [127]

Component category (Peacoc)	**Component category (*Huang et al.*)**
Central Processing Units	CPU
IC chips and transistors	ST, ILT, PT, FET, Thyrstor and Chip
MLCC + Ta capacitors	SC, MLCC, SMD-R and SMD-D
Small transistors and small IC chips	SMD-T and OC
Blue and black rectangular connectors (VGA)	Port
Rectangular connectors (USB, HDMI etc.)	Port
Golden connectors (RCA)	Port
Round gray connector (RCA)	Port
Plastic connectors with pins and others	Connector
Large steel and aluminium cases	Tuner
Inductors and transformers	FI, HPI, SMP-P, TI, TR and Transformer
Al electrolytic capacitors	ETC, PC, CEC and Relay
Blue capacitors	FC, CC and HVCC
Resistors	AI, MFR, CR, CFR, ZD and RD
Quartz resonators	PCO
Heatsinks	Heatsink
Cables	-
Connectors of plastic with golden pins	-
Connectors of plastic with silver pins (SCART)	Port
Other	-

Table A.12: The CRM concentrations (mg/kg component) from *Huang et al.* to the Peacoc component categories [127]. Not all component categories could be matched.

	Ba	**Be**	**Co**	**Mg**	**Sb**	**Ti**	**V**	**Pt**
Central Processing Units	30,760	110	150	1,190	4,070	2,810	50	0
IC chips and transistors	71	20	156	393	4,343	2,860	63	2
MLCC + Ta capacitors	77,028	33	180	1,333	2600	2,003	40	1
Small transistors and small IC chips	55	200	65	315	7,410	5,000	125	0
Blue and black rectangular connectors (VGA)	320	0	10	1,560	5,360	160	40	0
Rectangular connectors (USB, HDMI etc.)	320	0	10	1,560	5,360	160	40	0
Golden connectors (RCA)	320	0	10	1,560	5360	160	40	0
Round gray connector (RCA)	320	0	10	1,560	5360	160	40	0
Plastic connectors with pins and others	10	0	30	440	2,580	2,940	40	9
Large steel and aluminium cases	4,400	0	8750	0	9450	19,850	1,050	0
Inductors and transformers	148	0	97	1,830	925	5,427	138	0
Al electrolytic capacitors	270	10	10	2,593	1868	5,100	68	0
Blue capacitors	59,640	2,123	1,777	22,847	89,947	3,860	620	3
Resistors	8,637	57	158	2,722	1,940	1363	92	0
Quartz resonators	29	19	4,060	1,020	340	0	60	0
Heatsinks	0	0	100	105,250	0	35,300	1,450	0
Cables	Not in data							
Connectors of plastic with golden pins	Not in data							
Connectors of plastic with silver pins (SCART)	320	0	10	1,560	5,360	160	40	0
Other	Not in data							

A.11. CRM concentrations in the bare PCBs

Table A.13: The CRM concentrations in the bare PCBs from different sources.

Source	**Ba (wt%)**	**Be (wt%)**	**Co (wt%)**	**Mg (wt%)**	**Sb (wt%)**	**Pt (wt%)**
[147]	0.0022, 0.16, 0.00, 0.00, 0.02			0.08, 0.10, 0.22, 0.00, 0.16	0.45, 1.97, 0.00, 0.00	
[148]	0.02	0.0038		0.16	0.34	0.0022
[149]		0.003			0.35	
[150]			0.292			
Average	0.0364	0.0034	0.292	0.11	0.52	0.0022

A.12. Energy requirements of a select number of Dutch municipalities

Table A.14: The energy requirements of a select number of Dutch municipalities.

Municipality	Number of houses [151]	Natural gas per house (m^3) [152]	Natural gas total (GJ)	Electricity per house (kWh) [152]	Electricity total (GJ)	Total energy (GJ)
Delft	51,495	850	1,443,559	2,350	435,648	**1,879,207**
Den Haag	265,959	950	8,332,761	2,339	2,239,481	**10,572,243**
Hattem	5,262	1,370	237,751	2,920	55,314	**293,065**
Leiden	60,538	820	1,637,165	2,360	514,331	**2,151,496**
Leiderdorp	12,379	1,020	416,425	2,790	124,335	**540,759**
Rijswijk	27,219	1,050	942,567	2,460	241,051	**1,183,618**
Voorschoten	11,504	1,160	440,106	2,850	118,031	**558,137**
Waddinxveen	12,797	1,060	447,368	2,880	132,679	**580,047**
Wageningen	18,086	1,000	596,476	2,460	160,170	**756,646**
Zwolle	59,491	1,020	2,001,253	2,500	535,419	**2,536,672**

Bibliography

[1] A. Ede and L.B. Cormack. *A History of Science in Society: From Philosophy to Utility, Third Edition*. G - Reference,Information and Interdisciplinary Subjects Series. University of Toronto Press, 2017. ISBN 9781442634992. URL https://books.google.nl/books?id=P5sSDQAAQBAJ.

[2] J.K. Rowling. *Harry Potter and the Philosopher's Stone*, volume 1. Bloomsbury Publishing, London, 1 edition, June 1997. ISBN 978-0747532699.

[3] G.B. Kauffman. The role of gold in alchemy. part ii. *Gold Bulletin*, 18(2):69–78, Jun 1985. ISSN 2190-7579. doi: 10.1007/BF03214689. URL https://doi.org/10.1007/BF03214689.

[4] C. Blair, M.C. Ross, P.E. Lasko, J.F. Hayward, H. Goetz, H.-U. Haedeke, E.J. Forsdyke, G.K. Geerling, E.L. Young, B. March, G.McK. Hughes, R. Sieber, J.T. Ulak, D.T. Easby, B.V. Gyllensvärd, S.V. Grancsay, W.W. Watts, and W.Y. Willetts. Metalwork, 2016. URL https://www.britannica.com/topic/metalwork/Silver-and-gold. Accessed: 2021-12-09.

[5] E. Schoenberger. Why is gold valuable? nature, social power and the value of things. *Cultural Geographies - CULT GEOGR*, 18:3–24, 01 2011. doi: 10.1177/1474474010377549.

[6] J. Kershaw and S.W. Merkel. Silver recycling in the viking age: Theoretical and analytical approaches. *Archaeometry*, n/a(n/a), 2021. doi: https://doi.org/10.1111/arcm.12709. URL https://onlinelibrary.wiley.com/doi/abs/10.1111/arcm.12709.

[7] European Commission, Entrepreneurship Directorate-General for Internal Market, Industry, SMEs, G. Blengini, C. El Latunussa, U. Eynard, C. Torres De Matos, D. Wittmer, K. Georgitzikis, C. Pavel, S. Carrara, L. Mancini, M. Unguru, M. Grohol, F. Mathieux, and D. Pennington. *Study on the EU's list of critical raw materials (2020) : non-critical raw materials factsheets*. Publications Office, 2020. doi: doi/10.2873/587825.

[8] European Commission, Entrepreneurship Directorate-General for Internal Market, Industry, SMEs, G. Blengini, C. El Latunussa, U. Eynard, C. Torres De Matos, D. Wittmer, K. Georgitzikis, C. Pavel, S. Carrara, L. Mancini, M. Unguru, M. Grohol, F. Mathieux, and D. Pennington. *Study on the EU's list of critical raw materials (2020) : critical raw materials factsheets*. Publications Office, 2020. doi: doi/10.2873/92480.

[9] C. Bracey, P. Ellis, and G. Hutchings. Application of copper-gold alloys in catalysis: Current status and future perspectives. *Chemical Society Reviews*, 38, 09 2009. doi: 10.1039/b817729p.

[10] T.A. Atia and J. Spooren. Fast microwave leaching of platinum, rhodium and cerium from spent non-milled autocatalyst monolith. *Chemical Engineering and Processing - Process Intensification*, 164:108378, 7 2021. ISSN 0255-2701. doi: 10.1016/J.CEP.2021.108378.

[11] C. Hagelüken and C. Corti. Recycling of gold from electronics: Cost-effective use through 'design for recycling'. *Gold Bulletin*, 43:209–220, 09 2010. doi: 10.1007/BF03214988.

[12] C. Helbig, L. Wietschel, A. Thorenz, and A. Tuma. How to evaluate raw material vulnerability - an overview. *Resources Policy*, 48:13–24, 2016. ISSN 0301-4207. doi: https://doi.org/10.1016/j.resourpol.2016.02.003. URL https://www.sciencedirect.com/science/article/pii/S0301420716300083.

[13] B. Buijs, H. Sievers, and L. Tercero. Limits to the critical raw materials approach. *Proceedings of the ICE - Waste and Resource Management*, 165:201–208(7), 11 2012. doi: 10.1680/warm.12.00010.

[14] E. Rietveld and T. Bastein. *In Search of an Appropriate Criticality Assessment of Raw Materials in the Dutch Economy*, chapter Chapter 8, pages 151–176. 2019. doi: 10.1142/9789813271050_0008. URL https://www.worldscientific.com/doi/abs/10.1142/9789813271050_0008.

[15] N.T. Nassar, T.E. Graedel, and E.M. Harper. By-product metals are technologically essential but have problematic supply. *Science Advances*, 1(3):e1400180, 2015. doi: 10.1126/sciadv.1400180. URL https://www.science.org/doi/abs/10.1126/sciadv.1400180.

[16] K. Lee and J. Cha. Towards improved circular economy and resource security in south korea. *Sustainability*, 13(1), 2021. ISSN 2071-1050. doi: 10.3390/su13010017. URL https://www.mdpi.com/2071-1050/13/1/17.

[17] J. Jacob. China tightens grip on rare earths supply, 9 2011. URL https://www.ibtimes.com/china-tightens-grip-rare-earths-supply-318698. Accessed: 2022-05-11.

[18] Engineering ToolBox. Electrical conductivity - elements and other materials, 2008. URL https://www.engineeringtoolbox.com/conductors-d_1381.html. Accessed: 2022-03-24.

[19] O. Loebich. The optical properties of gold. *Gold Bulletin*, 5(1):2–10, Mar 1972. ISSN 2190-7579. doi: 10.1007/BF03215148. URL https://doi.org/10.1007/BF03215148.

[20] P. Cyganowski, K. Garbera, A. Leśniewicz, J. Wolska, P. Pohl, and D. Jermakowicz-Bartkowiak. The recovery of gold from the aqua regia leachate of electronic parts using a core–shell type anion exchange resin. *Journal of Saudi Chemical Society*, 21(6):741–750, 2017. ISSN 1319-6103. doi: https://doi.org/10.1016/j.jscs.2017.03.007. URL https://www.sciencedirect.com/science/article/pii/S131961031730042X.

[21] T. Huang, J. Zhu, X. Huang, J. Ruan, and Z. Xu. Assessment of precious metals positioning in waste printed circuit boards and the economic benefits of recycling. *Waste Management*, 139:105–115, 2022. ISSN 0956-053X. doi: https://doi.org/10.1016/j.wasman.2021.12.030. URL https://www.sciencedirect.com/science/article/pii/S0956053X21006759.

[22] S. Glöser-Chahoud, M. Pfaff, R. Walz, and F. Schultmann. Simulating the service lifetimes and storage phases of consumer electronics in europe with a cascade stock and flow model. *Journal of Cleaner Production*, 213:1313–1321, 3 2019. ISSN 0959-6526. doi: 10.1016/J.JCLEPRO.2018.12.244. product lifetime modelling of electronics.

[23] G.F. Cardamone, F. Ardolino, and U. Arena. About the environmental sustainability of the european management of weee plastics. *Waste Management*, 126:119–132, 2021. ISSN 0956-053X. doi: https://doi.org/10.1016/j.wasman.2021.02.040. URL https://www.sciencedirect.com/science/article/pii/S0956053X21001094.

[24] J.M. Valero Navazo, G. Villalba Méndez, and L. Talens Peiró. Material flow analysis and energy requirements of mobile phone material recovery processes. *The International Journal of Life Cycle Assessment*, 19(3):567–579, Mar 2014. ISSN 1614-7502. doi: 10.1007/s11367-013-0653-6. URL https://doi.org/10.1007/s11367-013-0653-6.

[25] Peacoc. Peacoc project, May 2021. URL https://www.peacoc-h2020.eu/. Accessed: 2022-5-11.

[26] N. Hultgren. Guidelines and design strategies for improved product recyclability - how to increase the recyclability of consumer electronics and domestic appliances through product design. 2012.

[27] F. Zhang, M. Rio, and P. Zwolinski. Dynamic eco-design strategic options for electric-electronic industry. In J.-L. Bessède, editor, *Eco-design in Electrical Engineering*, pages 29–40, Cham, 2018. Springer International Publishing. ISBN 978-3-319-58172-9.

[28] CDS Manufacturing. Precision roll sorters, 2022. URL https://www.cdsmanufacturing.com/product-category/products/precision-roll-sorters/. Accessed: 2022-05-11.

[29] Sormac B.V. Roller grader rs, 2022. URL https://www.sormac.eu/en/machines/roller-grader-rs/. Accessed: 2022-05-11.

[30] D.G. Batchelder. Roll grader sizing of agricultural seeds. Master's thesis, Oklahoma State University, May 1962.

[31] M.Y. Ibrahim and S. Sultana. Study on fresh fish sorting techniques. pages 462 – 467, 08 2006. doi: 10.1109/ICMECH.2006.252571.

[32] G. Mir. Portable walnut grading machine best replacement for perforated cylindrical grader. *Business Dimensions, an International Journal of Research & Innovation*, 3:82–86, 07 2016.

[33] S. Sultan and T. Venkatachalam. Performance evaluation of a divergent roller grader for selected vegetables. *Ama, Agricultural Mechanization in Asia, Africa & Latin America*, 40:60–62, 10 2009.

[34] E.N. Maull. Fruit grader, 7 1911. URL https://patents.google.com/patent/US1035887A/.

[35] F. Stebler. Fruit grader, 10 1924. URL https://patents.google.com/patent/US1651847A/.

[36] E.R. Scott. Apple-grader, 6 1919. URL https://patents.google.com/patent/US1363818A/.

[37] H. Nakamura, K. Tazawa, and T. Teshigawara. Method of regenerating catalyst, 8 2004. URL https://patents.google.com/patent/JP2005095874A/.

[38] L.E. Allen III, B.L. Riise, P.C. Allen, R.C. Rau, and M.B. Biddle. Multistep separation of plastics, 4 2003. URL https://patents.google.com/patent/EP1494843B1/.

[39] P. Piekaj. Modern grinding balls sorting machines. *New Trends in Production Engineering*, 2 (1):86–95, 2019. doi: doi:10.2478/ntpe-2019-0009. URL https://doi.org/10.2478/ntpe-2019-0009.

[40] L. Kitinoja and A. Kader. *Small scale postharvest handling practices: a manual for horticultural crops (5th edition)*. 11 2015.

[41] R. Visvanathan and Y.P. Ashok. A divergent type grader for cocoa pods (theobroma cacao l.). *CIGR*, 23(4):283–294, 2021. doi: http://orcid.org/0000-0001-5560-0503.

[42] D. Ghanbarian, A. Ghorbani-marghmaleki, M.A. Ghazavi, and Sh. Besharati. Design, development and evaluation of a divergent roller sizer for almond kernels. *Journal of Agricultural Machinery*, 5(2):228–241, 2015. ISSN 2228-6829. doi: doi:10.22067/jam.v5i2.27009. URL https://www.ingentaconnect.com/content/doaj/22286829/2015/00000005/00000002/art00001.

[43] S. Garg, V.S. Kolli, and S.S. Shirkole. 3 - sorting operations for the classification of agricultural crops. In Seid Mahdi Jafari, editor, *Postharvest and Postmortem Processing of Raw Food Materials*, pages 53–76. Woodhead Publishing, 2022. ISBN 978-0-12-818572-8. doi: https://doi.org/10.1016/B978-0-12-818572-8.00011-5. URL https://www.sciencedirect.com/science/article/pii/B9780128185728000115.

[44] J. Oberteuffer. Magnetic separation: A review of principles, devices, and applications. *IEEE Transactions on Magnetics*, 10(2):223–238, 1974. doi: 10.1109/TMAG.1974.1058315.

[45] O. Olsvik, T. Popovic, E. Skjerve, K.S. Cudjoe, E. Hornes, J. Ugelstad, and M. Uhlén. Magnetic separation techniques in diagnostic microbiology. *Clinical Microbiology Reviews*, 7(1):43–54, 1994. doi: 10.1128/CMR.7.1.43. URL https://journals.asm.org/doi/abs/10.1128/CMR.7.1.43.

[46] S.K. Roy, D. Nayak, and S.S. Rath. A review on the enrichment of iron values of low-grade iron ore resources using reduction roasting-magnetic separation. *Powder Technology*, 367:796–808, 2020. ISSN 0032-5910. doi: https://doi.org/10.1016/j.powtec.2020.04.047. URL https://www.sciencedirect.com/science/article/pii/S0032591020303338.

[47] Y. Qin, Z. Yao, J. Ruan, and Z. Xu. Motion behavior model and multistage magnetic separation method for the removal of impurities from recycled waste plastics. *ACS Sustainable Chemistry & Engineering*, 9(32):10920–10928, 2021. doi: 10.1021/acssuschemeng.1c03580. URL https://doi.org/10.1021/acssuschemeng.1c03580.

[48] C. Kittel. *Introduction to Solid State Physics, 8th Ed.* 11 2004. ISBN 978-0-471-41526-8.

[49] Wamag. Overband magnetic separators, n.d. URL https://www.wamag.cz/en/products/overband-magnetic-separators. Accessed: 2022-5-11.

[50] A. Müller and I. Martins. *Processing of Construction and Demolition Waste*, pages 65–126. Springer Fachmedien Wiesbaden, Wiesbaden, 2022. ISBN 978-3-658-34609-6. doi: 10.1007/978-3-658-34609-6_4. URL https://doi.org/10.1007/978-3-658-34609-6_4.

[51] Resources & Recycling. Polymers recycling, 2013. URL https://www.tudelft.nl/citg/over-faculteit/afdelingen/engineering-structures/sections-labs/resources-recycling/research-innovation/recycling-technologies/polymers-recycling. Accessed: 2022-8-22.

[52] S. Serranti, V. Luciani, G. Bonifazi, B. Hu, and P.C. Rem. An innovative recycling process to obtain pure polyethylene and polypropylene from household waste. *Waste Management*, 35:12–20, 2015. ISSN 0956-053X. doi: https://doi.org/10.1016/j.wasman.2014.10.017. URL https://www.sciencedirect.com/science/article/pii/S0956053X14005017.

[53] M. Bauer, M. Lehner, D. Schwabl, H. Flachberger, L. Kranzinger, R. Pomberger, and W. Hofer. Sink–float density separation of post-consumer plastics for feedstock recycling. *Journal of Material Cycles and Waste Management*, 20, 05 2018. doi: 10.1007/s10163-018-0748-z.

[54] V. Luciani, G. Bonifazi, P. Rem, and S. Serranti. Upgrading of pvc rich wastes by magnetic density separation and hyperspectral imaging quality control. *Waste Management*, 45:118–125, 2015. ISSN 0956-053X. doi: https://doi.org/10.1016/j.wasman.2014.10.015. URL https://www.sciencedirect.com/science/article/pii/S0956053X14004991. Urban Mining.

[55] E.J. Bakker, P.C. Rem, and N. Fraunholcz. Upgrading mixed polyolefin waste with magnetic density separation. *Waste Management*, 29(5):1712–1717, 2009. ISSN 0956-053X. doi: https://doi.org/10.1016/j.wasman.2008.11.006. URL https://www.sciencedirect.com/science/article/pii/S0956053X08003954. First international conference on environmental management, engineering, planning and economics.

[56] J.J. Kosse, M. Dhallé, P.C. Rem, H.J.M. ter Brake, and H.H.J. ten Kate. Fundamental electromagnetic configuration for generating one-directional magnetic field gradients. *IEEE Transactions on Magnetics*, 57(8):1–10, 2021. doi: 10.1109/TMAG.2021.3080183.

[57] J.J. Kosse, W.A.J Wessel, C. Zhou, M. Dhallé, G. Tomás, H.J.G. Krooshoop, H.J.M. ter Brake, and H.H.J. ten Kate. Mechanical design of a superconducting demonstrator for magnetic density separation. *Superconductor Science and Technology*, 34(11):115019, oct 2021. doi: 10.1088/1361-6668/ac2c0f. URL https://doi.org/10.1088/1361-6668/ac2c0f.

[58] J.J. Kosse. *Superconducting magnets for magnetic density separation: A NbTi based demonstrator*. PhD thesis, University of Twente, Netherlands, March 2021.

[59] E. Bakker, A.J. Berkhout, L. Hartmann, and P. Rem. Turning magnetic density separation into green business using the cyclic innovation model. *The Open Waste Management Journal*, 3, 05 2010. doi: 10.2174/1876400201003010099.

[60] B. Hu. *Magnetic density separation of polyolefin wastes*. PhD thesis, Delft University of Technology, 2014.

[61] P. Rem, F. Di Maio, B. Hu, G. Houzeaux, L. Baltes, and M. Tierean. Magnetic fluid equipment for sorting secondary polyolefins from waste. *Environmental engineering and management journal*, 12:951–958, 05 2013. doi: 10.30638/eemj.2013.118.

[62] B. Hu, N. Fraunholz, and P.C. Rem. Wetting technologies for high-accuracy sink-float separations in water- based media. *The Open Waste Management Journal*, 3:71–80, 2010.

[63] J.R.A. Koning, E. Bakker, and P. Rem. Sorting of vegetable seeds by magnetic density separation in comparison with liquid density separation. *Seed Science and Technology*, 39, 10 2011. doi: 10.15258/sst.2011.39.3.06.

[64] L. Muchova, E. Bakker, and P. Rem. Precious metals in municipal solid waste incineration bottom ash. *Water, Air, & Soil Pollution: Focus*, 9:107–116, 2009. doi: 10.1007/s11267-008-9191-9.

[65] Umincorp. Umincorp how, 2021. URL https://umincorp.com/how. Accessed: 2021-12-09.

[66] P.H. Brunner and H. Rechberger. *Handbook of Material Flow Analysis: For Environmental, Resource, and Waste Engineers, Second Edition (2nd ed.)*. CRC Press, Boca Raton Fl, 2016. ISBN 978-13-153-1345-0. doi: https://doi.org/10.1201/9781315313450.

[67] T.E. Graedel. Material flow analysis from origin to evolution. *Environmental Science & Technology*, 53(21):12188–12196, 2019. doi: 10.1021/acs.est.9b03413. URL https://doi.org/10.1021/acs.est.9b03413. PMID: 31549816.

[68] O. Cencic and H. Rechberger. Material flow analysis with software stan. *Journal of Environmental Engineering and Management*, 18:3–7, 01 2008.

[69] W.-Q. Chen and T.E. Graedel. Anthropogenic cycles of the elements: A critical review. *Environmental Science & Technology*, 46(16):8574–8586, 2012. doi: 10.1021/es3010333. URL https://doi.org/10.1021/es3010333. PMID: 22803614.

[70] A. Elshkaki, T.E. Graedel, L. Ciacci, and B.K. Reck. Resource demand scenarios for the major metals. *Environmental Science & Technology*, 52(5):2491–2497, 2018. doi: 10.1021/acs.est.7b05154. URL https://doi.org/10.1021/acs.est.7b05154. PMID: 29380602.

[71] Y. Wang and H. Ma. Analysis of uncertainty in material flow analysis. *Journal of Cleaner Production*, 170:1017–1028, 2018. ISSN 0959-6526. doi: https://doi.org/10.1016/j.jclepro.2017.09.202. URL https://www.sciencedirect.com/science/article/pii/S0959652617322047.

[72] T. Fishman, R.J. Myers, O. Rios, and T.E. Graedel. Implications of emerging vehicle technologies on rare earth supply and demand in the united states. *Resources*, 7(1), 2018. ISSN 2079-9276. doi: 10.3390/resources7010009. URL https://www.mdpi.com/2079-9276/7/1/9.

[73] F. Krausmann, D. Wiedenhofer, C. Lauk, W. Haas, H. Tanikawa, T. Fishman, A. Miatto, H. Schandl, and H. Haberl. Global socioeconomic material stocks rise 23-fold over the 20th century and require half of annual resource use. *Proceedings of the National Academy of Sciences*, 114(8):1880–1885, 2017. doi: 10.1073/pnas.1613773114. URL https://www.pnas.org/doi/abs/10.1073/pnas.1613773114.

[74] H. Wu, Z. Yuan, Y. Zhang, L. Gao, S. Liu, and Y. Geng. Data uncertainties in anthropogenic phosphorus flow analysis of lake watershed. *Journal of Cleaner Production*, 69:74–82, 2014. ISSN 0959-6526. doi: https://doi.org/10.1016/j.jclepro.2014.01.043. URL https://www.sciencedirect.com/science/article/pii/S0959652614000560.

[75] G. Liu and D.B. Müller. Centennial evolution of aluminum in-use stocks on our aluminized planet. *Environmental Science & Technology*, 47(9):4882–4888, 2013. doi: 10.1021/es305108p. URL https://doi.org/10.1021/es305108p. PMID: 23480626.

[76] M. Keersemaker. *Critical Raw Materials*, pages 69–82. Springer International Publishing, Cham, 2020. ISBN 978-3-030-40268-6. doi: 10.1007/978-3-030-40268-6_9. URL https://doi.org/10.1007/978-3-030-40268-6_9.

[77] W. Rabe, G. Kostka, and K. Smith Stegen. China's supply of critical raw materials: Risks for europe's solar and wind industries? *Energy Policy*, 101:692–699, 2017. ISSN 0301-4215. doi: https://doi.org/10.1016/j.enpol.2016.09.019. URL https://www.sciencedirect.com/science/article/pii/S0301421516304852.

[78] T.E. Graedel, J. Allwood, J.-P. Birat, M. Buchert, C. Hagelüken, B.K. Reck, S.F. Sibley, and G. Sonnemann. What do we know about metal recycling rates? *Journal of Industrial Ecology*, 15(3):355–366, 2011. doi: https://doi.org/10.1111/j.1530-9290.2011.00342.x. URL https://onlinelibrary.wiley.com/doi/abs/10.1111/j.1530-9290.2011.00342.x.

[79] European Commission, Entrepreneurship Directorate-General for Internal Market, Industry, SMEs, G. Blengini, C. El Latunussa, U. Eynard, C. Torres De Matos, D. Wittmer, K. Georgitzikis, C. Pavel, S. Carrara, L. Mancini, M. Unguru, D. Blagoeva, F. Mathieux, and D. Pennington. *Study on the EU's list of critical raw materials (2020) : final report*. Publications Office, 2020. doi: doi/10.2873/11619.

[80] S. Glöser, L. Tercero Espinoza, C. Gandenberger, and M. Faulstich. Raw material criticality in the context of classical risk assessment. *Resources Policy*, 44:35–46, 2015. ISSN 0301-4207. doi: https://doi.org/10.1016/j.resourpol.2014.12.003. URL https://www.sciencedirect.com/science/article/pii/S0301420715000021.

[81] D. Schrijvers, A. Hool, G.A. Blengini, W.-Q. Chen, J. Dewulf, R. Eggert, L. van Ellen, R. Gauss, J. Goddin, K. Habib, C. Hagelüken, A. Hirohata, M. Hofmann-Amtenbrink, J. Kosmol, M. Le Gleuher, M. Grohol, A. Ku, M.-H. Lee, G. Liu, K. Nansai, P. Nuss, D. Peck, A. Reller, G. Sonnemann, L. Tercero, A. Thorenz, and P.A. Wäger. A review of methods and data to determine raw material criticality. *Resources, Conservation and Recycling*, 155:104617, 2020. ISSN 0921-3449. doi: https://doi.org/10.1016/j.resconrec.2019.104617. URL https://www.sciencedirect.com/science/article/pii/S0921344919305233.

[82] G. Gunn. *Critical Metals Handbook*. 12 2013. ISBN 9780470671719. doi: 10.1002/9781118755341.

[83] T. Graedel, R. Barr, C. Chandler, T. Chase, J. Choi, L. Christoffersen, E. Friedlander, C. Henly, C. Jun, N. Nassar, D. Schechner, S. Warren, M.-Y. Yang, and C. Zhu. Methodology of metal criticality determination. *Environmental science & technology*, 46:1063–70, 12 2011. doi: 10.1021/es203534z.

[84] European Commission, Entrepreneurship Directorate-General for Internal Market, Industry, and SMEs. *COMMUNICATION FROM THE COMMISSION TO THE EUROPEAN PARLIAMENT, THE COUNCIL, THE EUROPEAN ECONOMIC AND SOCIAL COMMITTEE AND THE COMMITTEE OF THE REGIONS TACKLING THE CHALLENGES IN COMMODITY MARKETS AND ON RAW MATERIALS*. Publications Office, 2011. URL https://eur-lex.europa.eu/legal-content/EN/TXT/?uri=CELEX:52011DC0025. Accessed: 2022-06-10.

[85] European Commission, Entrepreneurship Directorate-General for Internal Market, Industry, and SMEs. *COMMUNICATION FROM THE COMMISSION TO THE EUROPEAN PARLIAMENT, THE COUNCIL, THE EUROPEAN ECONOMIC AND SOCIAL COMMITTEE AND THE COMMITTEE OF THE REGIONS On the review of the list of critical raw materials for the EU and the implementation of the Raw Materials Initiative*. Publications Office, 2014. URL https://eur-lex.europa.eu/legal-content/EN/TXT/?uri=CELEX:52014DC0297. Accessed: 2022-06-10.

[86] European Commission, Entrepreneurship Directorate-General for Internal Market, Industry, and SMEs. *Study on the review of the list of critical raw materials : final report*. Publications Office, 2017. doi: doi/10.2873/876644.

[87] European Commission, Entrepreneurship Directorate-General for Internal Market, Industry, SMEs, D. Pennington, E. Tzimas, C. Baranzelli, J. Dewulf, S. Manfredi, P. Nuss, M. Grohol, A. Van Maercke, Y. Kayam, S. Solar, B. Vidal-Legaz, L. Talens Peirò, L. Mancini, C. Ciupagea,

L. Godlewska, P. Dias, C. Pavel, D. Blagoeva, G. Blengini, V. Nita, C. Latunussa, C. Torres De Matos, F. Mathieux, and A. Marmier. *Methodology for establishing the EU list of critical raw materials : guidelines*. Publications Office, 2017. doi: doi/10.2873/769526.

[88] E. Hertwich. Increased carbon footprint of materials production driven by rise in investments. *Nature Geoscience*, 14:1–5, 03 2021. doi: 10.1038/s41561-021-00690-8.

[89] Michael F. Ashby. Chapter 15 - material profiles. In M.F. Ashby, editor, *Materials and the Environment (Second Edition)*, pages 459–595. Butterworth-Heinemann, Boston, second edition edition, 2013. ISBN 978-0-12-385971-6. doi: https://doi.org/10.1016/B978-0-12-385971-6.00015-4. URL https://www.sciencedirect.com/science/article/pii/B9780123859716000154.

[90] C. Hagelüken. Recycling of electronic scrap at umicore. precious metals refining. volume 12, pages 111–120, 06 2006.

[91] C. Hageluken. Metals recovery from e-scrap in a global environment. In *6th session of OEWG Basel Convention, Geneva*, 2007.

[92] Peacoc. Refining stage optimisation, June 2022. URL https://www.peacoc-h2020.eu/news/refining-stage-optimisation/. Accessed: 2022-8-22.

[93] A. Priya and S. Hait. Extraction of metals from high grade waste printed circuit board by conventional and hybrid bioleaching using acidithiobacillus ferrooxidans. *Hydrometallurgy*, 177:132–139, 2018. ISSN 0304-386X. doi: https://doi.org/10.1016/j.hydromet.2018.03.005. URL https://www.sciencedirect.com/science/article/pii/S0304386X17309465.

[94] M. Ghodrat, M.A. Rhamdhani, G. Brooks, M. Rashidi, and B. Samali. A thermodynamic-based life cycle assessment of precious metal recycling out of waste printed circuit board through secondary copper smelting. *Environmental Development*, 24:36–49, 2017. ISSN 2211-4645. doi: https://doi.org/10.1016/j.envdev.2017.07.001. URL https://www.sciencedirect.com/science/article/pii/S221146451730009X.

[95] M. Goosey and R. Kellner. Recycling technologies for the treatment of end of life printed circuit boards (pcb). *Circuit World*, 29:33–37, 09 2003. doi: 10.1108/03056120310460801.

[96] M. Bigum, L. Brogaard, and T.H. Christensen. Metal recovery from high-grade weee: A life cycle assessment. *Journal of Hazardous Materials*, 207-208:8–14, 2012. ISSN 0304-3894. doi: https://doi.org/10.1016/j.jhazmat.2011.10.001. URL https://www.sciencedirect.com/science/article/pii/S0304389411012283. Selected papers presented at the 2nd International Conference CRETE 2010, October 2010 - Industrial and Hazardous Waste Management.

[97] V. Forti, C. Baldé, and R. Kuehr. *E-Waste statistics Guidelines on classification, reporting and indicators*. 04 2018. ISBN 978-92-808-9067-9.

[98] R. Kaufmann, G. Isella, A. Sanchez-Amores, S. Neukom, A. Neels, L. Neumann, A. Brenzikofer, A. Dommann, C. Urban, and H. von Kaenel. Near infrared image sensor with integrated germanium photodiodes. *JOURNAL OF APPLIED PHYSICS*, 110, 07 2011. doi: 10.1063/1.3608245.

[99] A. Buekens and J. Yang. Recycling of weee plastics a review. *J Mater Cycles Waste Manag*, 16, 03 2014. doi: 10.1007/s10163-014-0241-2.

[100] S. Ruggeri, G. Fontana, V. Basile, M. Valori, and I. Fassi. Micro-robotic handling solutions for pcb (re-)manufacturing. *Procedia Manufacturing*, 11:441–448, 2017. ISSN 2351-9789. doi: https://doi.org/10.1016/j.promfg.2017.07.132. URL https://www.sciencedirect.com/science/article/pii/S2351978917303360. 27th International Conference on Flexible Automation and Intelligent Manufacturing, FAIM2017, 27-30 June 2017, Modena, Italy.

[101] K. Feldmann, J. Franke, and F. Schüßler. Development of micro assembly processes for further miniaturization in electronics production. *CIRP Annals*, 59(1):1–4, 2010. ISSN 0007-8506. doi: https://doi.org/10.1016/j.cirp.2010.03.005. URL https://www.sciencedirect.com/science/article/pii/S0007850610000065.

[102] Y. Liu, Q. Song, L. Zhang, and Z. Xu. Novel approach of in-situ nickel capture technology to recycle silver and palladium from waste nickel-rich multilayer ceramic capacitors. *Journal of Cleaner Production*, 290:125650, 2021. ISSN 0959-6526. doi: https://doi.org/10.1016/j.jclepro.2020.125650. URL https://www.sciencedirect.com/science/article/pii/S0959652620356961.

[103] Y. Liu, L. Zhang, Q. Song, and Z. Xu. Recovery of palladium and silver from waste multilayer ceramic capacitors by eutectic capture process of copper and mechanism analysis. *Journal of Hazardous Materials*, 388:122008, 2020. ISSN 0304-3894. doi: https://doi.org/10.1016/j.jhazmat.2019.122008. URL https://www.sciencedirect.com/science/article/pii/S0304389419319624.

[104] R. Panda, O.S. Dinkar, M.K. Jha, and D.D. Pathak. Hydrometallurgical processing of waste multilayer ceramic capacitors (mlccs) to recover silver and palladium. *Hydrometallurgy*, 197:105476, 2020. ISSN 0304-386X. doi: https://doi.org/10.1016/j.hydromet.2020.105476. URL https://www.sciencedirect.com/science/article/pii/S0304386X19308758.

[105] G. Prabaharan, S.P. Barik, and B. Kumar. A hydrometallurgical process for recovering total metal values from waste monolithic ceramic capacitors. *Waste Management*, 52:302–308, 2016. ISSN 0956-053X. doi: https://doi.org/10.1016/j.wasman.2016.04.010. URL https://www.sciencedirect.com/science/article/pii/S0956053X16301738.

[106] C.P. Baldé, M. Wagner, G. Iattoni, and R. Kuehr. In-depth review of the weee collection rates and targets in the eu-28, norway, switzerland, and iceland. Technical report, Bonn, Germany, 2020.

[107] European Commission. A new circular economy action plan for a cleaner and more competitive europe. Technical report, European Commission, 2020.

[108] Rijksoverheid. Uitvoeringsprogramma circulaire economie 2021-2023. Technical report, Het ministerie van Infrastructuur en Waterstaat, mede namens de ministeries van Economische Zaken en Klimaat, Binnenlandse Zaken en Koninkrijksrelaties, Landbouw, Natuur en Voedselkwaliteit en Buitenlandse Zaken., 2021.

[109] V.M. Van Straalen, A.J. Roskam, and C.P. Baldé. Waste over time [computer software]. Available at http://github.com/Statistics-Netherlands/ewaste (2022/06/07), 2016.

[110] J. Huisman, P. Leroy, F. Tertre, M. Ljunggren, P. Chancerel, D. Cassard, A. Løvik, P. Wäger, D. Kushnir, V. Rotter, P. Mählitz, L. Herreras, J. Emmerich, A. Hallberg, H. Habib, M. Wagner, and S. Downes. Prospecting secondary raw materials in the urban mine and mining wastes (prosum) - final report. Technical report, 12 2017.

[111] Eurostat. Population on 1 january by age and sex. https://ec.europa.eu/eurostat/databrowser/bookmark/537afe3a-cd84-4caa-914e-cec8f43cb564?lang=en, 2022. Accessed: 2022-06-07.

[112] Eurostat. Population on 1st january by age, sex and type of projection. https://ec.europa.eu/eurostat/databrowser/bookmark/17d99692-d418-42fa-84eb-96637f27912b?lang=en, 2021. Accessed: 2022-06-07.

[113] M.A. Wagner, J. Huisman, A.N. Løvik, H. Habib, P. Mählitz, and E. van der Voet. Methodology to prospect electronics compositions and flows, illustrated by material trends in printed circuit boards. *Journal of Cleaner Production*, 307:127164, 2021. ISSN 0959-6526. doi: https://doi.org/10.1016/j.jclepro.2021.127164. URL https://www.sciencedirect.com/science/article/pii/S0959652621013834.

[114] A. Rohatgi. Webplotdigitizer - web based plot digitizer. Available at https://apps.automeris.io/wpd/ (2022/06/07), 2021.

[115] H. Escaith. Trade collapse, trade relapse and global production networks: Supply chains in the great recession. *University Library of Munich, Germany, MPRA Paper*, 10 2009. doi: 10.2139/ssrn.1497512.

[116] S. Althaf, C.W. Babbitt, and R. Chen. The evolution of consumer electronic waste in the united states. *Journal of Industrial Ecology*, 25(3):693–706, 2021. doi: https://doi.org/10.1111/jiec.13074. URL https://onlinelibrary.wiley.com/doi/abs/10.1111/jiec.13074.

[117] Y. Kalmykova, J. Patrício, L. Rosado, and P. EO Berg. Out with the old, out with the new – the effect of transitions in tvs and monitors technology on consumption and weee generation in sweden 1996–2014. *Waste Management*, 46:511–522, 2015. ISSN 0956-053X. doi: https://doi.org/10.1016/j.wasman.2015.08.034. URL https://www.sciencedirect.com/science/article/pii/S0956053X1530101X.

[118] Eurostat. Waste electrical and electronic equipment (weee) by waste management operations - open scope, 6 product categories (from 2018 onwards). https://ec.europa.eu/eurostat/databrowser/bookmark/59cc974f-28f2-47c9-8e37-43a984c6cef6?lang=en, 2022. Accessed: 2022-08-01.

[119] Eurostat. Waste electrical and electronic equipment (weee) by waste management operations. https://ec.europa.eu/eurostat/databrowser/bookmark/879f067c-8644-4929-bef9-de1944ac4696?lang=en, 2022. Accessed: 2022-08-01.

[120] H. Li, J. Eksteen, and E. Oraby. Hydrometallurgical recovery of metals from waste printed circuit boards (wpcbs): Current status and perspectives – a review. *Resources, Conservation and Recycling*, 139:122–139, 2018. ISSN 0921-3449. doi: https://doi.org/10.1016/j.resconrec.2018.08.007. URL https://www.sciencedirect.com/science/article/pii/S092134491830288X.

[121] Platirus. Platirus project, April 2021. URL https://www.platirus.eu/. Accessed: 2022-8-22.

[122] G. Nicol, E. Goosey, D. Yıldız, E. Loving, V. Nguyen, S. Riaño, I. Yakoumis, A. Martinez, A. Siriwardana, A. Unzurrunzaga, J. Spooren, Thomas Abo A., Bart M., X. Dominguez-Benetton, and O. Lanaridi. Platinum group metals recovery using secondary raw materials (platirus): Project overview with a focus on processing spent autocatalyst. *Johnson Matthey Technology Review*, 65, 01 2021. doi: 10.1595/205651321x16057842276133.

[123] L. Zhang and Z. Xu. A review of current progress of recycling technologies for metals from waste electrical and electronic equipment. *Journal of Cleaner Production*, 127:19–36, 2016. ISSN 0959-6526. doi: https://doi.org/10.1016/j.jclepro.2016.04.004. URL https://www.sciencedirect.com/science/article/pii/S0959652616302451.

[124] I. Birloaga and F. Vegliò. Study of multi-step hydrometallurgical methods to extract the valuable content of gold, silver and copper from waste printed circuit boards. *Journal of Environmental Chemical Engineering*, 4(1):20–29, 2016. ISSN 2213-3437. doi: https://doi.org/10.1016/j.jece.2015.11.021. URL https://www.sciencedirect.com/science/article/pii/S221334371530066X.

[125] A. Batnasan, H. Kazutoshi, A. Narankhuu, S. Kawamura, and S. Atsushi. Leaching and adsorption of gold from waste printed circuit boards using iodine-iodide solution and activated carbon. *Engineering Journal*, 20:29–40, 2016.

[126] Council of European Union. Directive 2012/19/eu of the european parliament and of the council of 4 july 2012 on waste electrical and electronic equipment (weee), 2018. https://eur-lex.europa.eu/legal-content/EN/TXT/?uri=CELEX:02012L0019-20180704.

[127] J. Huang, Y. Deng, Y. Han, J. Shu, R. Wang, S. Huang, O.A. Ogunseitan, K. Yu, M. Shang, Y. Liu, S. Li, Y. Han, Z. Cheng, and M. Chen. Toxic footprint and materials profile of electronic components in printed circuit boards. *Waste Management*, 141:154–162, 2022. ISSN 0956-053X. doi: https://doi.org/10.1016/j.wasman.2022.01.019. URL https://www.sciencedirect.com/science/article/pii/S0956053X22000204.

[128] L. Sundqvist Ökvist, X. Hu, J. Eriksson, J. Kotnis, Y. Yang, E. Yli-Rantala, J. Bacher, H. Punkkinen, T. Retegan, M. González Moya, and M. Drzazga. *Production technologies of CRM from secondary resources*. European Union, 2018.

[129] L. Prause. Chapter 10 - conflicts related to resources: The case of cobalt mining in the democratic republic of congo. In Alena Bleicher and Alexandra Pehlken, editors, *The Material Basis of Energy Transitions*, pages 153–167. Academic Press, 2020. ISBN 978-0-12-819534-5. doi: https://doi.org/10.1016/B978-0-12-819534-5.00010-6. URL https://www.sciencedirect.com/science/article/pii/B9780128195345000106.

[130] J. Lee, Y. Kim, and J.-C. Lee. Disassembly and physical separation of electric/electronic components layered in printed circuit boards (pcb). *Journal of Hazardous Materials*, 241-242:387–394, 2012. ISSN 0304-3894. doi: https://doi.org/10.1016/j.jhazmat.2012.09.053. URL https://www.sciencedirect.com/science/article/pii/S0304389412009776.

[131] S. Park, S. Kim, Y. Han, and J. Park. Apparatus for electronic component disassembly from printed circuit board assembly in e-wastes. *International Journal of Mineral Processing*, 144: 11–15, 2015. ISSN 0301-7516. doi: https://doi.org/10.1016/j.minpro.2015.09.013. URL https://www.sciencedirect.com/science/article/pii/S0301751615300302.

[132] Respose Waste Management & Research Private Limited (Respose India). Double shaft waste pcb shredder, capacity: 15-60 hp, 2022. URL https://www.indiamart.com/proddetail/waste-pcb-shredder-12643362488.html. Accessed: 2022-06-14.

[133] Shreddingtech. E-waste pcb shredder, 2022. URL https://www.shreddingtech.com/shredding-machines/e-waste-pcb-shredder-machine.html. Accessed: 2022-06-14.

[134] Engineering ToolBox. Conveyors - load & power consumption, 2009. URL https://www.engineeringtoolbox.com/conveyor-power-load-d_1560.html. Accessed: 2022-06-14.

[135] World Nuclear Association. Heat values of various fuels, 2022. URL https://world-nuclear.org/information-library/facts-and-figures/heat-values-of-various-fuels.aspx. Accessed: 2022-08-24.

[136] A. Domínguez and A. Valero. Global gold mining: Is technological learning overcoming the declining in ore grades? *Journal of Environmental Accounting and Management*, 1, 03 2013. doi: 10.5890/JEAM.2012.01.007.

[137] T.G. Gutowski, S. Sahni, J.M. Allwood, M.F. Ashby, and E. Worrell. The energy required to produce materials: constraints on energy-intensity improvements, parameters of demand. *Philosophical Transactions of the Royal Society A: Mathematical, Physical and Engineering Sciences*, 371(1986):20120003, 2013. doi: 10.1098/rsta.2012.0003. URL https://royalsocietypublishing.org/doi/abs/10.1098/rsta.2012.0003.

[138] G. Wernet, C. Bauer, B. Steubing, J. Reinhard, E. Moreno Ruiz, and B. Weidema. The ecoinvent database version 3 (part i): Overview and methodology. *The International Journal of Life Cycle Assessment*, 21:1–13, 09 2016. doi: 10.1007/s11367-016-1087-8.

[139] C. Meskers and C. Hagelüken. Green recycling of eee:special and precious metal recovery from eee. 02 2009.

[140] M. Xue, A. Kendall, Z. Xu, and J.M. Schoenung. *Waste Management of Printed Wiring Boards: A Life Cycle Assessment of the Metals Recycling Chain from Liberation through Refining*, pages 287–288. Springer International Publishing, Cham, 2016. ISBN 978-3-319-48768-7. doi: 10.1007/978-3-319-48768-7_44. URL https://doi.org/10.1007/978-3-319-48768-7_44.

[141] Z. Li, L.A. Diaz, Z. Yang, H. Jin, T.E. Lister, E. Vahidi, and F. Zhao. Comparative life cycle analysis for value recovery of precious metals and rare earth elements from electronic waste. *Resources, Conservation and Recycling*, 149:20–30, 2019. ISSN 0921-3449. doi: https://doi.org/10.1016/j.resconrec.2019.05.025. URL https://www.sciencedirect.com/science/article/pii/S0921344919302381.

[142] K.-G. Namlis and D. Komilis. Influence of four socioeconomic indices and the impact of economic crisis on solid waste generation in europe. *Waste Management*, 89:190–200, 2019. ISSN 0956-053X. doi: https://doi.org/10.1016/j.wasman.2019.04.012. URL https://www.sciencedirect.com/science/article/pii/S0956053X19302259.

[143] J. Huisman. Weee recast: From 4kg to 65%: The compliance consequences, 01 2010.

[144] Y. van Fan, J.J. Klemeš, and C.T. Lee. Roles of e-waste in a circular economy: Eu-27. In *2021 6th International Conference on Smart and Sustainable Technologies (SpliTech)*, pages 1–4, Sep. 2021. doi: 10.23919/SpliTech52315.2021.9566394.

[145] Eurostat. Immigration by age group, sex and citizenship. https://ec.europa.eu/eurostat/databrowser/bookmark/dc665ef7-6d12-4214-b7ce-97657166ad99?lang=en&page=time:2018, 2022. Accessed: 2022-06-22.

[146] Eurostat. Emigration by age group, sex and country of next usual residence. https://ec.europa.eu/eurostat/databrowser/bookmark/98515ab2-dc0c-4e1f-80a0-a6d7a154fea2?lang=en&page=time:2018, 2022. Accessed: 2022-06-22.

[147] J. Szałatkiewicz. Metals content in printed circuit board waste. *Polish Journal of Environmental Studies*, 23:2365–2369, 01 2014.

[148] X. Wang and G. Gaustad. Prioritizing material recovery for end-of-life printed circuit boards. *Waste Management*, 32(10):1903–1913, 2012. ISSN 0956-053X. doi: https://doi.org/10.1016/j.wasman.2012.05.005. URL https://www.sciencedirect.com/science/article/pii/S0956053X1200195X.

[149] C. Yuan, H.-C. Zhang, G. Mckenna, C. Korzeniewski, and J. Li. Experimental studies on cryogenic recycling of printed circuit board. *The International Journal of Advanced Manufacturing Technology*, 34:657–666, 10 2007. doi: 10.1007/s00170-006-0634-z.

[150] A.-G. Guezennec, K. Bru, J. Jacob, and P. d'Hugues. Co-processing of sulfidic mining wastes and metal-rich post-consumer wastes by biohydrometallurgy. *Minerals Engineering*, 75:45–53, 2015. ISSN 0892-6875. doi: https://doi.org/10.1016/j.mineng.2014.12.033. URL https://www.sciencedirect.com/science/article/pii/S0892687514004403. Biohydrometallurgy.

[151] CBS. Voorraad woningen en niet-woningen; mutaties, gebruiksfunctie, regio. https://opendata.cbs.nl/#/CBS/nl/dataset/81955NED/table?dl=6E0F4, 2022. Accessed: 2022-09-04.

[152] CBS. Energieverbruik particuliere woningen; woningtype en regio's. https://opendata.cbs.nl/#/CBS/nl/dataset/81528NED/table?dl=6E0F5, 2021. Accessed: 2022-09-04.